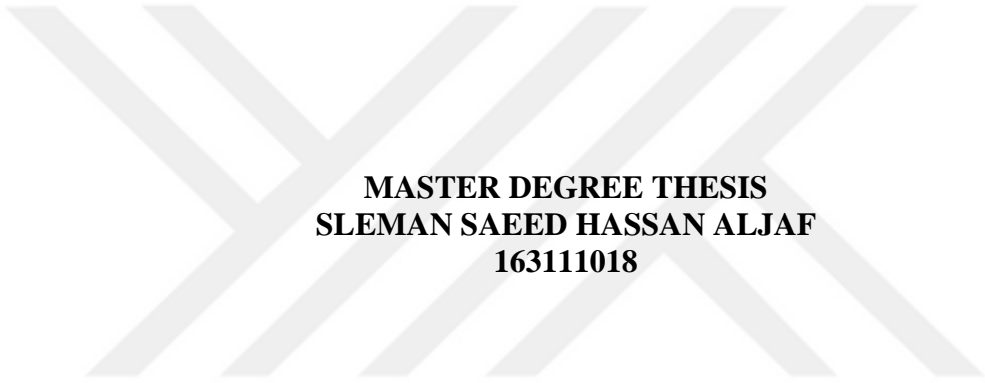


**REPUBLIC OF TURKEY
SİİRT UNIVERSITY
GRADUATE SCHOOL OF NATURAL AND APPLIED SCIENCES**

IMAGE DENOISING IN MULTIREOLUTION WAVELET DOMAIN



**MASTER DEGREE THESIS
SLEMAN SAEED HASSAN ALJAF
163111018**

Department of Electrical and Electronics Engineering

Supervisor: Assoc. Prof. Dr. Musa ATAŞ

**JUNE – 2019
SIIRT**

THESIS ACCEPTANCE AND APPROVAL

This thesis entitled as". Prepared by "Image Denoising in Multiresolution Wavelet Domain", prepared by Sleman Saeed Hassan AL-JAF under the supervision of Assoc. Prof. Dr. Musa ATAŞ has been accepted as thesis study on the data 21/06/2019, as a Master degree in the Department of Electrical and Electronic Engineering at Siirt University, with majority votes by the jury below.

Jury Members

Signature

President

Assoc. Prof. Dr. İbrahim Berkan AYDİLEK



Supervisor

Assoc. Prof. Dr. Musa ATAŞ



Member

Assist. Prof. Dr. Melih KUNCAN



I confirm the above results.



Assoc. Prof. Dr. Fevzi HANSU
Director of the Graduate School of
Natural and Applied Sciences

THESIS NOTIFICATION

I hereby declare that this study is my unique authorial work, which I have worked out on my own. Every information bases, references, and literature used or excerpted through explanation of this work are correctly cited and listed complete reference to the owing cause.

Signature

Sleman Saeed Hassan AL JAF

A handwritten signature in blue ink, consisting of several loops and a long horizontal stroke at the end.

Note: In this thesis, the use of original and other source notifications, Tables, Figures and photographs without reference, it is subject to provision of law No. 5846 on Intellectual and Artistic Works.

ACKNOWLEDGMENT

First of all, thanks to Allah for giving me the strength and confidence to achieve my goals. I sincerely wish to express my gratitude to all individuals who in one way or another provided me the help of any kind when conducting this study.

I would like to express my gratitude and appreciation to my supervisor Assoc. Prof. Dr. Musa Ataş, for his academic guidance that he enabled me to work through the thesis and to complete this thesis successfully, Allah bless him.

I would also like to express my profound gratitude to Dr. Firas M. Mustafa for guiding me throughout the study.

My sincere appreciation is extended to senior lecturer Dr. Naseem Yousif Hanna for his continuous support, who worked with me as encouraging advisor. I also appreciate the help of assistant lecturer Mr. Hussein Ahmad Mustafa, at Salahaddin University for his continuous support and instruction regarding the practical side of the study. Last but not least, I would like to thank my family for their generous encouragement.

2019

Sleman Saeed Hassan ALJAF

CONTENTS

| | <u>Page</u> |
|--|-------------|
| ACKNOWLEDGEMENT | iii |
| CONTENTS | iv |
| LIST OF TABLES | vi |
| LIST OF FIGURES | vii |
| ABBREVIATIONS AND SYMBOLS LISTS | ix |
| ÖZET | x |
| ABSTRACT..... | xi |
| 1. INTRODUCTION | 1 |
| 1.1. Digital images Processing..... | 1 |
| 1.2. Wavelet Transformation | 1 |
| 1.2.1. Definition | 1 |
| 1.2.2. Fourier Transform and Short-Time Fourier analysis (STFT)..... | 2 |
| 1.2.3. Comparison between Wavelet Transform and Fourier Transform..... | 2 |
| 1.3. The Theory of Wavelets | 3 |
| 1.4. Continuous Wavelet Transform (CWT) | 5 |
| 1.5. Discrete Wavelet Transform (DWT) | 5 |
| 1.5.1. Discrete Wavelet Transform for One-Dimension Signal (1D DWT)..... | 5 |
| 1.5.2. Discrete Wavelet Transform of Images (Two-Dimension 2D DWT) | 6 |
| 1.5.2.1. Two Dimensions DWT Decomposition (Analysis) Phase | 7 |
| 1.5.2.2. Two Dimensions DWT Reconstruction (Synthesis) Phase | 11 |
| 1.6. The Standard Families of the Filters for the Wavelet Transformation | 14 |
| 1.6.1. Daubechies Filters Family | 14 |
| 1.6.2. Coiflets Filters Family | 15 |
| 1.6.3. Symmetry Filter Family..... | 15 |
| 1.6.4. Biorthogonal Filter Family | 15 |
| 1.6.5. Reverse Biorthogonal Filter Family | 16 |
| 1.7. The Noise | 16 |
| 1.7.1. Additive White Gaussian Noise..... | 16 |
| 1.8. Research Aim..... | 18 |
| 1.9. Objectives of the Study..... | 18 |
| 1.10. Digital Image Denoising | 18 |
| 2. LITERATURE REVIEW | 19 |
| 3. MATERIALS AND METHODS | 23 |
| 3.1. Materials | 23 |
| 3.2. Methods | 23 |
| 3.2.1. Robust Median Estimator | 25 |
| 3.2.2. Peak Signal to Noise Ratio (PSNR)..... | 26 |
| 3.2.3. Threshold Techniques..... | 27 |

| | |
|--|-----------|
| 3.2.3.1. Hard Thresholding Technique | 28 |
| 3.2.3.2. Soft Thresholding Technique..... | 30 |
| 3.2.3.3. Penalized Thresholding Technique..... | 31 |
| 3.2.4. Proposed Method..... | 32 |
| 3.2.4.1. Image Denoising by the Threshold Methods Only..... | 32 |
| 3.2.4.2. Image Denoising with Removing High Frequencies Bands..... | 34 |
| 3.2.4.2.1. Image Denoising with Removing one High Frequencies Bands..... | 34 |
| 3.2.4.2.2. Image Denoising with Removing two High Frequencies Bands..... | 34 |
| 3.2.4.2.3. Image Denoising with Removing all High Frequencies Bands..... | 34 |
| 4. RESULTS..... | 35 |
| 4.1. Experimental Results of Butterfly Image..... | 55 |
| 4.1.1. Results of Butterfly Image Denoising by the Hard Threshold Methods..... | 37 |
| 4.1.2. Results of Butterfly Image Denoising by the Soft Penalized Threshold Methods..... | 40 |
| 4.2. Experimental Results of Lena Image..... | 43 |
| 4.2.1. Results of Lena Image Denoising by the Hard Threshold Methods..... | 43 |
| 4.2.2. Results of Lena Image Denoising by the Soft Penalized Threshold Methods..... | 47 |
| 4.3. Experimental Results of the Camera Image..... | 50 |
| 4.3.1. Results of Camera Image Denoising by the Hard Threshold Methods..... | 50 |
| 4.3.2. Results of Camera Image Denoising by the soft Penalized Threshold Methods..... | 54 |
| 4.4. Experimental Results of the Peppers Image..... | 57 |
| 4.4.1. Results of Peppers Image Denoising by the Hard Threshold Methods..... | 57 |
| 4.4.2. Results of Peppers Image Denoising by the Soft Penalized Threshold Methods..... | 61 |
| 4.5. Comparisons of the Threshold Techniques..... | 64 |
| 5. CONCLUSION AND DISCUSSION..... | 66 |
| 5.1 Results Discussion..... | 66 |
| 5.1.1 Results Discussion for the Hard Threshold Cases..... | 66 |
| 5.1.2 Results Discussion for the Soft Penalized Threshold Cases..... | 68 |
| 5.2 The Conclusion..... | 69 |
| 6. REFERENCES..... | 71 |
| CURRICULUM VITAE..... | 74 |

LIST OF TABLES

| | <u>Page</u> |
|--|-------------|
| Table 3.1. Noise Estimation by Using Robust Median Estimator..... | 25 |
| Table 4.1. The Comparison Between the Hard Threshold, and Soft Penalized Threshold Cases for the Four Test Images with the Noise Sigma =15..... | 64 |
| Table 4.2. The Comparison between the hard Threshold, and Soft Penalized Threshold Cases for the Four Test Images with the Noise Sigma =25..... | 65 |



LIST OF FIGURES

| | <u>Page</u> |
|---|-------------|
| Figure 1. The Time-Frequency Plane Representation for the Fourier Transform and Wavelet Transform..... | 3 |
| Figure 1.2. One-Dimension Discrete Wavelet Transform for a Signal and for two Levels..... | 6 |
| Figure 1.3. The Analysis Phase for one Level 2D Discrete Wavelet Transform..... | 8 |
| Figure 1.4. The Bands for one level 2D DWT Analysis Phase. | 9 |
| Figure 1.5. The Analysis Phase for two Levels 2D Discrete Wavelet Transform..... | 10 |
| Figure 1.6. The Bands for two Levels 2D Discrete Wavelet Transform Analysis phase. | 11 |
| Figure 1.7. The 2D Inverse Discrete Wavelet Transform Synthesis Phase for one level..... | 12 |
| Figure 1.8. The process of the Synthesis Phase for one Level 2D Inverse Discrete Wavelet Transform..... | 13 |
| Figure 1.9. The Graphical of Gaussian Noise Distribution..... | 17 |
| Figure 3.1. The Scheme for the Image Denoising..... | 23 |
| Figure 3.2. The Original Image..... | 24 |
| Figure 3.3. The Bands for Three levels 2D Discrete Wavelet Transform Analysis phase.. | 27 |
| Figure 3.4. The Hard Thresholding Function..... | 29 |
| Figure 3.5. The Soft Threshold Function..... | 31 |
| Figure 3.6. The Flowchart for 1-level Analysis Image Denoising by the Threshold Methods only..... | 33 |
| Figure 3.7. The Flowchart for 1-level Analysis Image Denoising by the Threshold Methods with Removing High Frequencies Bands. | 35 |
| Figure 4.1. The Results of the Butterfly Image with Noise Sigma =15, by Using the Hard Threshold Methods..... | 37 |
| Figure 4.2. The results of the Butterfly Image with Noise Sigma =25, by Using the Hard Threshold Methods..... | 37 |
| Figure 4.3. The Butterfly Image Results with Noise Sigma =15, by Using the Hard Threshold Methods..... | 38 |
| Figure 4.4. The Butterfly Image Results with Noise Sigma =25, by Using the Hard Threshold Methods..... | 39 |
| Figure 4.5. The Results of the Butterfly Image with Noise Sigma =15, by Using the Soft Penalized Threshold Methods..... | 40 |
| Figure 4.6. The Results of the Butterfly Image with Noise Sigma =25, by Using the Soft Penalized Threshold Methods..... | 40 |
| Figure 4.7. The Results of the Butterfly Image with Noise Sigma =15, by Using Soft Penalized Threshold Methods..... | 41 |
| Figure 4.8. The Results of the Butterfly Image with Noise Sigma =25, by Using Soft Penalized Threshold Methods..... | 42 |
| Figure 4.9. The results of the Lena Image with Noise Sigma =15, by Using the Hard Threshold Methods..... | 44 |
| Figure 4.10. The Results of the Lena Image with Noise Sigma = 25, by Using the Hard Threshold Methods..... | 44 |
| Figure 4.11. The Lena Image Results with Noise Sigma =15, by Using the Hard Threshold Methods..... | 45 |
| Figure 4.12. The Lena Image Results with Noise Sigma =25, by using the Hard Threshold Methods..... | 46 |

| | |
|--|----|
| Figure 4.13. The Results of the Lena Image with Noise Sigma = 15, by Using the Soft Penalized Threshold Methods..... | 47 |
| Figure 4.14. The Results of the Lena Image with Noise Sigma = 25, by Using the Soft Penalized Threshold Methods..... | 47 |
| Figure 4.15. The Results of the Lena Image with Noise Sigma =15, by Using Soft Penalized Threshold Methods..... | 48 |
| Figure 4.16. The Results of the Lena Image with Noise Sigma =25, by Using Soft Penalized Threshold Methods..... | 49 |
| Figure 4.17. The Results of the Camera Image with Noise Sigma = 25, by Using the Hard Threshold Methods..... | 51 |
| Figure 4.18. The Results of the Camera Image with Noise Sigma = 25, by Using the Hard Threshold Methods..... | 51 |
| Figure 4.19. The Camera Image Results with Noise Sigma =15, by Using the Hard Threshold Methods..... | 52 |
| Figure 4.20. The Camera Image Results with Noise Sigma =25, by Using the Hard Threshold Methods..... | 53 |
| Figure 4.21. The Results of the Camera Image with Noise Sigma = 15, by Using the Soft Penalized Threshold Methods..... | 54 |
| Figure 4.22. The results of the Camera Image with Noise Sigma = 25, by Using the Soft Penalized Threshold Methods..... | 54 |
| Figure 4.23. The Results of the Camera Image with Noise Sigma =15, by Using Soft Penalized Threshold Methods..... | 55 |
| Figure 4.24. The Results of the Camera Image with Noise Sigma =25, by Using Soft Penalized Threshold Methods..... | 56 |
| Figure 4.25. The Results of the Image of the Pepper With Noise Sigma = 15, by Using the Hard Threshold Methods..... | 58 |
| Figure 4.26. The Results of the Peppers Image with Noise Sigma = 25, by Using the Hard Threshold Methods..... | 58 |
| Figure 4.27. The Peppers Image Results with Noise Sigma =15, by Using the Hard Threshold Methods..... | 59 |
| Figure 4.28. The Peppers Image Results with Noise Sigma =25, by Using the Hard Threshold Methods..... | 60 |
| Figure 4.29. The Results of the Peppers Image with Noise Sigma = 15, by Using the Soft Penalized Threshold Methods..... | 61 |
| Figure 4.30. The Results of the Peppers Image with Noise Sigma = 25, by Using the Soft Penalized Threshold Methods..... | 61 |
| Figure 4.31. The Results of the Peppers Image with Noise Sigma =15, by Using Soft Penalized Threshold Methods..... | 62 |
| Figure 4.32. The Results of the Peppers Image with Noise Sigma =25, by Using Soft Penalized Threshold Methods..... | 63 |

ABBREVIATIONS AND SYMBOLS LIST

| <u>Abbreviation</u> | <u>Explanation</u> |
|----------------------------|---|
| PSNR | : Peak Signal Noise Ratio |
| MSE | : Mean Square Error |
| CWT | : Continuous Wavelet Transform |
| DWT | : Discrete Wavelet Transform |
| IDWT | : Inverse Discrete Wavelet Transform |
| HH | : High-high Subband |
| HL | : High-low Subband |
| LH | : Low-high Subband |
| LL | : Low-low Subband |
| QMF | : Quadrature Mirror Filters |
| <i>Thb</i> | : The Threshold Value for the <i>b</i> Band |
| AWGN | : Additive White Gaussian Noise |
| STFT | : Short-Time Fourier Transform |
| V1 | : The Vertical details band for first analysis level in wavelet |
| H1 | : The Horizontal details band for first analysis level in wavelet |
| D1 | : The Diagonal details band for first analysis level in wavelet |
| rbio | : The Reverse Biorthogonal Wavelets Filter Family |
| bior | : The Biorthogonal Wavelets Filter Family |
| sym | : The Symmetry Wavelets Filter Family |
| coif | : The Coiflets Wavelets Filter Family |
| db | : The Daubechies Wavelets Filter Family |

SYMBOLS

| | <u>Description</u> |
|---------------|--|
| σ_{xy} | : Covariance between X and Y Images |
| σ^2 | : Variance of the Noise. |
| φ | : Scaling Function. |
| ψ | : Wavelet Function. |
| $\eta(x, y)$ | : The Noise of the Additive White Gaussian Noise Type. |
| De | : It is the Denoised Image. |
| U | : It is the Pixel of the Noisy Image. |

ÖZET

YÜKSEK LİSANS TEZİ

ÇOK ÇÖZÜNÜRLÜKLÜ DALGACIK ALANINDA İMGE GÜRÜLTÜ UZAKLAŞTIRMA

Yüksek Lisans Tezi
Sleman Saeed HASSAN ALJAF

Siirt Üniversitesi Fen Bilimleri Enstitüsü
Elektrik-Elektronik Mühendisliği Anabilim Dalı

Danışman: Doç. Dr. Musa ATAŞ

Haziran 2019, 74 sayfa

Günümüzde, gelişen teknoloji ile birlikte dijital görüntü kalitesinde kayda değer iyileştirmeler yaşanmaktadır. Kullanıcının dijital görüntüleri günlük yaşamı kolaylaştıran uygulamalarda kullanarak verimli kararlar alması her zamankinden daha daha kolay ve etkin bir şekilde yapılmaktadır. Dijital görüntüler çoğunluğu donanım kaynaklı olmak üzere çeşitli parazitlere/gürültülere maruz kalmaktadırlar. Dijital görüntülerden parazit giderme adına kullanılan renklendirme teknikleri oldukça önemli bir işlemdir. Görüntülerin kalitesinin artırılmasında ve bu görüntülerin bilgisinin kullanılmasına bağlı uygulamalara uyması için netleştirilmesinde bu teknikler etkili bir şekilde kullanılmaktadır. Bu çalışmada, hem sert hem de yumuşak eşik gürültü temizleme tekniklerinin performansının değerlendirilebilmesi açısından çok çözünürlüklü dalgacık uzayında yüksek frekanslı alt bantların iptal edilmesine ve dalgalanma alanındaki etkisinin ölçülmesine bağlı bazı yeni yaklaşımlar önerilmiştir. Bununla birlikte dijital görüntülerdeki gürültü temizleme yönteminin etkinliğini ölçmek için Ortalama Kare Hata (OKH) ve Tepe Sinyalinin Gürültüye Oranı (TSGO) metrikleri çerçevesinde bir değerlendirme yapılmıştır.

Anahtar kelimeler: Ayrık, Dalgacık, Denoising, Dönüşümü, Eşik, Görüntü, Gürültü, Tepe Sinyali Gürültü Oranı.

ABSTRACT

M.Sc. THESIS

IMAGE DENOISING IN MULTIREOLUTION WAVELET DOMAIN

Sleman Saeed Hassan

**The Graduate School of Natural and Applied Science of Siirt University
The Degree of Master of Science
In Electrical-Electronics Engineering**

Supervisor : Assoc. Prof. Dr. Musa ATAŞ

2019, 74 pages

Today, with the advancing technology, there are significant improvements in digital image quality. It is easier and more efficient than ever to make decisions by using digital images in applications that make everyday life easier. Digital images are subject to various noises, most of which is hardware-based. Coloring techniques used to eliminate noise from digital images are a very important process. These techniques are used effectively to improve the quality of the images and to clarify them to suit the applications associated with the use of the information. In this study, some new approaches have been proposed in order to evaluate the performance of both hard and soft threshold noise cleaning techniques (denoising) due to the cancellation of high frequency subbands in multi-resolution wavelet space and measuring the effect of the ripple field. However, in order to measure the effectiveness of noise removal method in digital images, an evaluation was made within the framework of Mean Square Error (MSE) and Peak Signal to Noise Ratio (PSNR) metrics.

Keywords: Discrete Wavelet Transform, Image Denoising, Mean Square Error Threshold, Noise, Peak Signal To Noise Ratio.

1. INTRODUCTION

In this section, the fundamentals of the wavelet transformation revealed by using filters, the DWT in a multiresolution analysis of the images, also how to apply the soft and hard threshold techniques for the denoising, PSNR, and MSE methods.

1.1. Digital Images Processing

The image processing is the process which applied on the digital images to acquire the desired changes using the digital computer. The changes in the digital image components can be in many fields like image enhancement, the noise removing, improved image details, divide the image and classified into regions to get useful information from it. Nowadays, image processing is one of the most critical technologies. It offers a wide area of research for the researchers in computer science and computer engineering disciplines (Niblack, 1986).

1.2. Wavelet Transformation

1.2.1. Definition

In the early 1980s, Morlet and Grossmann introduced the wavelet mechanism. The word wavelet referred to as small waves, so the small waves originated from the wave propagation, field of time-frequency signal analysis, and the sampling theory. For the analysis of nonstationary signals, by using translation and dilation of the single function called the mother wavelets, then the main idea of using wavelets as a group of constructed functions was introduced first by Morlet. Including audio signals and images as several types of information, the wavelets represent a useful mathematical method that can be used to obtain information from those signals. For analyzing the data thoroughly, a set of wavelets generally needed. The signal with finite energy in the spatial domain as a standard in the modular spatial area can be decomposed by the wavelet transform into a set of the function of orthogonal. Then in the modular spatial domain, the characteristics of the signal can be analyzed (Graps, 1995).

Wavelet transformation provides an excellent platform for many applications that analyze the information available within the signals, where it is difficult to deal with data as it is directly, especially in the case of gray images pixels. The lighting conditions control this value. Also, the local variations of the image intensity play an

essential role. The extent of the objects that want to analyze will affect the size of the neighborhood adapted. The resolution of reference for measuring the local variations of the image will be defined by this size too (Mallat, 1989).

However, the selection of the efficient methods used for the wavelet basis functions computation, and to find the robust method for their definition, can be considered as the main goal of the wavelet transform. The wavelet transform is a time-frequency analysis method with fixed window size and varied shape with time. The principle of the denoising by wavelet transform is that the noise mostly appears as a piece of high-frequency information (Liu et al., 2014).

1.2.2. Fourier Transform and Short-Time Fourier Analysis (STFT)

The mechanism of Fourier analysis was produced in 1807, by Joseph Fourier. The periodic signals can represent through the method of using a series of sine, cosine functions. Even if the signal is not periodically to end its role to infinity, there is a develop implement by produces what is known as “Fourier transform” transfer the signal to the domain of frequency from the domain of time (Mallat, 1989).

In 1946, Fourier transform disadvantage has a solution which reached by Gabor. The windowing of the signal Short-Time Fourier transformation (STFT) which measured as a new mechanism maps the signal into the domain of time and frequency as a two-dimensional function. The STFT is analyzing a small section of the signal at a time. While it produces an amount of information about both sides as when and at what a signal event occurs of the frequencies. Thus, the case when selecting a respective time window size, then all rates have the same window, this considered as the disadvantage of STFT. For more accurately to determine either time or frequency, a variable window size required for many signals (Graps, 1995).

1.2.3. Fourier Transform and Wavelet Transform Comparison

Burrus (2012), the wavelet transform provides a location for both time and frequency, while the Fourier transform acquire the frequencies of the length over the time limit alternatively of viewing how these frequencies modification over time (Newland, 1993). It also shows the interference in both time and frequency which is unavailable in the Fourier transforms (Mallat, 1989). The wavelet transform will be faster than Fourier transform because Fourier transform needs in its most rapid

condition $O(n \log n)$ of mathematics operations, while $O(n)$ of mathematics operations are required for the wavelet transform (Burrus, 2012).

The Fourier transform has circular change whereas the energy concentrates in time and frequency limit by the rules for the wavelet transform. Also, the wavelet transform includes multiresolution in the (time-frequency domain) limit while Fourier transform contains fixed resolution in the (time-frequency domain) limit (Burrus, 2012), as shown in Figure 1.1.

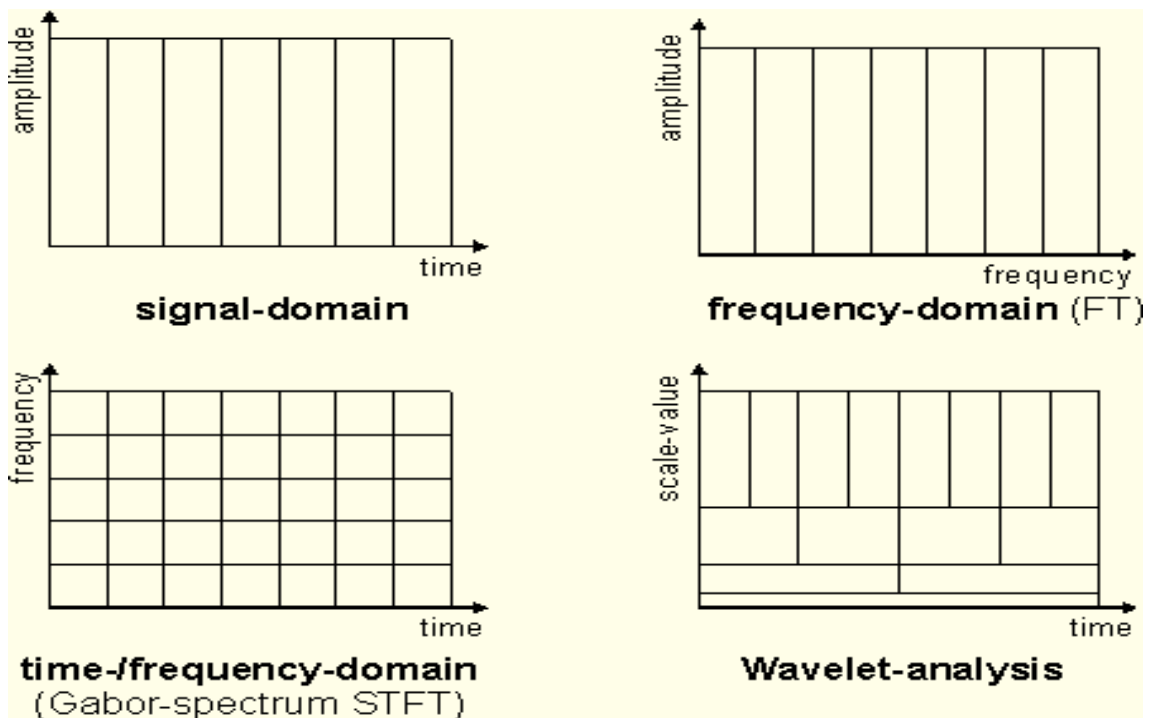


Figure 1.1. The Time-Frequency Plane Representation for the Fourier Transform and Wavelet Transform (Burrus, 2012).

1.3. The Theory of Wavelets

About a century after the introduction of the Fourier Transform, by the French J. Fourier, a German mathematician introduced the first wavelet transform holds his name, Haar. The function for the wavelet basis Haar has small support and integer coefficients. In both of the development of the theory related to the wavelet or towards its application in various fields, different works have been carried out (Toufik and Mokhtar, 2012).

A perfect mathematical tool or technique a wavelet transforms defined. For refining the wavelet definition, Sweldens and Daubechies added the three following characteristics (Burrus, 2012):

- 1) Through using one scaling function or wavelet function and through the scaling and translating operation, a wavelet system generated.
- 2) For representing a signal derived from the original function at many levels, the different weighted sums can be transformed.
- 3) Through the use of filter bank which defined as a system composed of several filters, and with the down-sampling and up-sampling operators, the lower level coefficients generating from, the higher-level coefficients can be achieved (Gomes and Velho, 2015).

The aim of split the signal (or a continuous function in time) into components with various scale can implement by using the wavelet transformation. The wavelet transform considers a proper mathematical technique. The frequency range can be assigned to each component scaled. Every component that has been scaled, then a specific resolution which matches its scale can be used. The signals are known as the daughter wavelets used as copies which scaled and translated of the or fast decaying oscillating waveform or a finite-length signal (known as the "mother wavelet") (Graps, 1995).

$$\psi_{a1,a2}(t) = \frac{1}{\sqrt{|a1|}} \psi \left(\frac{t-a2}{a1} \right), \quad a1, a2 \in \mathbb{R}, a \neq 0 \quad (1.1)$$

ψ : A wavelet functions.

a1: Measures the degree of compression or scale and called a scaling parameter.

a2: It determines the time location of the wavelet and called a translation parameter.

Graps (1995), the advantages for the wavelet transform compared with the Fourier transforms for showing the functions with sharp peaks, and discontinuities. Also for accurately dismantling and rebuilding finite, non-stationary, and a periodic signals. The STFT method developed through wavelet transform by changing the width of the window instead of using a constant width of the window, varying the width of the window is useful to obtain many information frequencies over the wavelet, therefore getting different wavelets frequency depending on the width of the window. The narrow window generates pressed wavelet includes elements of high-frequency (detailed operators), and the large window generates elongate wavelet contains low frequency (approximate operators) (Misiti et al., 1997). The differences with the STFT transform are shown in Figure 1.1, which also shows the plane of time-frequency of the wavelet transform.

1.4. Continuous Wavelet Transform (CWT)

Similar to the STFT, the CWT was analysed, for a certain scale length (a certain width of the window); the window shifted along with the signal, and then the process is repeated for many windows sizes (scales). The treatment process (and the amount of analysis of information that also produced) demands a very long time because of the problem that appeared in the massive number of wavelets arising due to the use of all windows sizes in operation (Misiti et al., 1997).

1.5. Discrete Wavelet Transform (DWT)

Ergen (2012), the decomposition of the signal into frequency bands done by using the discrete wavelet transform, many application areas for signal processing are used the DWT (as an example: the signal analysis or the signal compression). The denoising process is the standard application of DWT, which used to remove the noise that assumed as the small part of the signal. All kind of signals generated from the physical environment have contained more or less noise. Therefore, the wavelet denoising procedure has applied one or two-dimensional signal after, particularly soft or hard threshold methods.

A constant number of scales (discrete samples) used in DWT, resulting in the small quantity of information (by preventing loss important information). That is the central distinction between CWT and DWT. Due to their discrete information, DWT is an individual transformation appropriate on a digital computer application (Gomes and Velho, 2015).

1.5.1. Discrete Wavelet Transform for One-Dimension Signal (1D DWT)

Through using the filter bank, the analysis (Decomposition) of the signal in one dimension discrete wavelet transforms applied, which defined as an amalgamation of a high pass filter (HPF) and low pass filter (LPF), both followed down sampling operator by 2 (Agrawal and Sahu, 2012). For synthesis (reconstruction) signal use inverse one dimension discrete wavelet transforms of the filter bank (Ergen, 2012). In Figure 1.2, $\downarrow 2$ and $\uparrow 2$ refers to down and upsampling operation, respectively.

FL: is the low pass filter used to generate the approximation band of the input signal.

FH: is the high pass filters used to generate the details or its high-frequency bands.

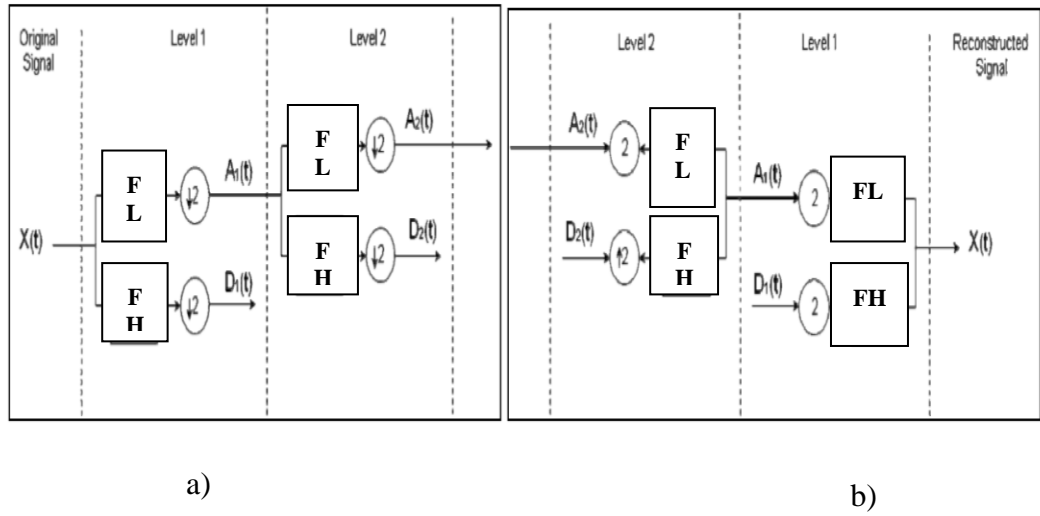


Figure 1.2. One-Dimension Discrete Wavelet Transform for a Signal and for two Levels. (a) The Decomposition. (b) The Reconstruction (Ergen, 2012).

1.5.2. Discrete Wavelet Transform of Images (Two-Dimension 2D DWT)

Gomes and Velho (2015), through using the orthonormal wavelet bases of one-dimensional signals, then the orthonormal wavelet bases of images (two-dimensions) can be constructed. Mallat (1989), developed the multiresolution representation and its relation to wavelets. In 2D DWT the image signal is considered as rows and columns as if they are one-dimensional signals using quadrature mirror filters QMF. The system represents the method of analysis low pass, and high pass filters (FL and FH) is the QMF system, together with their associated synthesis filters (FL' and FH') (Misiti et al., 1997).

So, in the relation of wavelets and QMF: wavelet function is specified by the high pass filter, which also generates the details of the wavelet analysis. The scaling function which is an additional function related with some but not all wavelets is very identical to the wavelet function, but the low pass filters determine it and so is related to the approximations of the wavelet decomposition. In the same convolving and up-sampling the high pass filter generates a form approximating the wavelet function, iteratively convolving, and up-sampling the low pass filter provides a form approximating the scaling function (Misiti et al., 1997).

Three functions as a mother wavelets $\psi_1(x)$, $\psi_2(x)$ and $\psi_3(x)$, with $x = (x_1, x_2) \in \mathbb{R}^2$, are expand by 2^j and translated by $2^j n$ with $n = (n_1, n_2) \in \mathbb{Z}^2$. It produces an

orthonormal basis of the space $L^2(\mathbb{R}^2)$ of finite energy functions $f(x) = f(x_1, x_2)$ (Mallat, 1989):

$$\left\{ \psi_{j,n}^k(x) = \frac{1}{2^j} \psi^k\left(\frac{x-2^j n}{2^j}\right) \right\}_{j \in \mathbb{Z}, n \in \mathbb{Z}^2, 1 \leq k \leq 3} \quad (1.2)$$

The 2D-DWT has two essential phases which they are:

- a) Decomposition (Analysis) Phase.
- b) Reconstruction (Synthesis) Phase.

1.5.2.1. Two Dimensions DWT Decomposition (Analysis) Phase

The first phase for applying the 2D DWT for the images is the analysis phase, which will convert and transform the pixels values from the spatial domain into the wavelet domain. The analysis phase starts by using digital filters and by applying the one-dimensional wavelet transform on the level of the original image and then the process iterative on the levels resulted from the rows' bands (Mallat, 1989).

Inside the original image, each point belongs to the specific row is filtered by a filter set with low pass filter FL, and high pass filter FH, and down sampling by 2. After that, the columns for the result two sub-images are filtered by a filter set with low pass filter FL, and high pass filter FH, then apply the operation of down sampling by 2 (Ismael and Mustafa, 2016). Figure 1.3 shows the analysis phase for one level 2D discrete wavelet transform. Four bands are generated as a result after finishing the steps of this process.

LL1: Called **A1**, or the Approximation band.

LH1: Called **H1**, or the Horizontal details band.

HL1: Called **V1**, or the Vertical details band.

HH1: Called **D1**, or the Diagonal details band.

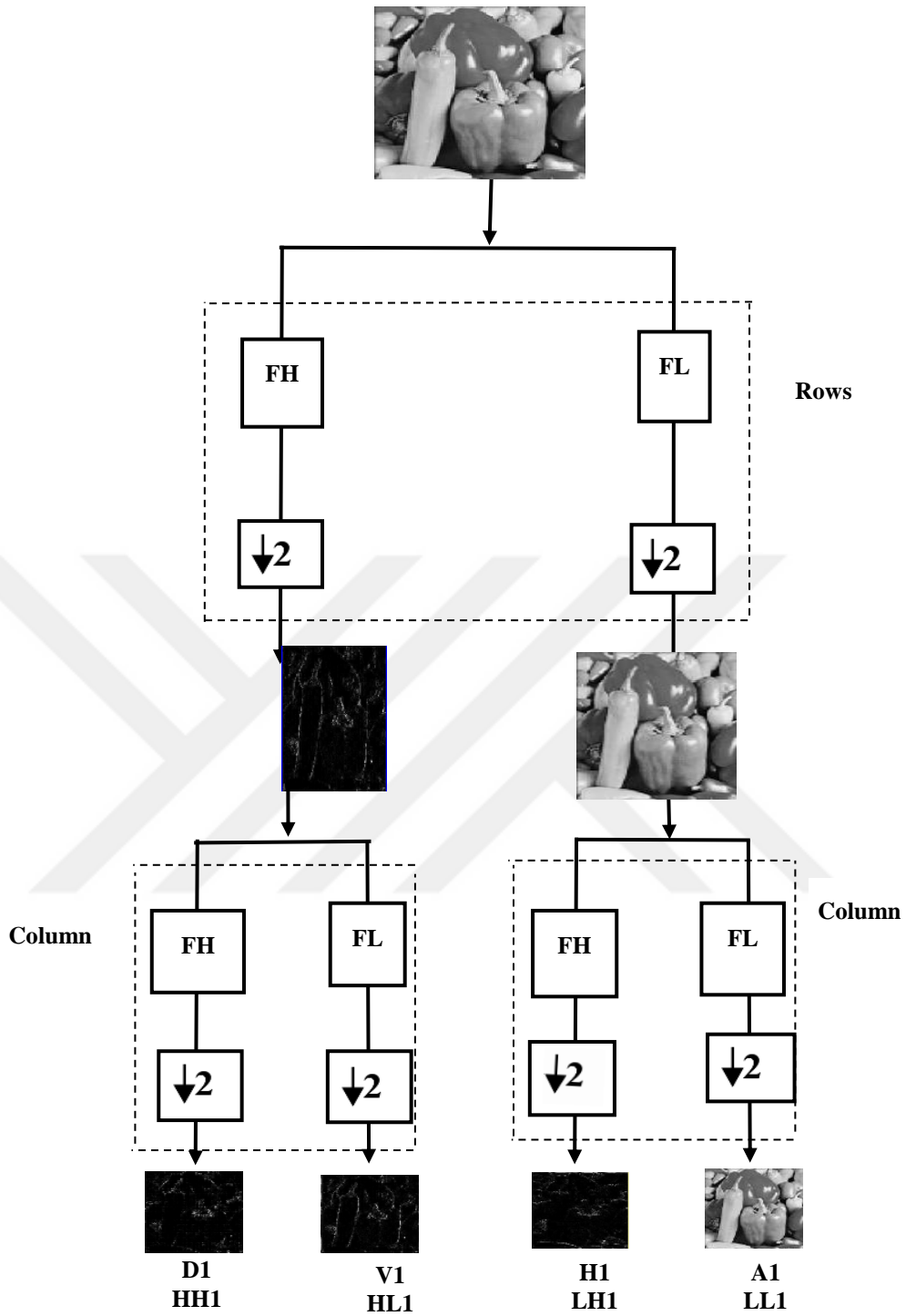


Figure 1.3. The Analysis Phase for One Level 2D Discrete Wavelet Transform.

Each band of the result sub-images of the original image has the quarter size of the original image due to the sub-sampling by 2 after each filtering operation, (Misiti et al., 1997) as Figure 1.4, displays the generated bands for using 2D DWT of one level analysis.

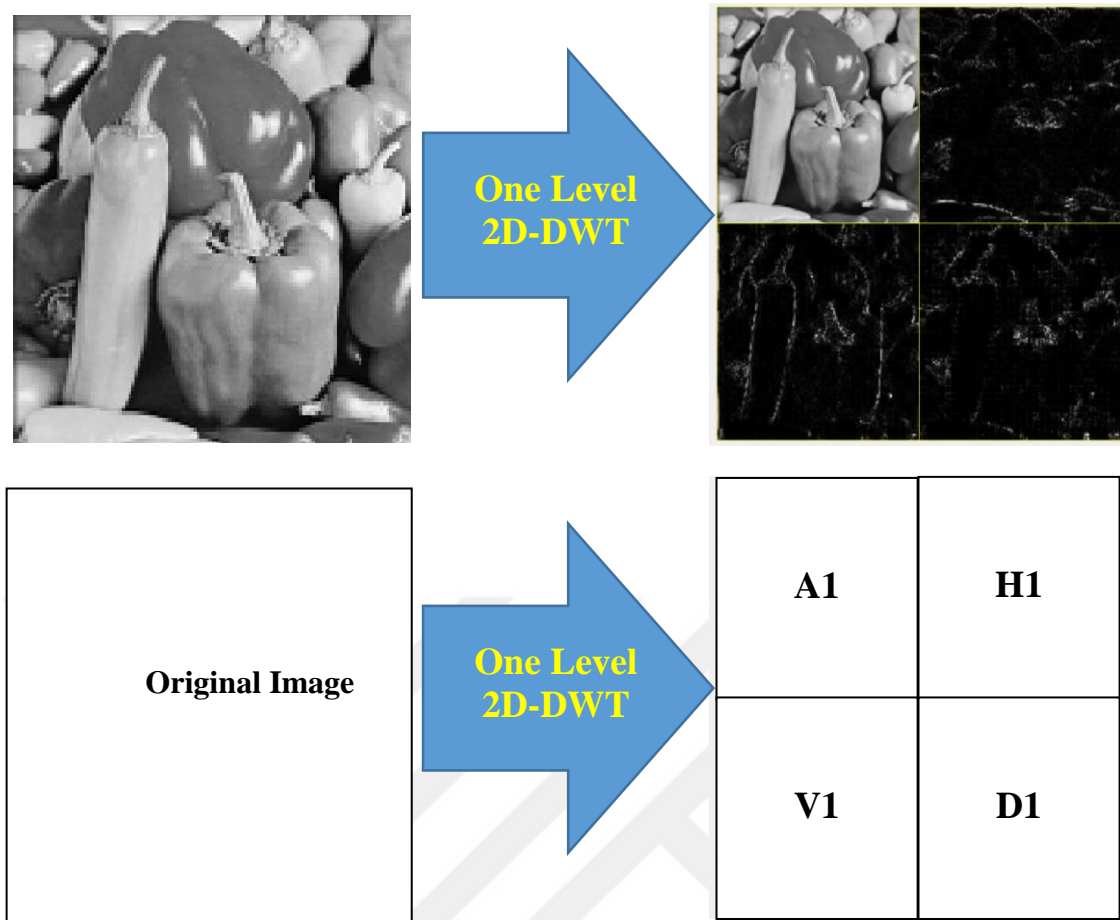


Figure 1.4. The Bands For One Level 2D DWT Analysis Phase.

For the second level of analysis, the approximation band LL1 then analysis to another four sub-bands A2, H2, V2, D2 as Figure 1.5, demonstrates the results as bands of using 2D DWT of two levels of analysis. For more level analysis apply DWT on (An) where n is (1, 2, 3.....n) the number of the analysis level (Ergen, 2012). Figure 1.6, displays the results as bands of using 2D DWT of two levels of analysis.

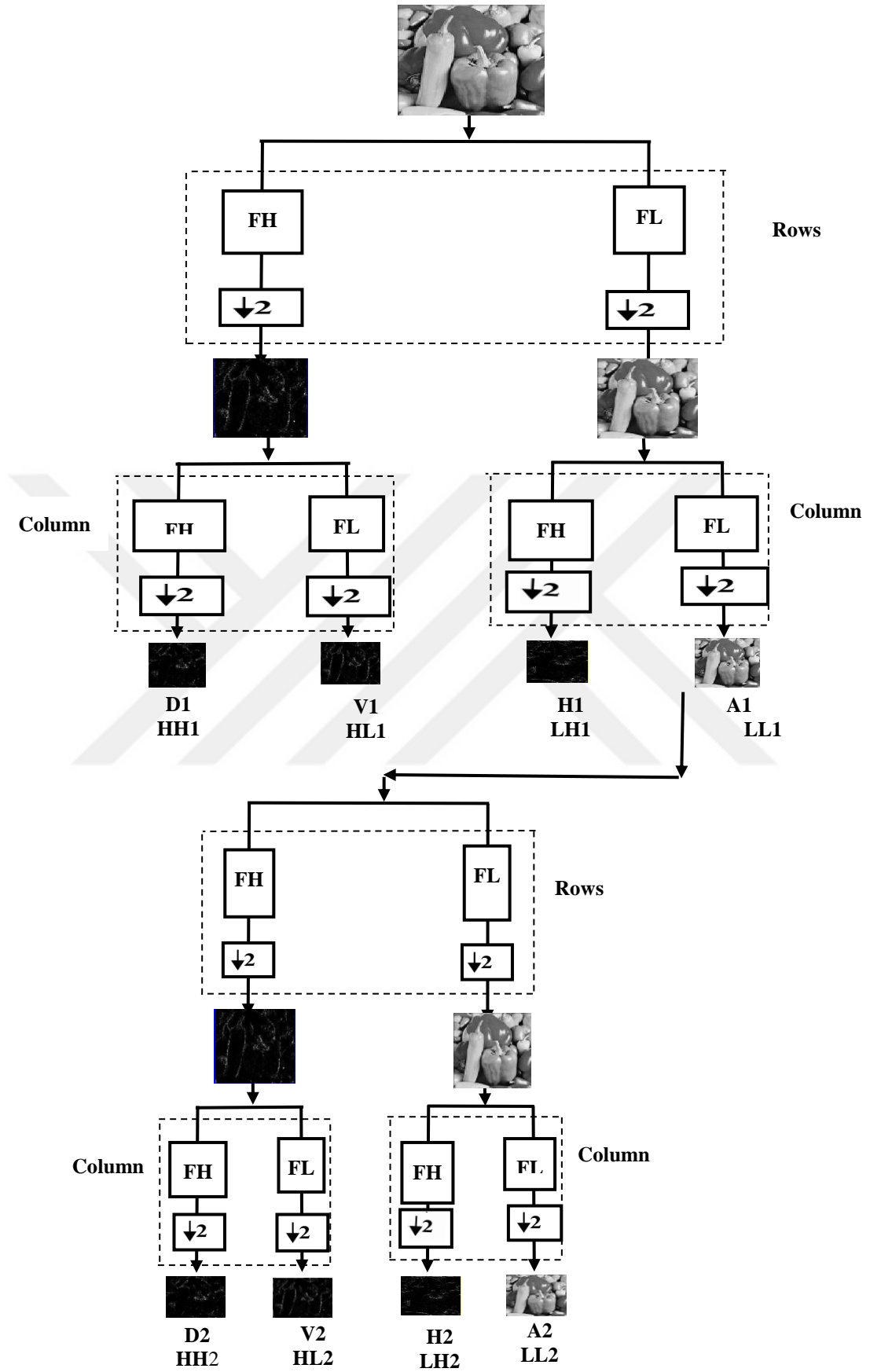


Figure 1.5. The Analysis phase for two levels 2D Discrete Wavelet Transform.

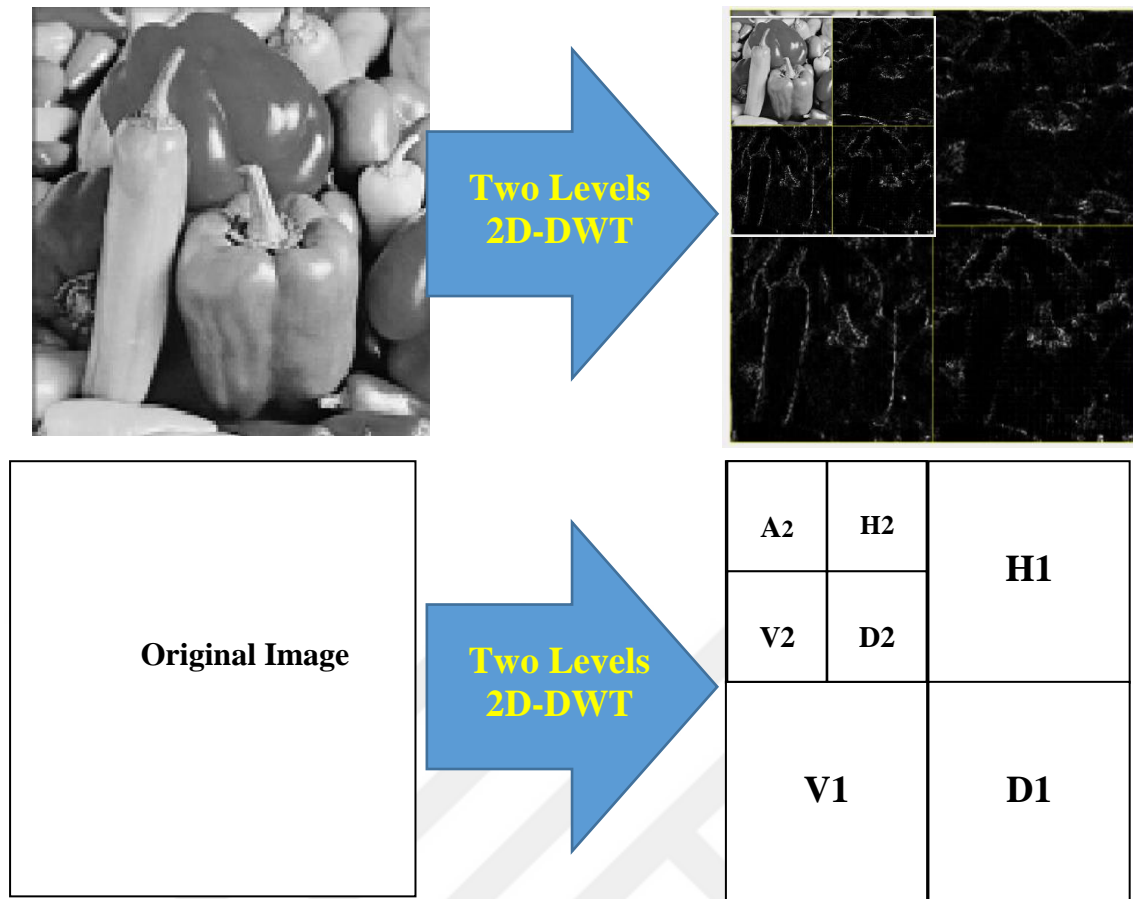


Figure 1.6. The Bands for two Levels 2D Discrete Wavelet Transform Analysis Phase.

The multiresolution representation for the image by using 2D DWT can be implemented with a repeat of the one-dimensional analysis scheme for n times by using the LL band for the current level to generate the four bands for the next level (Ramadhan et al., 2017).

1.5.2.2. Two Dimensions DWT Reconstruction (Synthesis) Phase

The reconstruction of the image from the 2D-DWT bands will be by using the inverse discrete wavelet transforms 2D-IDWT need to be used. With the same concepts like the 2D-DWT, the 2D-IDWT starts from the use of the 1D filter bank which is after applied to the column's values of the image then it has been applied to the values of the row. Figure 1.7 shows the IDWT, and Figure 1.8 shows the synthesis of bands result from 2D IDWT, the (FL) is a low pass filter, (FH) is a high pass filter, $\uparrow 2$ refers to up sampling by 2 (Ergen, 2012).

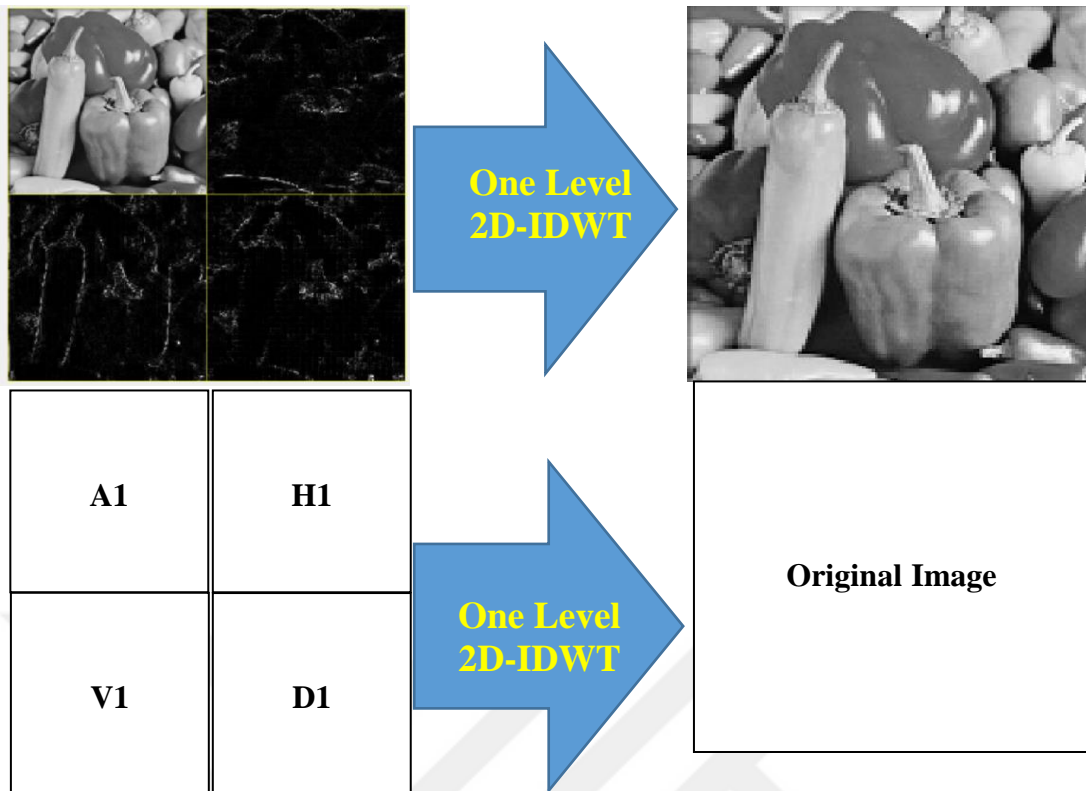


Figure 1.7. The 2D Inverse Discrete Wavelet Transform Synthesis Phase for One Level.

Levicky et al. (1996), the operation of rebuilding the original image from the sub-bands is the inverse of the analysis level where it begins from the final details of the transformation coefficients (Bregovic and Gotchev, 2014). If one analysis level can be assumed, then the formation level will be done as the following:

- a) Every band of the four bands (A, H, V, and D) will be used as an input for the interpolation operation that will be conducted on the racks by inserting a column with the value of zeros between every two rows.
- b) By using the filter bank FH and FL, the operation of the filtering process on the rows resulting from the first step for each of the synthesis bands will be applied and then merging the results. The bands (A, and V) filtered by the filter (FL) and the results collected. While the bands (H, and D) will filter by using the filter (FH), the results obtained are shown in Figure 1.8.
- c) Between every two columns for each band obtained from step (b), a new row that includes zeros will be inserted to implement the conducting of the interpolation operation on the columns.

d) For the bands that are resulting from the step (c), the filter (FL) will be used with the bands (A, V), while the filter (FH) used with the bands (H, D), then the results will be collected as shown in Figure 1.8.

e) The obtaining of the original image done by raising both bands resulting from step (d).

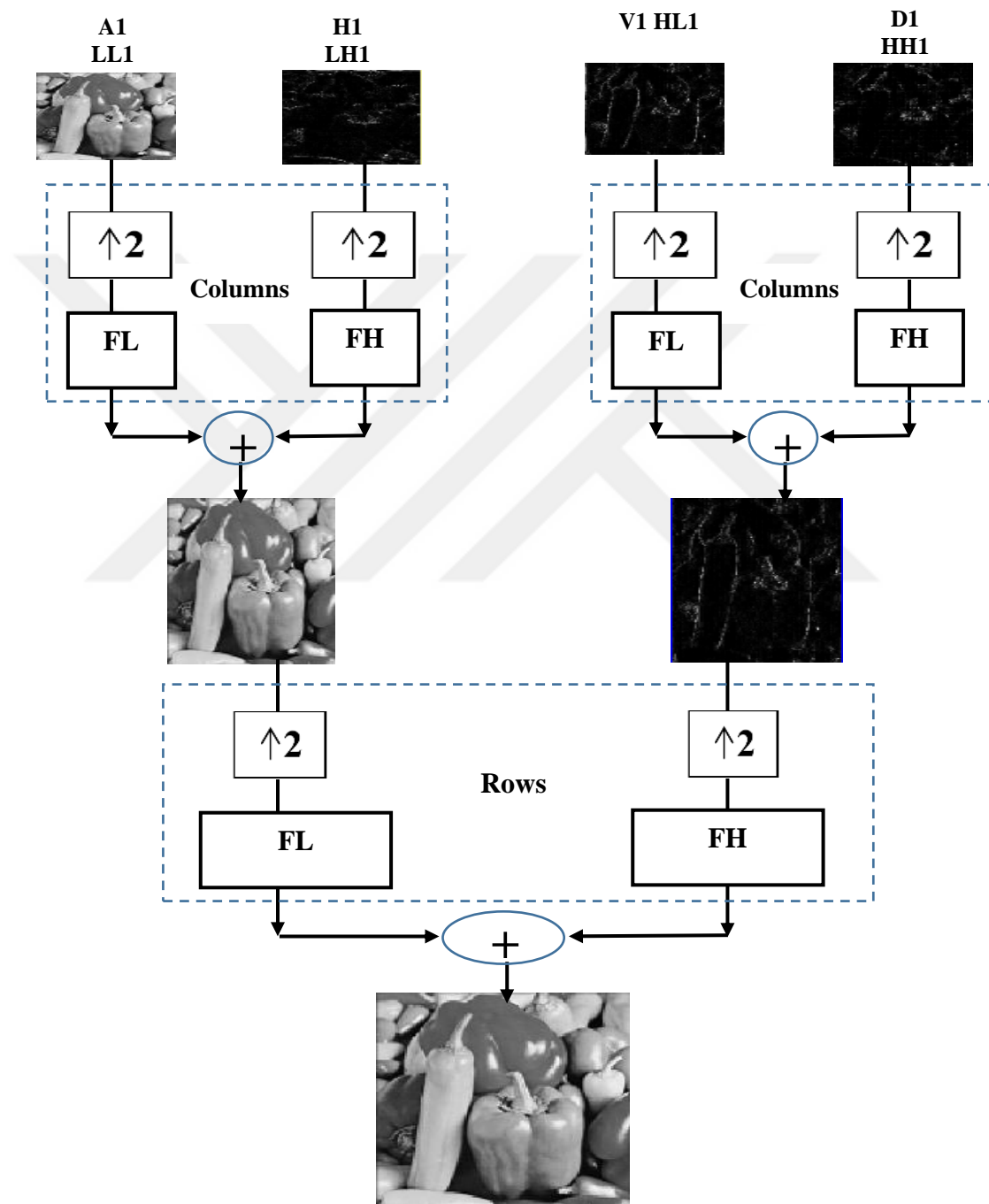


Figure 1.8. The Process of the Synthesis Phase for One Level 2D Inverse Discrete Wavelet Transform.

1.6. The Standard Families of the Filters for the Wavelet Transformation

Misiti et al. (1997), in wavelet analysis, the analysis and synthesis filters bank are considered as the keys opened the way to apply the DWT. The wavelet transform can be implemented by using the filter bank in an easier way than using the scaling function and wavelet function. Now the use and the performance of the wavelet transform depends on the kind of the filter used for the analysis and synthesis process; wavelet transformation has many types of filters classified as families. The wavelet filter families are different in terms of many significant properties (Ismael and Mustafa, 2016):

- Support of the wavelet in the rate of decay and, frequency, and time.
- The reconstruction filters have linear phase.
- Symmetry or antisymmetric of the wavelet.
- A number of vanishing moments. For a large class of signals and images, the increasing of vanishing moments for the wavelets will result in sparse representations.
- The regularity of the wavelet. The smoother wavelets have obtained, the sharper frequency resolution. As well, iterative algorithms for wavelet construction gather faster.
- The presence of a scaling function, ϕ .

In the same regard, Ergen (2012), mentioned that the most familiar wavelets showing the orthogonality attributes are Daubechies, symlets, and coiflets to provide rebuilding using the fast algorithms.

1.6.1. Daubechies Filters Family

Burrus (2012), the compactly supported orthonormal wavelets have been invented by Ingrid Daubechies, and this wavelet makes the DWT practicable. The family of Daubechies wavelets names is signed dbN (where N is the number of vanishing moments). The form of the functions will not be linear in the filters of the Daubechies wavelets family. In this family, the regularity for this filter increases with the increase of the length of the filter, so this family is the vanishing moments for the wavelet function. The Haar wavelet filter which is the same as db1 wavelet is the only orthogonal wavelet with linear phase (Misiti et al., 1997).

1.6.2. Coiflets Filters Family

These candidates named after the researcher Coifman who suggested the idea of obtaining vanishing momentums for the functions ψ , ϕ instead of limiting the vanishing moments to only (ψ) (Ismael and Mustafa, 2016). The vanishing moments also offered by the scaling functions for the Coiflet filters. In $\text{coif}N$, N is the number of vanishing moments for both of the scaling, and wavelet functions. The number of the filter coefficients is used to assign to this filter (Misiti et al, 1997).

These filters are abbreviated as $(\text{coif } N)$, where (N) is the grade for the filters (Al Jumah, 2013). The numbers of vanishing momentums for these filters are $L = 2N-1$. The shape of the function ψ , ϕ are connected with the family of these filters in symmetry (Ismael and Mustafa, 2016).

1.6.3. Symmetry Filter Family

The functions ψ , ϕ filters for this family are close symmetry, which is why it was called Symmetry Filter and is abbreviated as $(\text{Sym } N)$ where N represents the grade of the filters. The grade has connected the length as $\text{Filter Length} = 2N$

This family contains vanishing momentums in the wavelet function. The numbers of momentums connected with the grade of the filter as the following (Al Jumah, 2013). $L_1 = N$ the filter (h) comes close to this family from the linear phase (Ismael and Mustafa, 2016).

1.6.4. Biorthogonal Filter Family

In addition to that, the Biorthogonal wavelets family has the advantage of being more flexible, and it also has most of the properties of the orthogonal wavelet. The number of biorthogonal wavelets is more than orthogonal ones. Because of these properties for the biorthogonal wavelets, they offer possibly a variety of design options and form the category of wavelets most used in practical applications. The biorthogonal wavelets constitute a generalization of the orthogonal wavelet. Biorthogonal wavelets can have symmetry. They are related to perfect decomposition, rebuilding filter banks (Gomes and Velho, 2015). Further argued that under this structure, instead of one orthogonal basis, pair of dual biorthogonal basis functions is used: One for the decomposition step and the other for the composition step (Gomes and Velho, 2015).

However, Misiti et al. (1997), the analysis and synthesis wavelets can have a variable number of vanishing moments and harmony properties. For the analysis, the wavelet with the higher number of vanishing moments can be used and resulting in a dispersed representation, while for the reconstruction, then the smoother wavelet can be used.

1.6.5. Reverse Biorthogonal Filter Family

The biorthogonal wavelet functions are used to generate this family (Reverse Biorthogonal Filter Family). Compactly supported biorthogonal spline wavelets for which symmetry and exact reconstruction are possible with (Misiti et al., 1997).

1.7. The Noise

Noise, in general, can be defined as any unwanted changes to specific data, in the digital image is referred to many types of changes as values that can add to the pixels values. The random modification of color information or brightness in images can be added by the scanner circuit and digital camera, these modifications produced this addition can behold as a noise. Noise produces undesirable effects and is much hard to remove from the digital images without the previously awareness for the model of the noise. Many kinds of noise can found in images. The three common styles of image noise are Speckle noise, Gaussian noise, and Salt & Pepper noise. In many cases, noise in digital images is found to be additive, and with conventional power in the whole bandwidth with Gaussian endurance apportionment, and such noise referred to as Additive White Gaussian Noise (AWGN). The noise with the AWGN type tested in this study for being the most common noises that affect images naturally (Boyat and Joshi, 2015). In the operation of image acquisition and transition, the image will be unavoidably affected by several types of noise, and the impact will minimize the visible effects of the image (Preibisch et al., 2009).

1.7.1. Additive White Gaussian Noise (AWGN)

The noise with the Gaussian type distributes over the signal moderately, that means each pixel in the noisy image is the aggregate of the random noise value of the Gaussian distribution with the real pixel value. The name of the noise AWGN indicates that this style of noise has a Gaussian distribution, which has the probability

distribution function seem to be like the bell shape. Besides, the prospect of showing this style of noise in digital images is more significant than the other kinds of noise, and the noisy image becomes more difficult during image denoising process with Gaussian noise. The additive Gaussian noise (AWGN) is revealed in Figure 1.9, and the equation is given by equation no. 3, as follow (Selami and Fadhil, 2016):

$$\text{Gaussian} = \frac{1}{\sqrt{2\pi\sigma^2}} e^{-\frac{(i-mf)^2}{2\sigma^2}} \quad (1.3)$$

Where:

i = gray level, mf = mean or average of the function, and

σ^2 = variance of the noise.

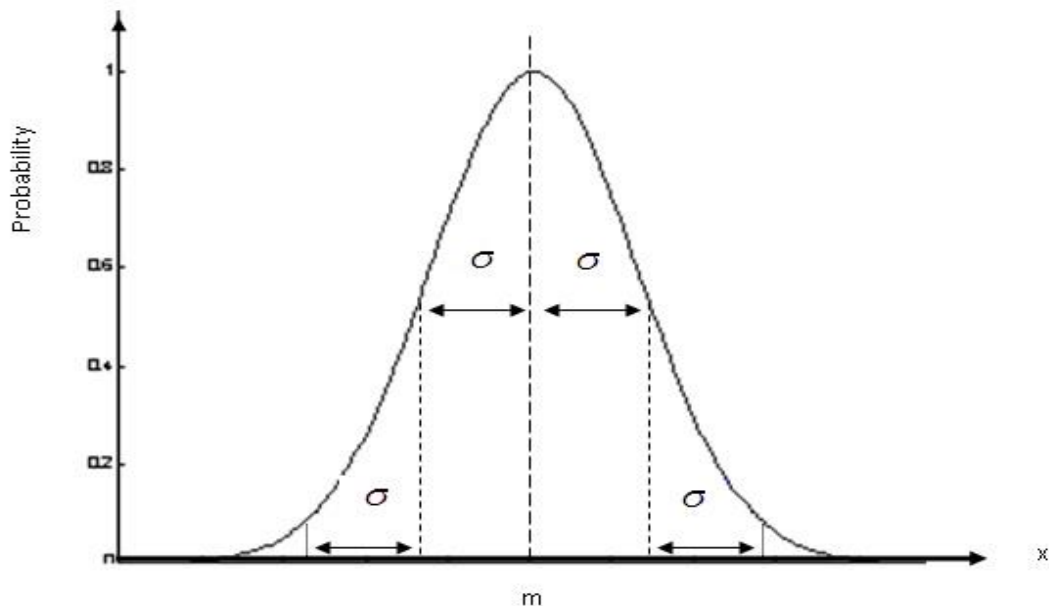


Figure 1.9. The Graphical of Gaussian Noise Distribution (Ismael and Mustafa, 2016).

1.8. Research Aim

This study aims to design a mechanism to remove noise from digital images which can be considered by applying the denoising mechanism. Through a comprehensive study of the theoretical basis for the wavelet transformation, the stage of development, and application of noise removal in the wavelet space and that the noise is reduced as much as possible to the digital image while trying to retain the most significant amount of original data in the image. Also, another aim of this study is to compare the noise-removing mechanisms with several cases with different percentage of the noise by measuring the PSNR criteria.

1.9. Study Objectives

The study was conducted to achieve the following objectives:

- To find out the efficiency of denoising (noise removal) methods by applying each method and with multiresolution analysis inside the wavelet domain by using the PSNR scale.
- To identify the effect and the performance improvement of the system in the case of applying the denoising (noise removal) mechanisms with cases of deletion the high-frequency bands in the wavelet domain.

1.10. Digital Image Denoising

In many applications, the quality of the image will consider the essential factor to decide to use that image to get specific information inside it or not. Noise will make the change and in general, will decrease the quality of the image, so, the operation that can remove as much it can of the noise from the image will be as a critical operation and can play an essential role in this field, this operation is called the denoising method. Image denoising is a significant part of image processing which required in many areas such as Astrophysics, weather forecasting, medical, etc. The essential challenge is to recapture the original image from the noisy image and to decrease the wastage of information due to the noise. The central point of the images denoising calculation is to accomplish both commotion lessening and highlight protection (Mohideen et al., 2018).

2. LITERATURE REVIEW

Mohideen et al. (2018), used the combination of three filters connected in series, and the hybrid filter composed. The hybridization has performed much better in case of the noise, and for most of the medical image type, either MRI, CT, SPECT, Ultra Sound, and for better visualization for the digital image and by applying the image denoising methods an improvement done to the results. PSNR values show a significant increase in comparison of other existing methods. The results obtained from the presented denoising experiments would be tried to be improved further by using this method with other transform domain methods. Also, the findings conclude that the proposed approach in terms of PSNR, improvement is outperformed.

Niblack (1986), an efficient study of image processing and its applications has been presented. By discussing the fundamentals of image processing, one of the critical application was image restoration and image enhancement to reduce noise and recover resolution loss. In which the results are more suitable for demonstration or more digital image analysis by removing the noise, sharpen, or brighten an image, leads to making it easier to distinguish critical properties. A comparative study of the image noise removing methods including the performance measurements for the denoising algorithms, is analyzed quantitatively by the PSNR index. Also, a part of this study was focused on the concept of image denoising, and discussing the hierarchy of image denoising methods.

Pang (2017), identified a new method presented to denoising an image. The 2D Haar wavelet thresholding method is used to implement the analysis of wavelet levels. Besides, a new thresholding function propose which realizes higher denoising performance in terms of the peak signal-to-noise ratio (PSNR) and mean squared error (MSE) than the soft thresholding method. So, at the high noise levels, the proposed new thresholding method outperforms hard thresholding, soft thresholding, and semi-soft thresholding methods. It utilizes the standard deviation values of the subbands to detect if the signal energy is strong or weak in the high-frequency subbands under the 2D Haar wavelet transform. Besides as a conclusion by this work, it will be useful to conduct more study to discover the effect of such prejudice values on the wavelet thresholding results.

Ramadhan et al. (2017), A new method of removing image noise based on using the median filter (MF) in the wavelet domain was proposed and tested, Many kinds of

filters for the wavelet transform used in coupling with the median filter in experimenting with the proposed method to get better results for the process of image noise removing, with the proposed method to get better results for the operation of image noise removing, and thus to select the better appropriate filter. The quality of images produced using the proposed denoising method on the digital images that carried the Gaussian noise compared in terms of PSNR against traditional techniques for the thresholding in 2D DWT and the median filter each alone. According to experimental results, the proposed method presents the higher levels of PSNR for the denoised images. Also, for estimating the noise ratio in the noisy images, the robust median estimator was used.

Ismael and Mustafa (2016), provided a study to implement and measure the performance of wavelet transform in the applications of the image denoising. Several techniques have been studied including (Robust Median Estimator). The quality of many digital images used and reconstructed by these techniques was evaluated for many ratios of the noise also. Through the results, an indication concluded that by using the wavelet transform in image denoising application a good quality as well as provide many other advantages which make it more appropriate for some form such as frequencies splitting, and removing noise in real time. By implementing the denoising algorithms at the wavelet domain, the results showed that the most noise concentrated at the first level of wavelet analysis distributed among the high frequencies bands HH, HL, and HL. The threshold technique used and when the threshold value adaptive for each band in the high-frequency bands can be considered as the primary factor controlling the performance of the denoising algorithm.

Selami and Fadhil (2016), applied for measuring the noise impact on the contours of the digital images, for this aim, many images used and each with carried the noise of the Gaussian noise type to represent the noisy images. Many cases of the mean and variance values were used at each time with the same images to measure several sets of noise parameters. Then, to remove the Gaussian noise, four distinct enhancement filters were utilized. The properties for original images, noisy images, and the denoised images are measured and compared. According to the texture properties, the average denoise filter came up with the superior results, but according to the wavelet-based features, the motion enhancement filter showed the best results.

Boyat and Joshi (2015), Several models of the noise that appeared in digital images have been reviewed and presented by The study classified that noise types can

be distinguished with the help of their original. The models of the noise provided by the probability density function using mean, variance and fundamentally gray levels in digital images. Image denoising is a substantial operation in the digital image processing action. Performing the denoising actions cannot be elaborate without the prior knowledge of the noise type.

Liu (2015), showed that according to the adjusting of wavelet coefficients in the wavelet domain, the wavelet thresholding could be used for noise removing. Then by setting threshold, the noise can be cleared. The denoising results estimate by using the genetic algorithm, and the image denoising can employ by using the wavelet transform. For the new algorithm, two images were used to confirm the validity, and by comparing the standard algorithm with the new algorithm, the results showed that there is an improvement in the values of the SNR by using the new algorithm.

Sontakke and Kulkarni (2015), various types of noises present in digital images and the different sources which are responsible for producing these noises have been we discussed with the various types of filters used to remove these noises.

Preibisch et al. (2009), many basic methods established on wavelet transform for the image denoising and other research techniques were shown. The threshold method in these methods of noise removing was used most widely because it is easy to perform and calculate instantly. However, the criteria used to select the proper threshold based on the environment, and it is still one of the fields oriented future research. In the practical side, both techniques can be used together or use many of the techniques to achieve superior results.

Saxena and Kourav (2014), shows the available denoising methods, such as filtering method, wavelet-based method, and multifractal method, and compare between their performance. Many kinds of noise used including additive and multiplicative types. The selection for the appropriate denoising algorithm depends on the application dependent. Also, to select the suitable denoising algorithm, it is requisite to know the noise type appeared in the image. The wavelet-based method finds applications in denoising images corrupted with Gaussian noise. In the case where the noise properties are involved, the multifractal method can be used. A quantitative mensuration of comparison shows the SNR of the image.

Al Jumah (2013), several wavelets with many threshold methods and measured the parameters such as Mean Square Error (MSE) and Signal-to-Noise Ratio (SNR) have been compared. After comparison, the results for MSE for HAAR global hard

wavelet threshold showed that it is the least between them all. SNR for HAAR SURE shrinks soft level 1 is the higher and the give the best results.

Agrawal and Sahu (2012), an algorithm of removing noise was proposed for denoising the medical image using discrete wavelet transform. The appearance of the noise in biomedical images is a big defy in image processing and analysis. Noise removing methods endeavored to remove the distortion from digital images while maintaining the quality of the image. The efficiency of the wavelet-based thresholding method at several levels with the appearance the random noise and measure the performance of the means of thresholding for many families of the wavelet filters in denoising the Image of a brain Magnetic Resonance, using the PSNR, and the MSE value and Mean Absolute Error estimation operators have been compared.



3. MATERIALS AND METHODS

3.1. Materials

The contents of most digital images can be inserted from smooth regions to the sharpen regions and this why most of the images have non-stationary properties, where the low frequencies regions represented by the smooth areas while the high frequencies regions represented by the sharpening area. The 2D-DWT has been used to obtain these regions of frequencies, where the approximation subband characterizes the low frequencies areas and the three details subbands characterize the high frequencies areas. The wavelet transforms considered as an appropriate tool to be used to study the characteristics of the digital images (Chun Lin, 2010). The following equation can represent the noisy image which contains normal noise of the type called additive white Gaussian noise:

$$R_n(x, y) = R(x, y) + \eta(x, y) \quad (3.1)$$

Where:

$R(x, y)$: It is representing the original image, image with no noise.

$R_n(x, y)$: It is representing the noisy image which means the original image with noise.

$\eta(x, y)$: It is representing the noise of the additive white Gaussian noise type.

The main aim is to obtain a result image that can be similar and near to be the original image $R(x, y)$ from the noisy image $R_n(x, y)$ by applying the noise reduction and to keep the information as much as can be proved by using the denoising method. Figure 3.1 represents the scheme for the image denoising.

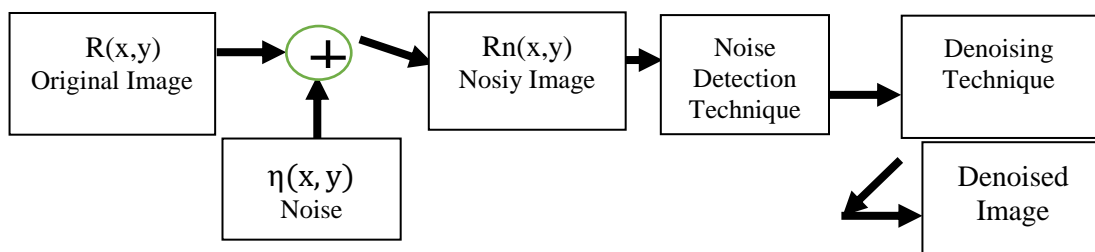


Figure 3.1. The Scheme for the Image Denoising.

Ismael and Mustafa (2016), argued that a wavelet transformation is a perfect tool for image denoising applications because it provides the separation of the frequencies to their respective frequency bands, thus limiting the frequency and ease of handling of these bands. To apply the denoising scheme than the first step which it is the transfer of the image into the domain of the wavelet by using the wavelet transformation and then remove the noise from the high-frequency bands by comparing it with a value called the threshold value. The selection for the threshold value is the second step and the basic point in the operation of the image denoising process. The selection of the threshold type and value play a critical role to remove most noise while maintaining data for the original image and the noise value should be lower than the data value of the original image because the higher the noise the greater the amount of data lost to the original image is also high.

In this study, four digital images were used as original images and each image was with (256 x 256) pixels sized gray color. The noise kind was additive Gaussian noise with zero means ($m = 0$), and the noise with two standard deviation values ($\sigma=15$, $\sigma=25$). Also, two kinds of the thresholding techniques were used in the wavelet domain with eight cases used for each threshold technique related with the four (LL, LH, HL, and HH) subbands in the first analysis level which have been obtained by applying the 2D-DWT to the selected noisy image. Figure 3.2, shows the original digital images which have been used in this study.



Butterfly



Lena



Camera



peppers

Figure: 3.2. Original Images.

3.2. Methods

In this study, eight cases used with each of the two methods of image denoising methods which used depends on the type of threshold techniques with using three-stages of analysis of the 2D-DWT applied to the image to transfer them into the wavelet domain. The algorithms for the proposed cases implemented by using MATLAB language. In this work, the three-level analysis of the wavelet transformation used. At each level, the threshold technique applied to the high frequencies of details bands in the wavelet domain.

3.2.1. Robust Median Estimator

Ramadhan et al. (2017), through the stages of the work mentioned in Figure 10, there is a critical stage before the denoising stage called the "Noise Estimation or noise detection" stage, this stage implemented by using the estimation method that called "Robust Median Estimator". For estimate the noise level inside the images, the noise estimator has been used, where the noisy image it is another copy of the original image however with added noise, by applying the following equation (Ismael and Mustafa, 2016):

$$\sigma = \text{Median} (|b(x,y)|) / kr \quad (3.2)$$

Where: $b(x,y)$: It represents the band (HH1) which is the diagonal subband for the first level analysis 2D-DWT of the image. $kr = 0.6745$.

The results shown in Table 3.1 are obtained by using the function in equation (3.2).

Table 3.1. Noise Estimation by Using Robust Median Estimator.

| Image Name | The standard deviation for the original image | The standard deviation for the noisy image with $\sigma=15$ | The standard deviation for the noisy image with $\sigma=25$ | The estimated noise standard deviation for the noisy image with $\sigma=15$ | The estimated noise standard deviation for the noisy image with $\sigma=25$ |
|------------|---|---|---|---|---|
| camera | 63.3729 | 64.3469 | 65.9484 | 14.6082 | 26.8597 |
| Lena | 48.5943 | 51.2133 | 54.9777 | 16.2917 | 28.8804 |
| Butterfly | 48.0703 | 50.5352 | 54.3618 | 16.8027 | 29.591 |
| peppers | 53.8455 | 56.0944 | 59.2166 | 15.6405 | 27.6837 |

3.2.2. Peak Signal to Noise Ratio (PSNR)

The criteria that used to show the improvement of the image quality due to the denoising was the PSNR, the increase in PSNR value indicate that there are an enhancement and a development for the image details and quality. Also, the PSNR used to measure the amount of congruence and convergence between the recovered image by removing the noise and the original pure image that does not contain noise. The steps and the terms used to calculate the PSNR has been shown by equations (3.3) and (3.4).

$$\text{MSE} = \frac{1}{K.S} \sum_{x=0}^{K-1} \sum_{y=0}^{S-1} [\text{Rd}(x,y) - R(x,y)]^2 \quad (3.3)$$

$$\text{PSNR} = 10. \text{Log} \left(\frac{mx^2}{\text{MSE}} \right) \quad (3.4)$$

Where:

R(x,y): The original image pixel.

Rd(x,y): The denoised image pixel.

K.S: Total number of the pixels inside the image.

mx: The max value of the pixels.

The equation (3.4) is used to calculate the PSNR, but in this equation, the MSE can be seen clearly as an essential part of it, the MSE gives an indication to the difference between the two compared cases which they are here the enhanced image and the image without noise respectively. So, the PSNR depends on the values of the MSE for the two compared images, and the relation between MSE and PSNR is mathematically an inverse relationship. When the difference MSE increased then PSNR will decrease, and vice versa. The lower the MSE, the higher the PSNR value, and this is logically true because the MSE is the value of the difference between the two images.

There are several types of measurements that can be used to measure the difference between two quantities in this case between two images, but because of the need to measure the quality of the image, these measurements MSE and PSNR are appropriate and clear in indicating the increase or decrease the quality of image recovered using denoising techniques.

3.2.3. Threshold Techniques

The role that played by the threshold technique can consider as the central part inside the denoising process, where the purpose is to reduce the noise as much as possible and to keep the original information as much as the method could. Thresholding in the wavelet domain is a simple non-linear method, which processes on one wavelet coefficient at a time. Each coefficient is thresholded by applying the comparing operation versus a threshold which is calculated using shrinkage methods (Abinaya and Amudha, 2015).

There are two primary thresholding methods:

- Hard thresholding.
- Soft thresholding.

For image denoising, soft and hard thresholding methods used. The basis of hard thresholding techniques is the principle of the keep and kill which is introduces artifacts in the images that are denoised while the basis of soft thresholding techniques is the principle of shrink and kill which shrinks the points more significant than the value of the threshold in absolute value to produce the denoised image. The soft thresholding is surpassed over hard thresholding because the soft thresholding reduces the abrupt sharp changes that appear in hard thresholding, and an additional visually delightful image will afford by using the soft thresholding (Anutam, 2014).

The threshold will be calculated in the wavelet domain and for each band of the details bands (High-frequencies bands), and all the analysis levels bands. Each band which belongs to the details bands in wavelet domain has a specific threshold value related to the properties for that band.

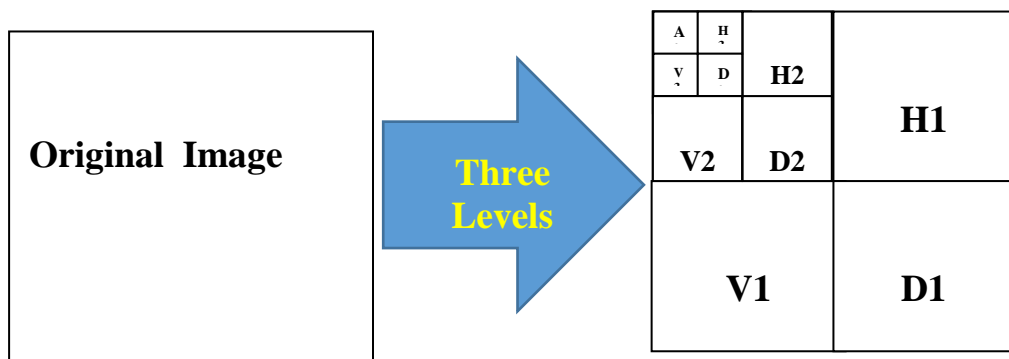


Figure 3.3. The Bands for Three levels 2D Discrete Wavelet Transform Analysis Phase.

In this study, and for each image of the four test images, the 3-levels of the 2D-DWT analysis operations have been used see Figure 3.3. For each band of the 3-levels, a specific threshold value will be calculated using the method that selected to apply on the image to implement the denoising. The threshold will be just for the high frequencies bands (details bands in wavelet domain), and for the 3-levels they are as follows:

After applying the 3-levels of the analysis operation for the 2D-DWT the following bands will be generated and used:

1-The bands for first analysis 2D-DWT level, and the threshold values:

A1: used to generate the bands for the second analysis level of 2D-DWT.

H1: ThH1 used as the threshold for this band.

V1: ThV1 used as the threshold for this band.

D1: ThD1 used as the threshold for this band.

2-The bands for second analysis 2D-DWT level, and the threshold values:

A2: used to generate the bands for the third analysis level of 2D-DWT.

H2: ThH2 used as the threshold for this band.

V2: ThV2 used as the threshold for this band.

D2: ThD2 used as the threshold for this band.

3-The bands for third analysis 2D-DWT level, and the threshold values:

A3: used to reconstruct the second level image by using the of 2D-Inverse DWT.

H3: ThH3 used as the threshold for this band.

V3: ThV3 used as the threshold for this band.

D3: ThD3 used as the threshold for this band.

3.2.3.1. Hard Thresholding Technique

The operator of the hard thresholding is defined as:

$$P(x, y) = \begin{cases} P_n(x, y), & P_n \geq Th_x \\ 0 & , \text{ otherwise} \end{cases} \quad (3.5)$$

Where :

$P_n(x, y)$: The noisy image sub-band pixel value.

$P(x, y)$: The denoised image pixel value.

Th_x : The threshold value.

As Figure 3.4, shows the hard threshold function.

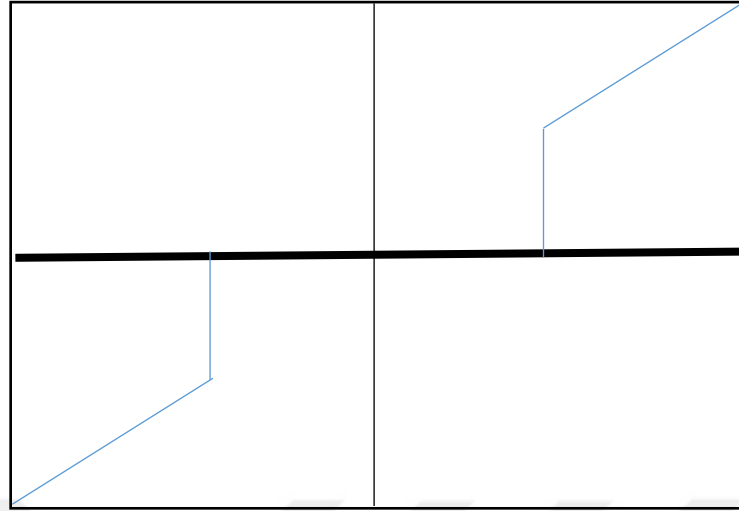


Figure 3.4. The Hard Thresholding Function.

The hard threshold value (Thb) can be calculated by using the following steps:

$$Thb = \frac{\sigma^2}{\sigma_b} \quad (3.6)$$

Where:

σ^2 : Noise level inside the noisy image.

σ_b : The standard deviation for one of these sub-bands (LH, HL, and HH), and can be found by equation (3.7).

$$\sigma = \sqrt{\frac{\sum_{k=0}^{N-1} (q_k - m)^2}{N}} \quad (3.7)$$

Where:

q: is the function for which the standard deviation is calculated.

σ : is the standard deviation for the function q.

m: the Mean.

N: the total elements of the function q.

For each subband, the value for the properties of the uniform threshold will be given by the standard deviation value for the specific subband. The standard deviation of each subband has an inverse relationship affect the threshold value for that subband, and the threshold value has a positive relationship with the standard deviation value of the noisy image. The noise power (σ^2) can compute by using equation (3.3), which represent the estimation method that called (Robust Median Estimator).

The hard threshold for each band from all of the high frequencies bands which generated after applying the 3-levels of the analysis operation for the 2D-DWT can be computed by using equation (3.6).

3.2.3.2. Soft Thresholding Technique

The thresholding method classified as a soft threshold method the operator of the threshold is defined as:

$$De = sgn(U) * \max(0, |Thb|) \quad (3.8)$$

Where:

De: it is the denoised image.

U: it is the pixel of the noisy image.

Thb: it is the threshold value related to the details subband b.

The soft thresholding function is implemented also by the following formula:

$$De = \begin{cases} U - Thb, & \text{if } U \geq Thb \\ U + Thb, & \text{if } U \leq -Thb \\ 0 & , \text{ if } |U| \leq Thb \end{cases} \quad (3.9)$$

Where:

De: it is the denoised image.

U: it is the pixel of the noisy image.

Thb: it is the threshold value related to the details subband b.

The soft threshold for each band from all of the high frequencies bands which generated after applying the 3-levels of the analysis operation for the 2D-DWT can be computed by using equations (3.8). Figure 3.5, shows the soft threshold function. As a soft threshold method, the Penalized threshold has been used in this study.

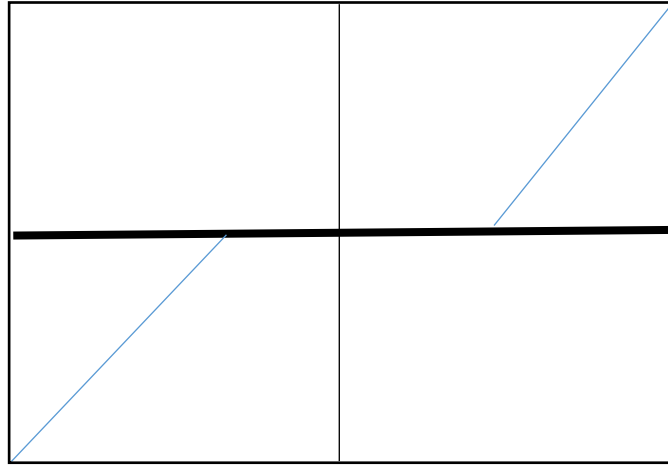


Figure 3.5. The Soft Threshold Function

3.2.3.3. Penalized Thresholding Technique

The Penalized threshold used as a soft threshold method and applied in wavelet domain in this study and for the 3-levels of the 2D-DWT. This is level wise threshold method which is provided by Birge and Massart. In this method the detail coefficients could be sort in descending order then according to equation (3.9), the threshold Thb can be computed as follows (Moghtased Azar and Gholamnia, 2014) :

$$Thb = argt_{min} [- \sum_{k=1}^t d_k^2 + 2\sigma^2 t . (\alpha s + \ln \frac{n}{t})] , t = 1, 2, 3, \dots, n \quad (3.10)$$

Where:

Thb : is the threshold value related to the details subband b .

σ : is the standard deviation of the zero mean Gaussian white noise in denoising model.

αs : is a tuning parameter for the penalty term. It must be a real number greater than 1.

d_k : are the wavelet coefficients sorted in decreasing order of their absolute value.

n : is the number of coefficients in the details subband b .

The sparsity of the wavelet representation of the denoised signal or image grows with αs which it must be a real number greater than 1.

3.2.4. Proposed Method

In this study, the aim is to apply the denoising methods to remove the noise from the images and based on using the thresholding methods in the wavelet domain. The threshold methods which has been used here are covered both hard and soft thresholds techniques. Through using the PSNR measurement to evaluate the threshold method performance.

The proposed idea is to test the effect of resetting the high frequencies bands of the first level for analysis the image by using the 2D-DWT, and each time on one image out of four test images. To evaluate the performance of proposed image denoising algorithm, a Matlab technical programming language is used for writing an image denoising program. With each type of the two methods for the threshold methods, there are eight cases that have been applied on the program and at each case, the result has been recorded.

3.2.4.1. Image Denoising by the Threshold Methods Only

The part of the cases that applied was started by using the pure value of the threshold method without removing any band of the high frequencies' bands, and for 3-levels of the analysis in 2D-DWT. For each kind of the threshold methods, the first case is called the normal hard threshold case for the hard threshold method, and normal Penalized threshold case for the soft threshold method.

By using the steps for the denoising algorithm, 2D-DWT applied to the noisy image and this will transform the noisy image into four subbands for each analysis level. The equations (3.6) and (3.7) are applied to the high frequencies bands respectively to compute the threshold value and applied into each subband for the hard threshold method, and the equations (3.8), and (3.10) are applied to the high frequencies bands respectively to compute the threshold value and applied into each subband for the soft (Penalized) threshold method. Then, the pixel values of each subband are compared with the computed threshold value by using the equation (3.5) for the hard threshold method, and by using the equation (3.9) for the soft threshold method. This process is repeated until all the pixels finished for the selected band.

Figure 3.6, illustrates the steps for image denoising by the threshold methods only for both types hard and soft threshold, and the noisy image for all noise ratios $\sigma=15$ and $\sigma=25$.

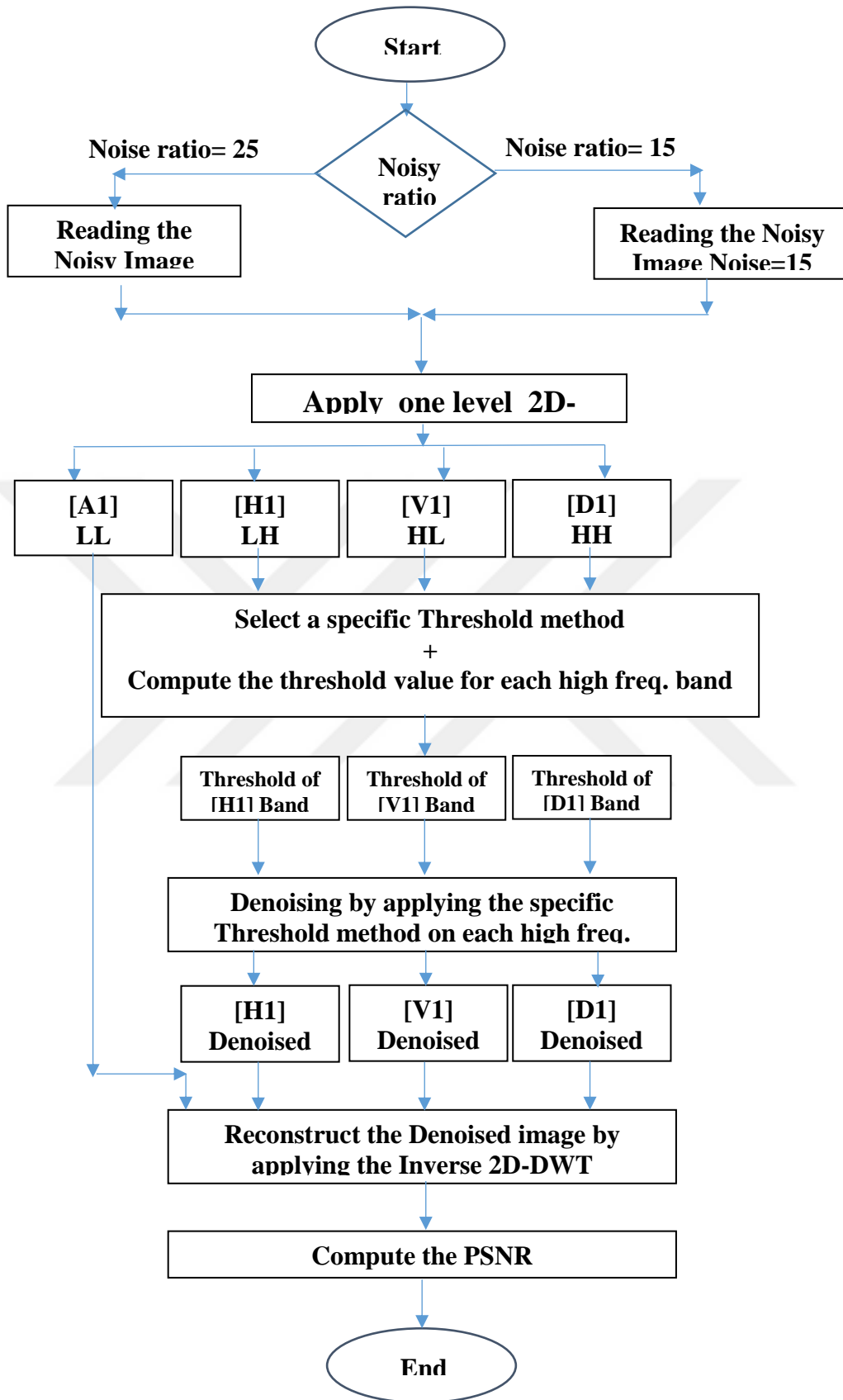


Figure 3.6. The Flowchart for 1-level Analysis Image Denoising by the Threshold Methods Only.

3.2.4.2. Image Denoising with Removing High Frequencies Bands

The method of image denoising with removing high frequencies bands is based on using one of the threshold techniques to be used into the subbands and also by reset (replace each pixel value with zero) one or more of the high frequencies bands. There are seven cases when using the threshold method with removing a specific number of the high frequencies bands, and for this study, only the details bands of the first level of the analysis of 2D-DWT used.

The idea for the removing these bands is because the 2D-DWT splits frequencies into bands and locate the high frequencies into these three details bands. The additive Gaussian noise contains values with small amplitude and high frequency added to the pixels values of the image, and then it will be easier to treat the noise located at that bands especially for the bands belong to the first levels of the 2D-DWT analysis. Figure 3.7, shows the flowchart of all techniques pertains to this method.

3.2.4.2.1. Image Denoising with Removing one High Frequencies Band

In this proposed technique, one band of the high frequencies bands for the first level of 2D-DWT analysis (V1, H1, and D1) removed by replacing all its pixels to the value zero during the denoising operation in the wavelet domain. There are three cases in this technique each related to one of the one band of the high frequencies bands for the first level of 2D-DWT analysis. The same steps implemented into the noisy image for all noise ratios $\sigma=15$ and $\sigma=25$.

3.2.4.2.2. Image Denoising with Removing two High Frequencies Bands

In this proposed technique, two bands of the high frequencies bands for the first level of 2D-DWT analysis removed by replacing all its pixels to the value in the wavelet domain. The same steps implemented into the noisy image for all noise ratios $\sigma=15$ and $\sigma=25$. There are three cases in this technique each related to the case to remove two bands together as follows: H1 with D1, V1 with D1, and V1 with H1.

3.2.4.2.3. Image Denoising with Removing all High Frequencies Bands

In this proposed technique, all of the three high frequencies bands for the first level 2D-DWT analysis (V1, H1, and D1) removed for all noise ratios $\sigma=15$ and $\sigma=25$.

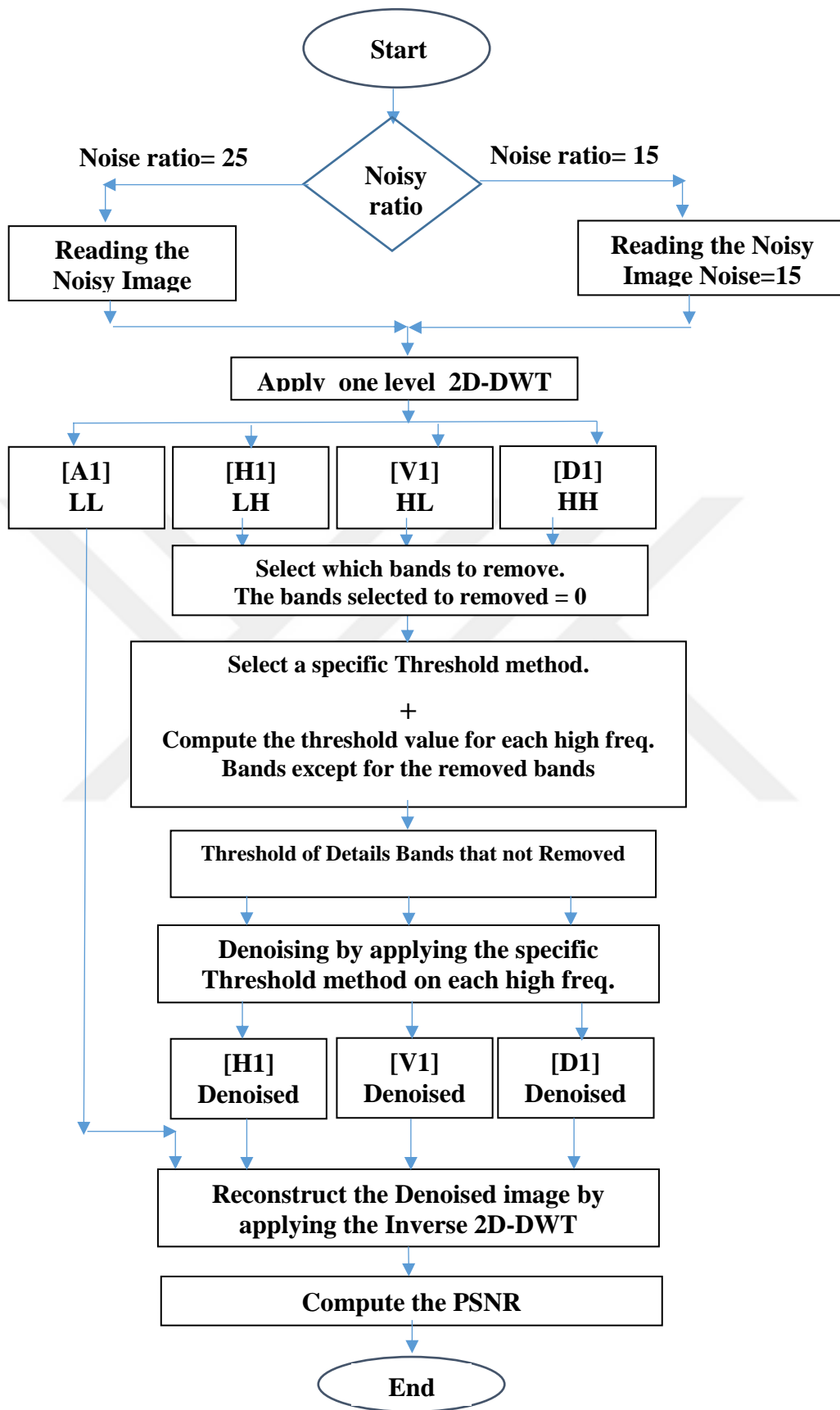


Figure 3.7. The Flowchart for 1-level Analysis Image Denoising by the Threshold Methods with Removing High Frequencies Bands.

4. RESULTS and DISCUSSION

The performance for all the methods has been evaluated by measure the results which are appeared as the PSNR value, the increase in the amount of PSNR indicates an enhancement for the performance related to the quality of the denoised image. Figure 3.6, and Figure 3.7 showed the steps for 1-level od 2D-DWT of both threshold techniques and all the cases belongs to them. The work is done in this study by expanded the actions of the flowcharts to cover the 3-levels of the analysis phase for 2D-DWT. Also, an iteration operation based on select the 2D-DWT filter form the wavelet filters families applied. The wavelet filters families contain about 110 filters and each with the specific threshold method for all the cases for both ratios of the noise in the noisy image $\sigma=15$ and $\sigma=25$.

The Robust Median Estimator has been used in this study and for each image of the four test images to estimate the additive noise ratio appears in the noisy image because the image denoising methods based on both techniques of thresholds need this information to use it in their steps.

4.1. Experimental Results of Butterfly Image

The original Butterfly image without noise showed in Figure 3.2, like an image with size 256x256 pixels gray level with a standard deviation equal to (48.0703). The two ratios of the noise ($\sigma=15$ and $\sigma=25$) with the type Additive Gaussian Noise are added to the original image to generate the two noisy Butterfly images, and the standard deviation becomes (50.5352) and (54.3618) respectively. After applying 2D-DWT for 3-analysis levels.

The image will be transformed into the wavelet domain as ten bands, the approximation band (A3) which contains a shrinking copy to the original image, and nine details bands (H1,V1,D1, H2,V2,D2, H3,V3,and D3) which they are the high frequencies bands. The denoising algorithm needs the value of the noise ratio in each noisy image; the Robust Median Estimator by equation 5, has been used to estimate the noise ratio. The results for the estimation noise ratio for the noisy Butterfly image shown in Table 3.1, and for the two ratios $\sigma=15$ and $\sigma=25$ they were equal to 16.8027, and 29.591 respectively.

4.1.1. Results of Butterfly Image Denoising by the Hard Threshold Methods

In this part, the results for implementing all the cases belong to the denoising the Butterfly image by the hard threshold methods and for the two ratios $\sigma=15$ and $\sigma=25$ are shown in the Figures 4.1, 4.2, 4.3, and 4.4 below.

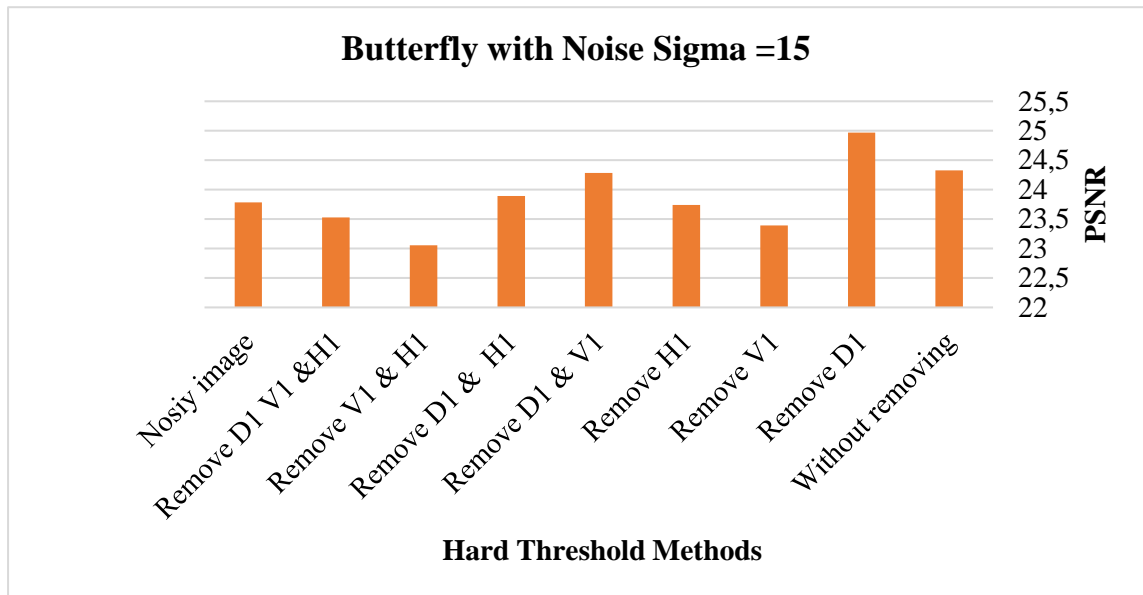


Figure 4.1. The Results of the Butterfly Image With Noise Sigma =15, by Using the Hard Threshold Methods .

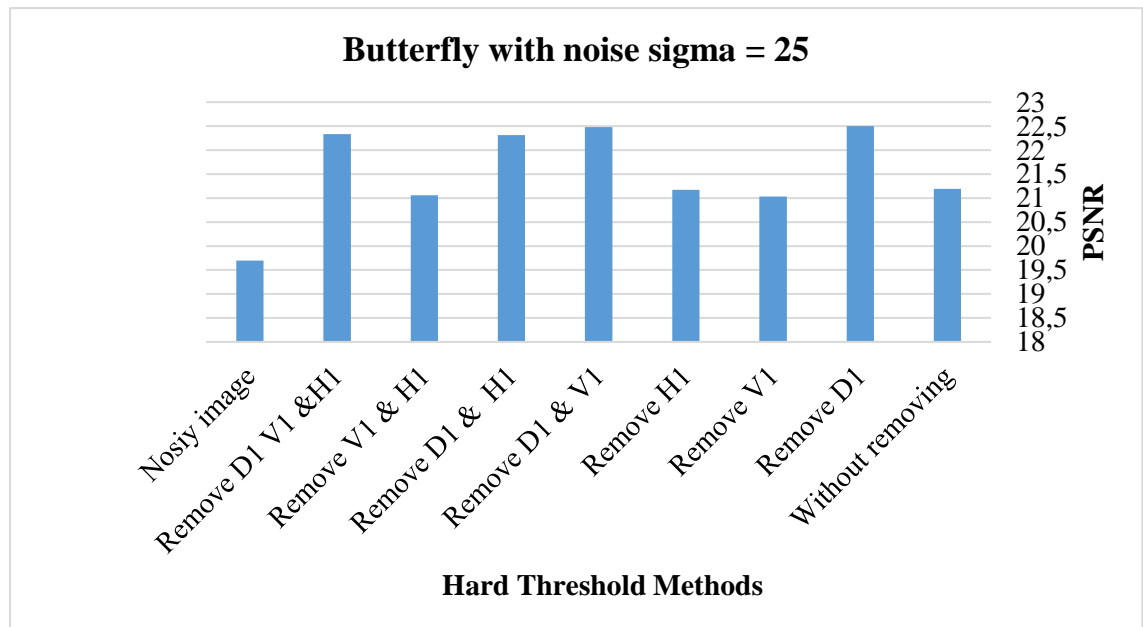


Figure 4.2. The Results of the Butterfly Image With Noise Sigma =25, by Using the Hard Threshold Methods .

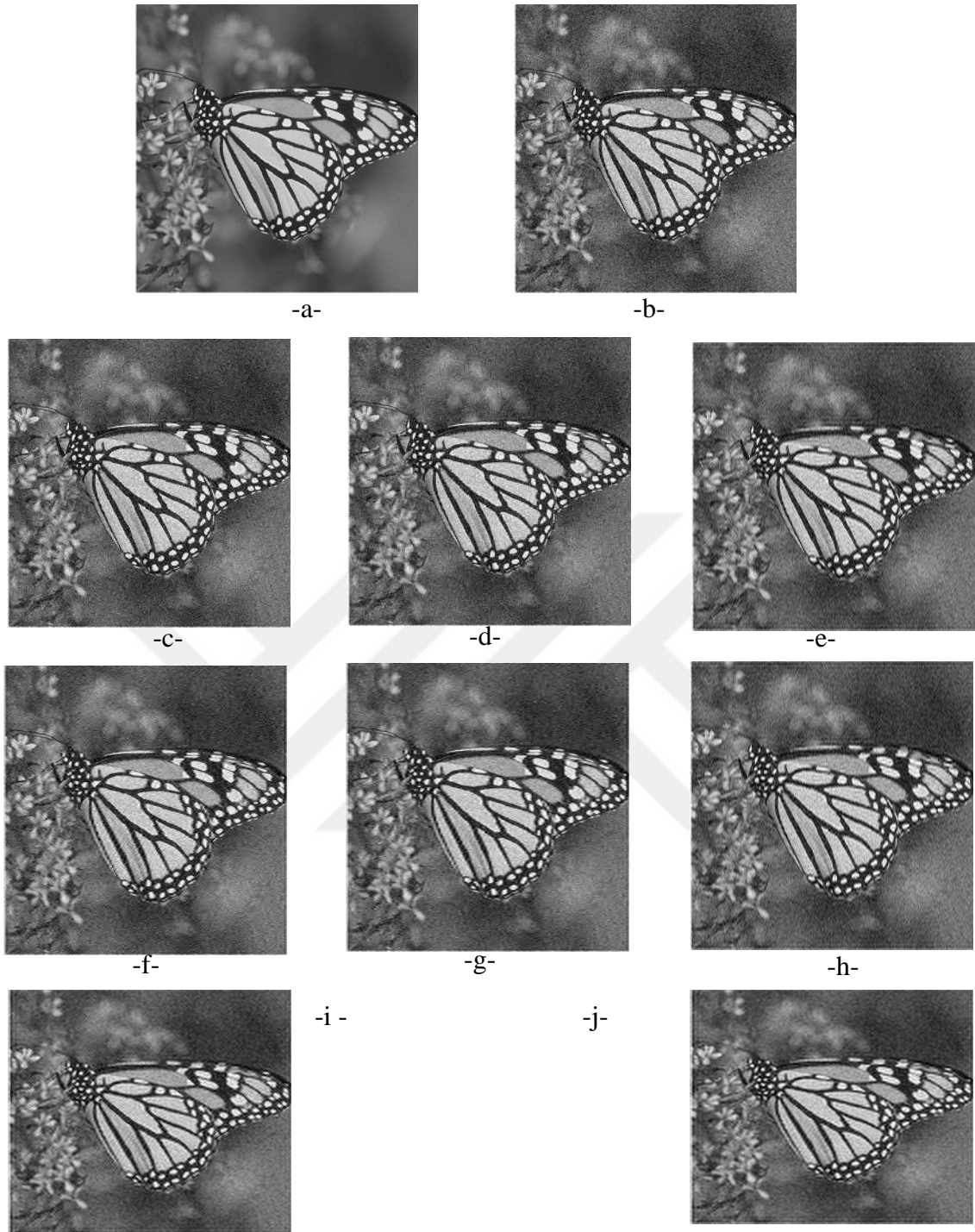


Figure 4.3. The Butterfly Image Results With Noise Sigma =15, by Using the Hard Threshold Methods.

| | | | | | |
|----|-------------------------------|----------------------|----|----------------------------------|----------------------|
| a- | Original image | | b- | Nosiy image | PSNR= 23.781 |
| c- | Hard Threshold | PSNR=24.325, rbio2.8 | d- | Hard Th, with removing D1 | PSNR=24.966, rbio2.8 |
| e- | Hard Th, with removing V1 | PSNR=23.391, db41 | f- | Hard Th, with removing H1 | PSNR=23.738, rbio2.8 |
| g- | Hard Th, with removing D1 &V1 | PSNR=24.285, rbio2.8 | h- | Hard Th, with removing D1&H1 | PSNR=23.892, sym36 |
| i- | Hard Th, with removing V1&H1 | PSNR=23.056, sym25 | j- | Hard Th, with removing D1,V1,&H1 | PSNR=23.528, sym25 |

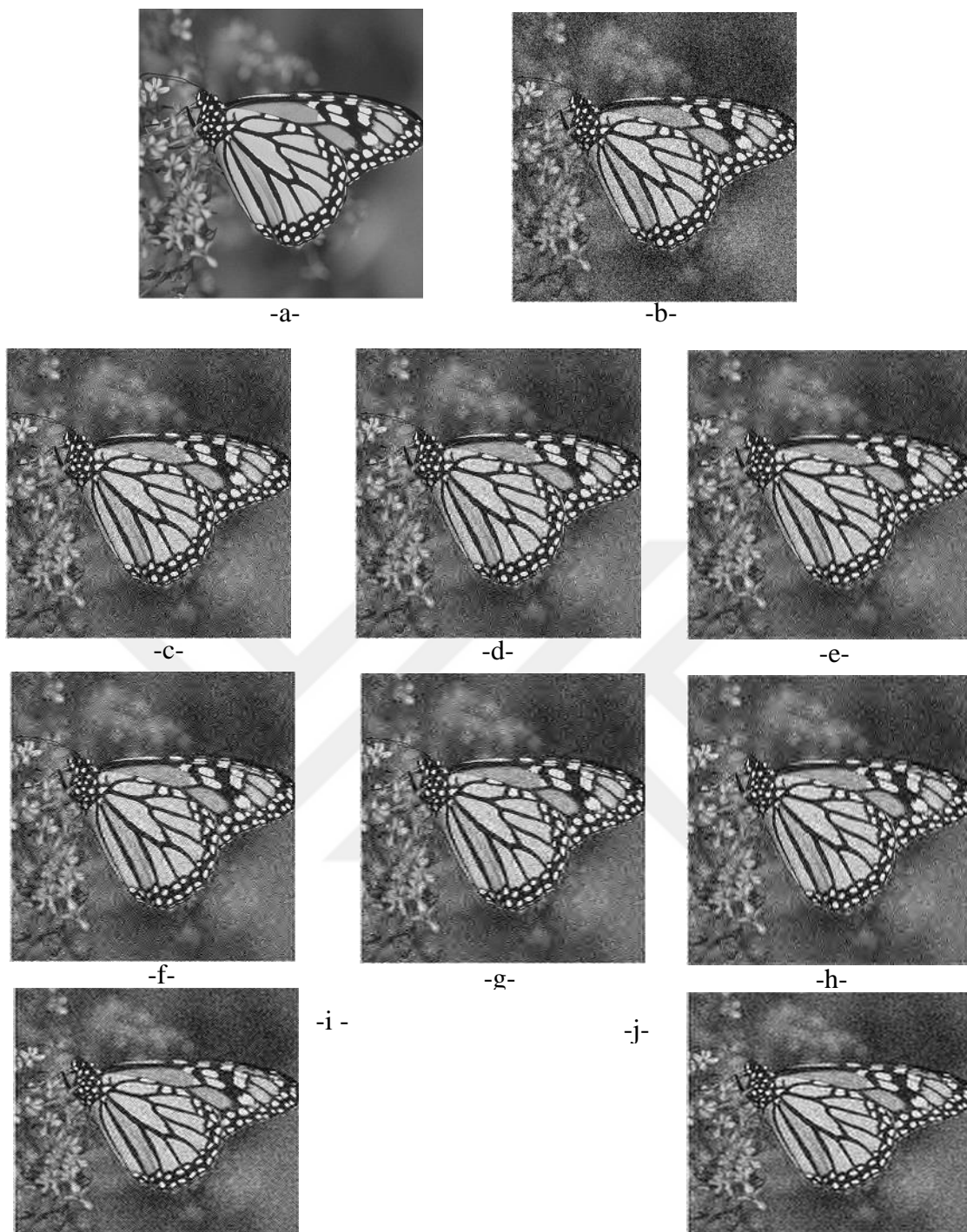


Figure 4.4. The Butterfly Image Results with Noise Sigma =25, by Using the Hard Threshold Methods .

| | | | | | |
|----|------------------------------|----------------------|----|----------------------------------|----------------------|
| a- | Original image | | b- | Nosiy image | PSNR= 19.697 |
| c- | Hard Threshold | PSNR=21.189, rbio2.8 | d- | Hard Th, with removing D1 | PSNR=22.503, rbio2.8 |
| e- | Hard Th, with removing V1 | PSNR=21.033, rbio2.8 | f- | Hard Th, with removing H1 | PSNR=21.173, rbio2.8 |
| g- | Hard Th, with removing D1 | PSNR=22.483, rbio2.8 | h- | Hard Th, with removing D1&H1 | PSNR=22.314, rbio2.8 |
| i- | Hard Th, with removing V1&H1 | PSNR=21.061, sym17 | j- | Hard Th, with removing D1,V1,&H1 | PSNR=22.335, sym29 |

4.1.2. Results of Butterfly Image Denoising by the Soft Penalized Threshold Methods

In this part, the results for implementing all the cases belong to the denoising the Butterfly image by the soft threshold methods and for the two ratios $\sigma=15$ and $\sigma=25$ are shown in the Figures 4.5, 4.6, 4.7, and 4.8 below.

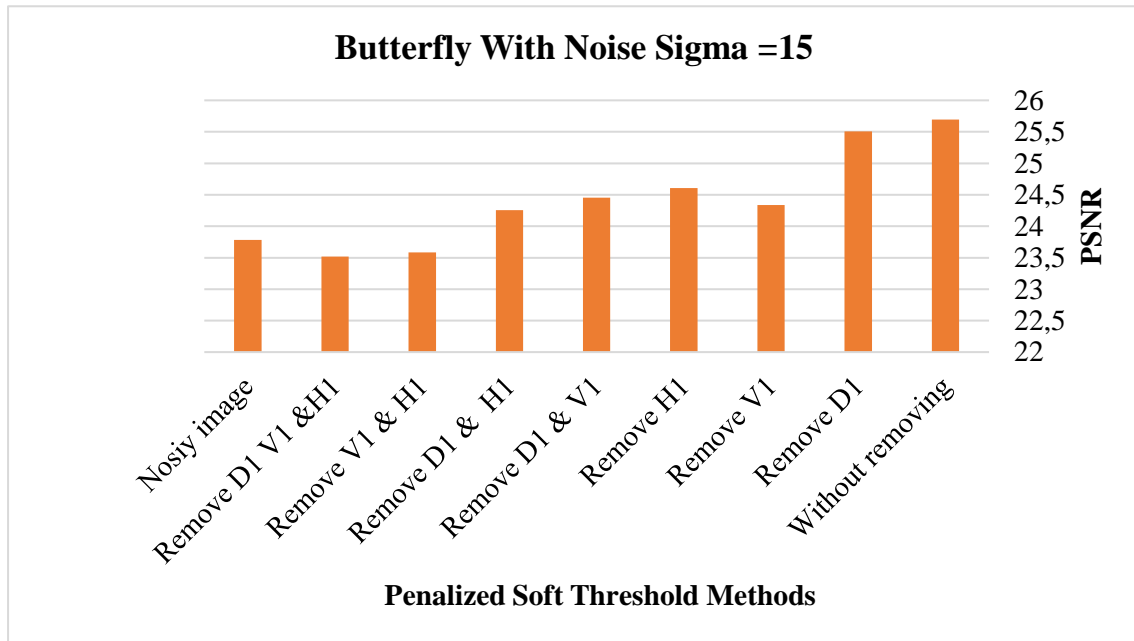


Figure 4.5. The Results of the Butterfly Image with Noise Sigma =15, By Using The Soft Penalized Threshold Methods .

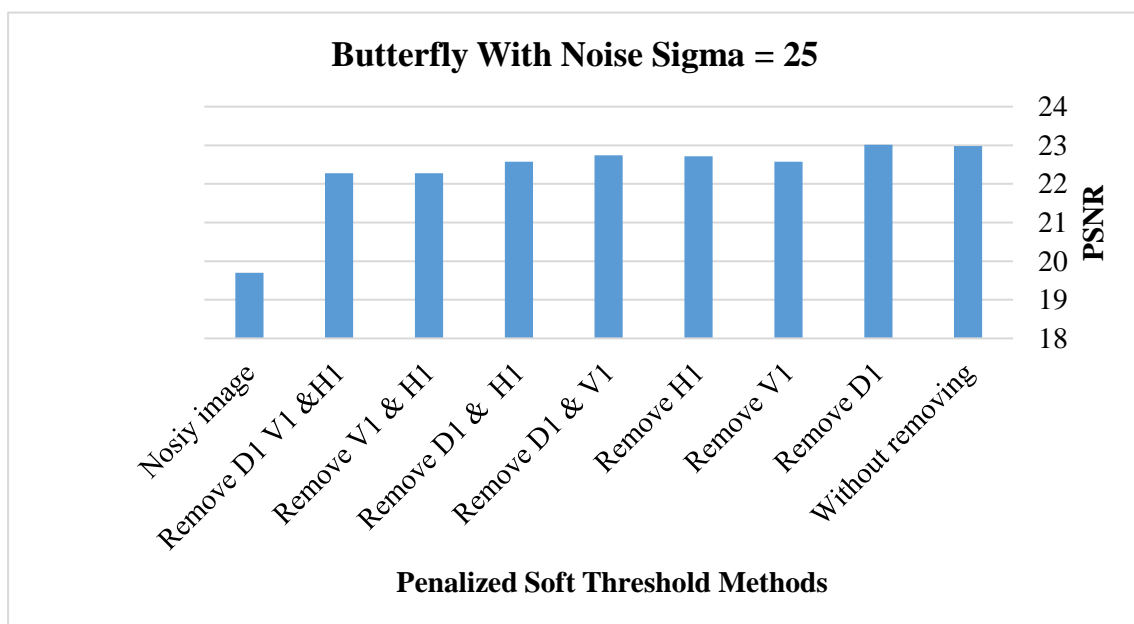


Figure 4.6. The Results of the Butterfly Image with Noise Sigma =25, by Using the Soft Penalized Threshold Methods .

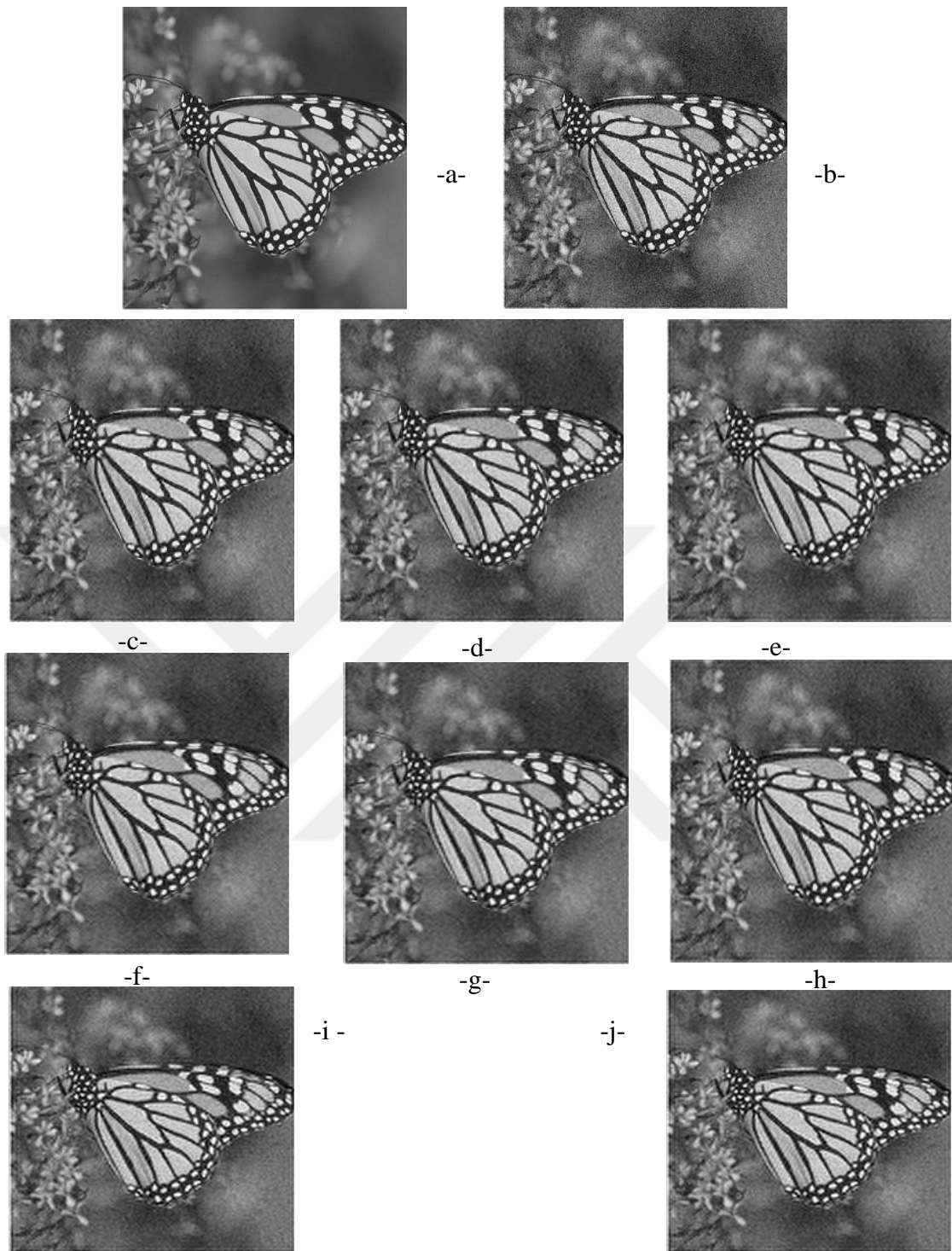


Figure 4.7. The Results of the Butterfly Image with Noise Sigma =15, by Using Soft Penalized Threshold Methods

| | | | | | |
|----|-----------------------------------|-------------------------|----|-------------------------------------|----------------------|
| a- | Original image | | b- | Nosiy image | PSNR= 23.781 |
| c- | Hard Threshold | PSNR=25.696, bior3.9 | d- | Hard Th, with removing D1 | PSNR=25.506, bior3.9 |
| e- | Hard Th, with removing V1 | PSNR=24.334, sym35 | f- | Hard Th, with removing H1 | PSNR=24.604, bior3.9 |
| g- | Hard Th, with removing D1 & V1 | PSNR=24.452, bior3.9 | h- | Hard Th, with removing D1&H1 | PSNR=24.255, sym35 |
| i- | Hard Th, with removing V1&H1 | PSNR=23.584, sym25 | j- | Hard Th, with removing D1,V1,&H1 | PSNR=23.516, sym25 |

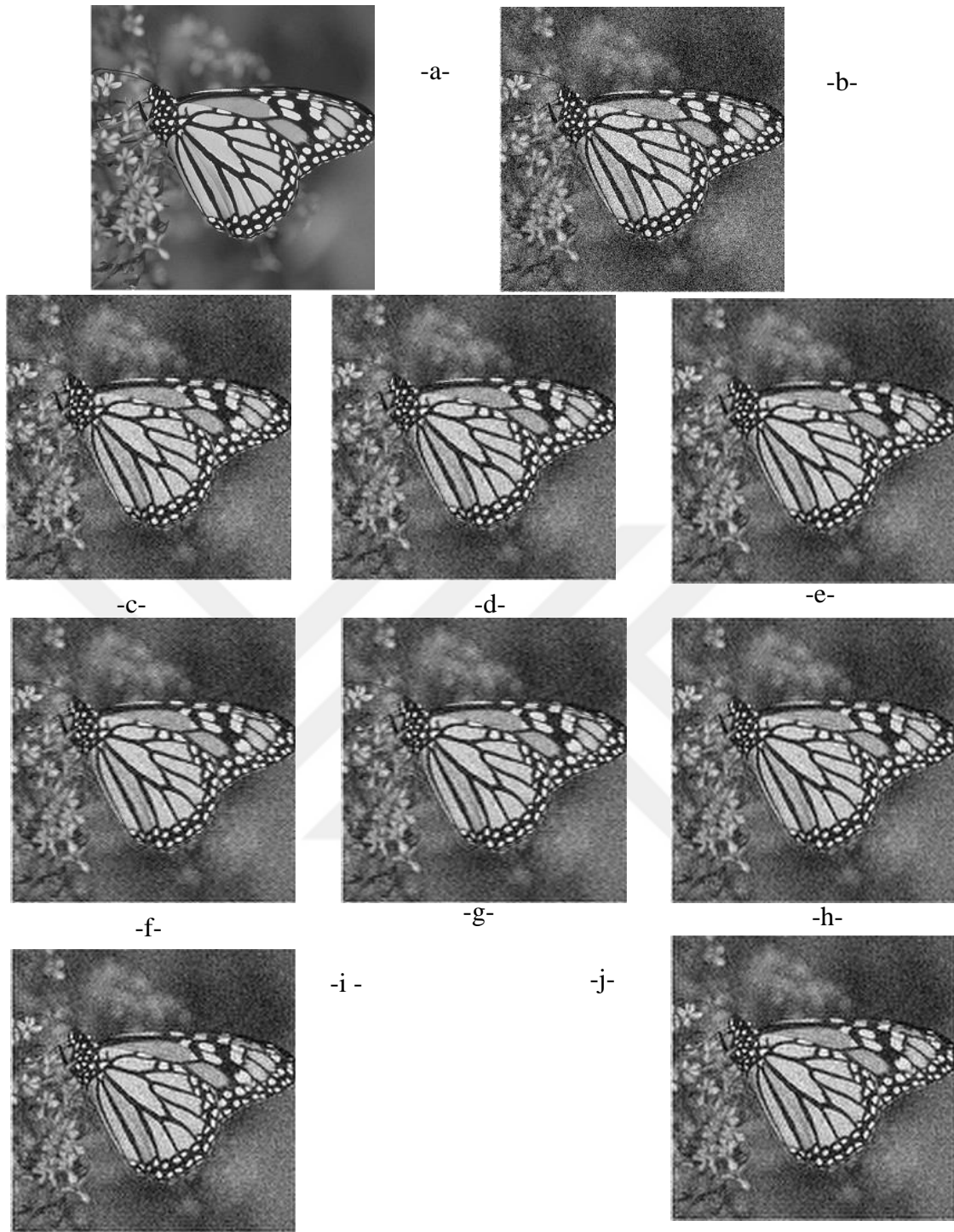


Figure 4.8. The Results of the Butterfly Image with Noise Sigma =25, by Using Soft Penalized Threshold Methods

| | | | | | |
|----|--------------------------------|----------------------|----|----------------------------------|-----------------------|
| a- | Original image | | b- | Nosiy image | PSNR= 19.697 |
| c- | Hard Threshold | PSNR=22.982, bior3.9 | d- | Hard Th, with removing D1 | PSNR=23.0123, bior3.9 |
| e- | Hard Th, with removing V1 | PSNR=22.576, sym36 | f- | Hard Th, with removing H1 | PSNR=22.716, bior3.7 |
| g- | Hard Th, with removing D1 & V1 | PSNR=22.738, bior3.9 | h- | Hard Th, with removing D1&H1 | PSNR=22.574, sym36 |
| i- | Hard Th, with removing V1&H1 | PSNR=22.279, sym29 | j- | Hard Th, with removing D1,V1,&H1 | PSNR=22.275, sym29 |

4.2. Experimental Results of Lena Image

The original Lena image without noise showed in Figure 3.2, like an image with size 256x256 pixels gray level with a standard deviation equal to (48.5943). The two ratios of the noise ($\sigma=15$ and $\sigma=25$) with the type Additive Gaussian Noise are added to the original image to generate the two noisy images, and the standard deviation become (51.2133) and (54.9777) respectively. After applying 2D-DWT for 3-analysis levels, the image will be transformed into the wavelet domain as ten bands, the approximation band (A3) which contains a shrinking copy to the original image, and nine details bands (H1,V1,D1, H2,V2,D2, H3,V3,and D3) which they are the high frequencies bands.

The denoising algorithm needs the value of the noise ratio in each noisy image; the Robust Median Estimator by equation 5, has been used to estimate the noise ratio. The results for the estimation noise ratio for the noisy Lena image shown in Table 3.1, and for the two ratios $\sigma=15$ and $\sigma=25$ they were equal to 16.2917, and 28.8804 respectively.

4.2.1. Results of Lena Image Denoising by the Hard Threshold Methods

In this part, the results for implementing all the cases belong to the denoising the Lena image by the hard threshold methods and for the two ratios $\sigma=15$ and $\sigma=25$ are shown in the Figures 4.9, 4.10, 4.11 and 4.12 below.

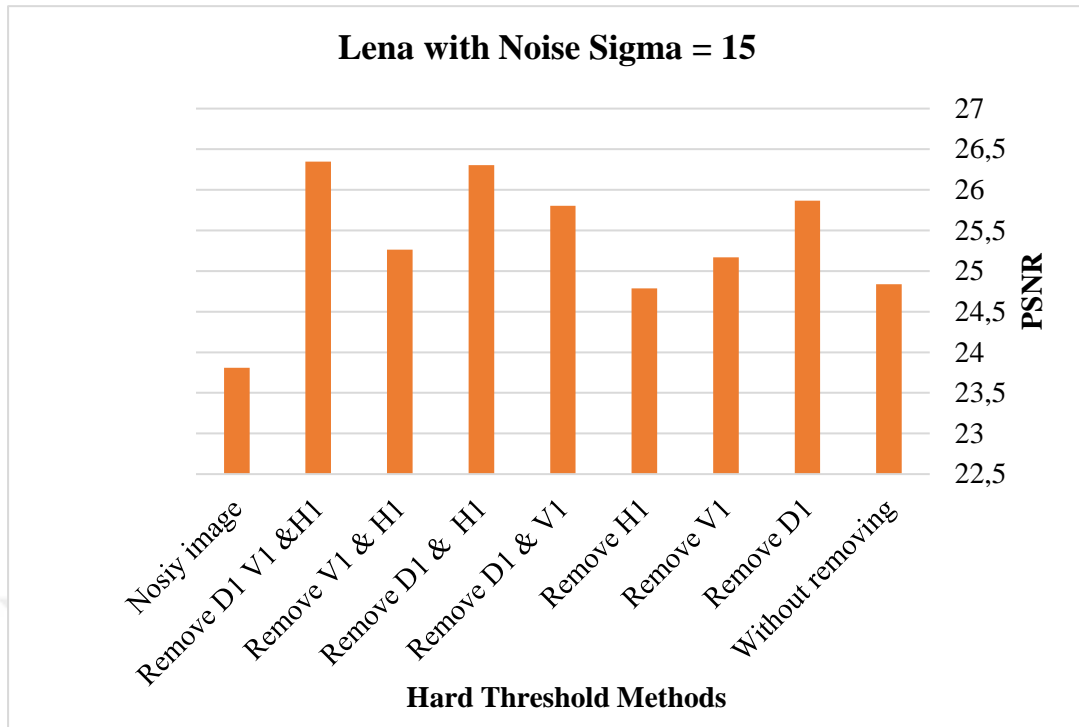


Figure 4.9. The Results of the Lena Image with Noise Sigma =15, by Using the Hard Threshold Methods.

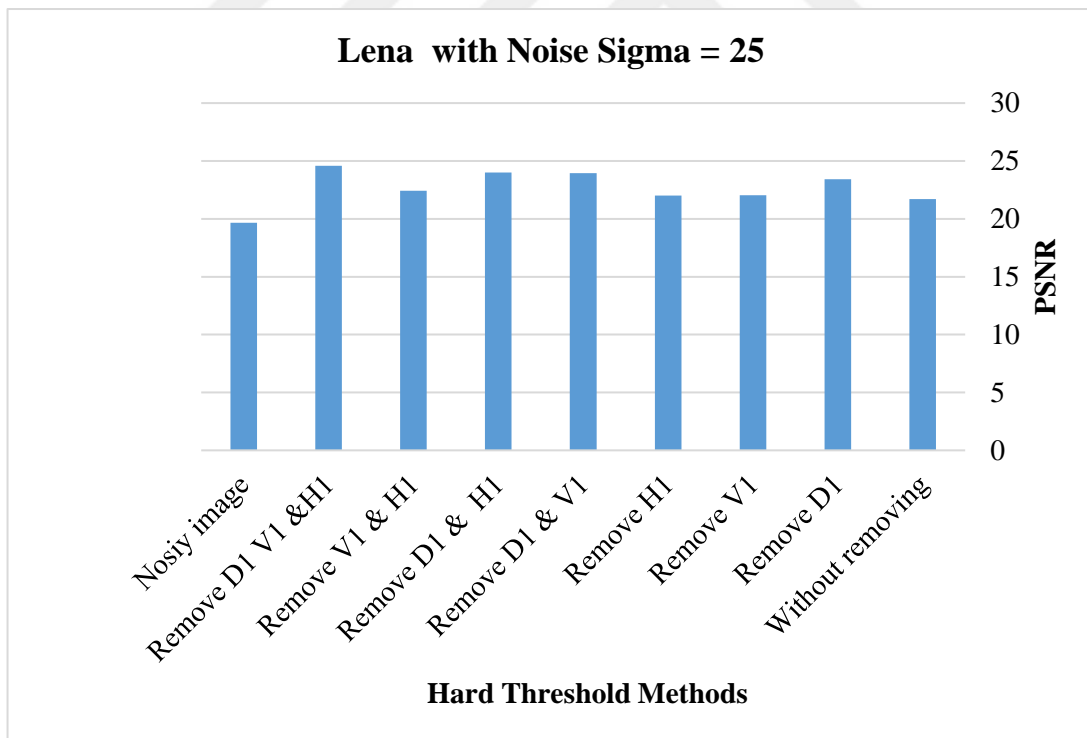


Figure 4.10. The Results of the Lena Image with Noise Sigma = 25, by Using the Hard Threshold Methods

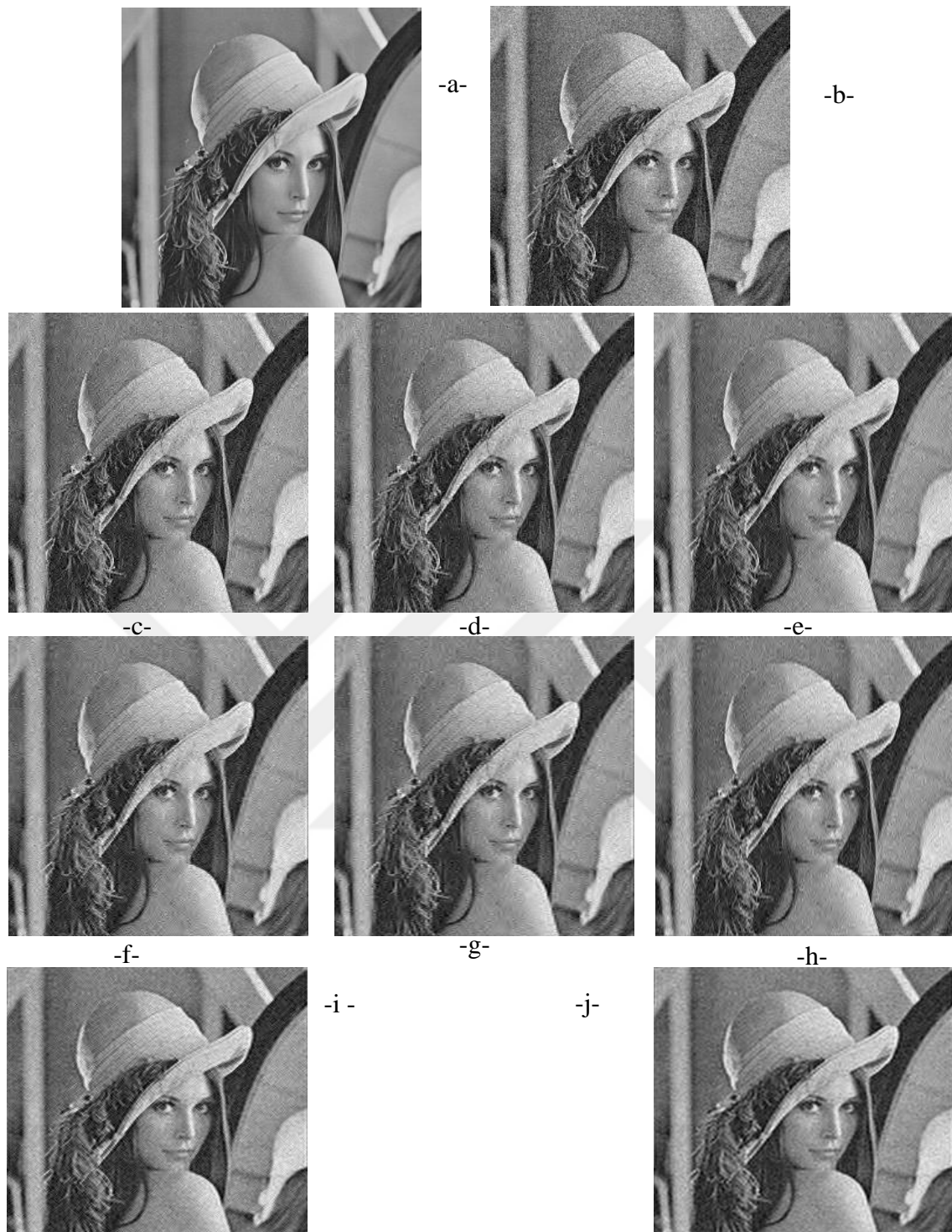


Figure 4.11. The Lena Image Results with Noise Sigma =15, by Using The Hard Threshold Methods .

| | | | | | |
|----|--------------------------------|----------------------|----|----------------------------------|----------------------|
| a- | Original image | | b- | Nosiy image | PSNR= 23.810 |
| c- | Hard Threshold | PSNR=24.836, rbio2.6 | d- | Hard Th, with removing D1 | PSNR=25.866, rbio2.6 |
| e- | Hard Th, with removing V1 | PSNR=25.170, rbio2.6 | f- | Hard Th, with removing H1 | PSNR=24.788, rbio2.6 |
| g- | Hard Th, with removing D1 & V1 | PSNR=25.803, rbio2.6 | h- | Hard Th, with removing D1&H1 | PSNR=26.303, rbio2.6 |
| j- | Hard Th, with removing V1&H1 | PSNR=25.262, sym25 | j- | Hard Th, with removing D1,V1,&H1 | PSNR=26.345, sym25 |

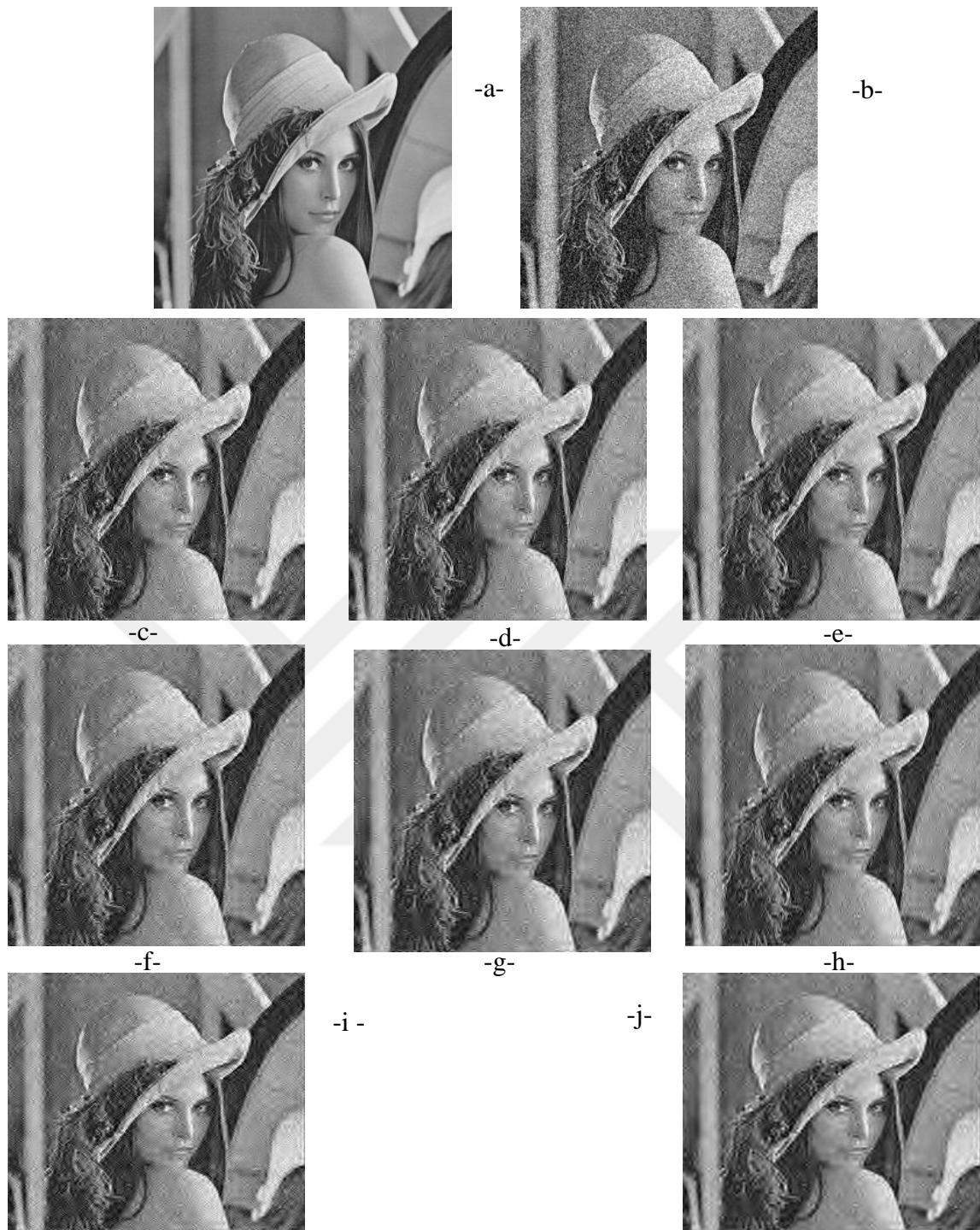


Figure 4.12. The Lena Image Results with Noise Sigma =25, by Using the Hard Threshold Methods .

| | | | | | |
|----|-------------------------------|----------------------|----|----------------------------------|----------------------|
| a- | Original image | | b- | Nosiy image | PSNR= 19.665 |
| c- | Hard Threshold | PSNR=21.693, rbio2.8 | d- | Hard Th, with removing D1 | PSNR=23.435, rbio2.8 |
| e- | Hard Th, with removing V1 | PSNR=22.051, rbio2.8 | f- | Hard Th, with removing H1 | PSNR=22.014, rbio2.8 |
| g- | Hard Th, with removing D1 &V1 | PSNR=23.954, rbio2.8 | h- | Hard Th, with removing D1&H1 | PSNR=23.998, rbio2.8 |
| i- | Hard Th, with removing V1&H1 | PSNR=22.413, rbio2.6 | j- | Hard Th, with removing D1,V1,&H1 | PSNR=24.596, rbio2.8 |

4.2.2. Results of Lena Image denoising by the Soft Penalized Threshold Methods

In this part, the results for implementing all the cases belong to the denoising the Lena image by the soft threshold methods and for the two ratios $\sigma=15$ and $\sigma=25$ are shown in the Figures 4.13, 4.14, 4.15, and 4.16 below.

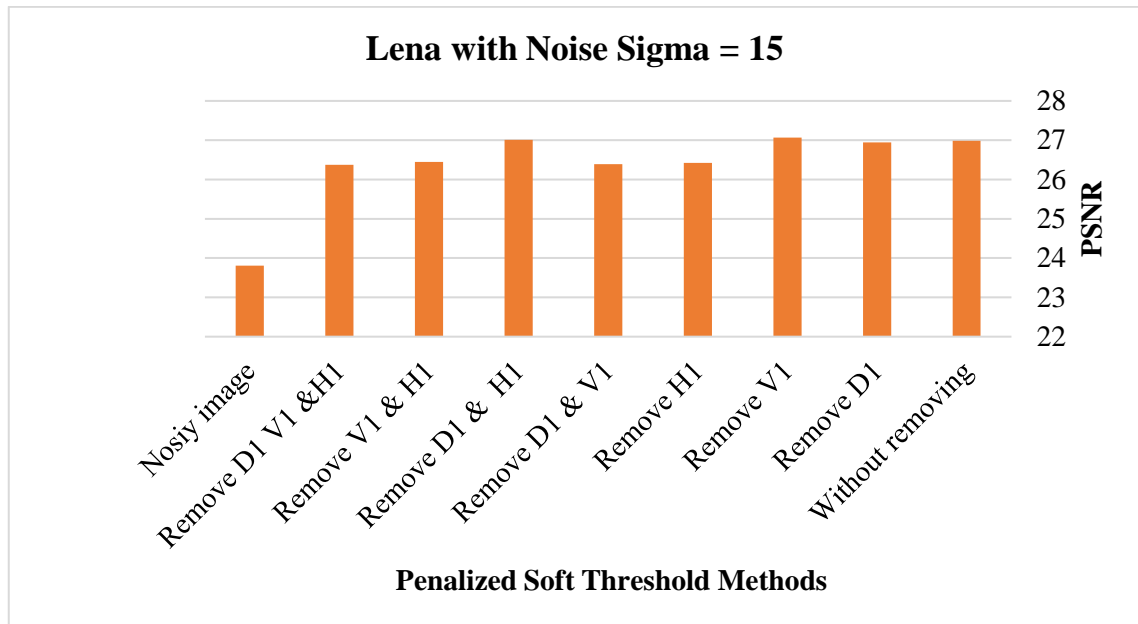


Figure 4.13. The Results of the Lena Image with Noise Sigma = 15, By Using The Soft Penalized Threshold Methods.

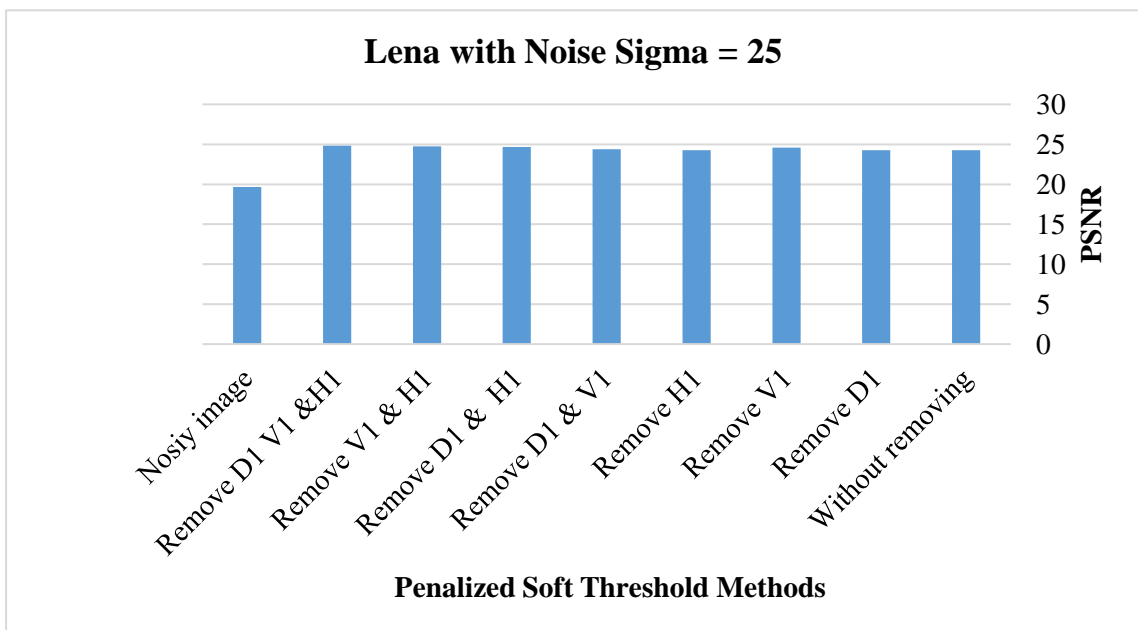


Figure 4.14. The Results of the Lena Image with Noise Sigma = 25, by Using the Soft Penalized Threshold Methods.



Figure 4.15. The Results of the Lena Image with Noise Sigma =15, By Using Soft Penalized Threshold Methods.

| | | | | | |
|----|--------------------------------|----------------------|----|----------------------------------|----------------------|
| a- | Original image | | b- | Nosiy image | PSNR= 23.810 |
| c- | Hard Threshold | PSNR=26.988, bior3.9 | d- | Hard Th, with removing D1 | PSNR=26.945, bior3.9 |
| e- | Hard Th, with removing V1 | PSNR=27.065, bior3.7 | f- | Hard Th, with removing H1 | PSNR=26.425, sym35 |
| g- | Hard Th, with removing D1 & V1 | PSNR=26.388, sym35 | h- | Hard Th, with removing D1&H1 | PSNR=27.012, bior3.9 |
| i- | Hard Th, with removing V1&H1 | PSNR=26.449, bior3.5 | j- | Hard Th, with removing D1,V1,&H1 | PSNR=26.372, bior3.9 |

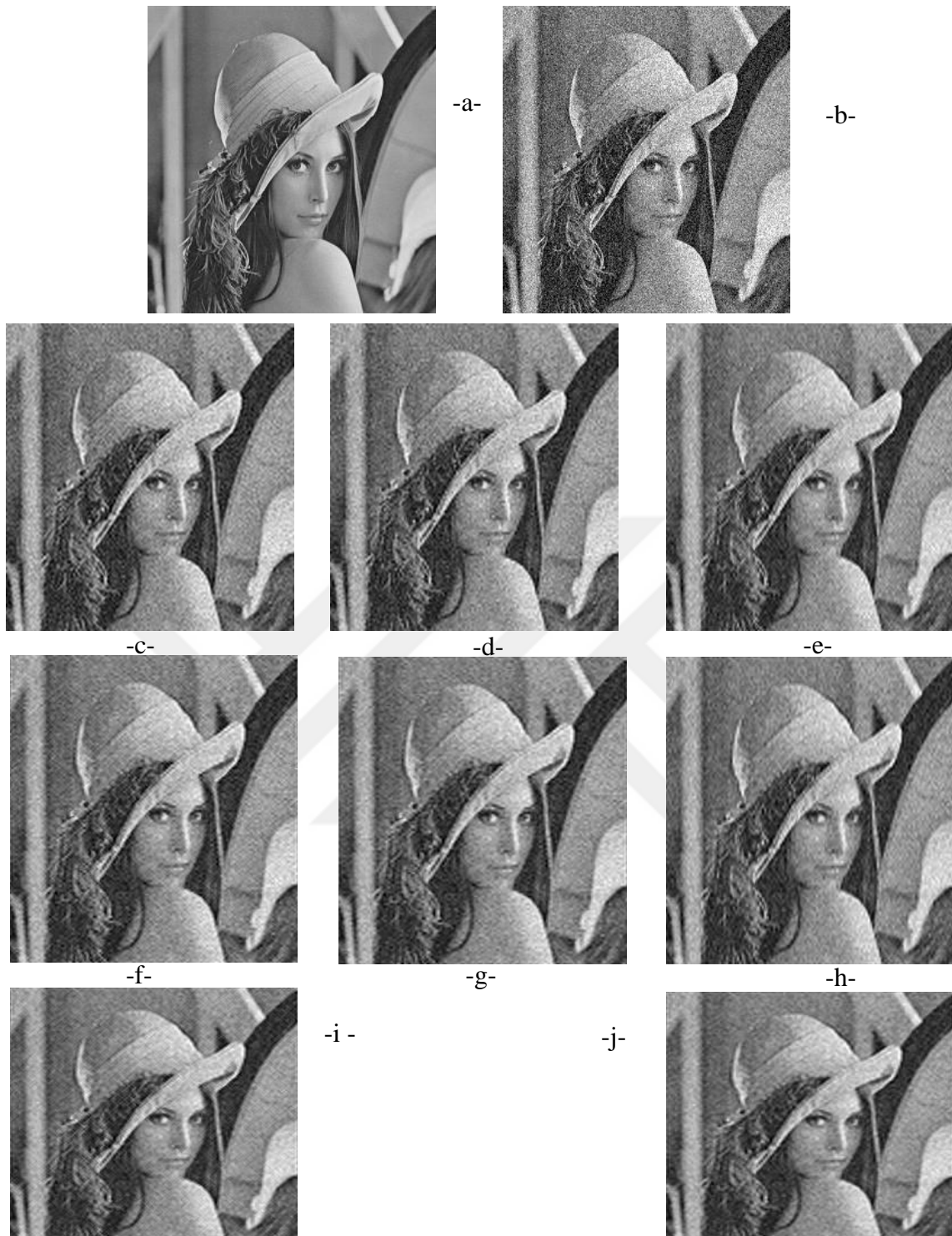


Figure 4.16. The Results of the Lena Image with Noise Sigma =25, By Using Soft Penalized Threshold Methods.

| | | | | | |
|----|-------------------------------|----------------------|----|----------------------------------|----------------------|
| a- | Original image | | b- | Nosiy image | PSNR= 19.666 |
| c- | Hard Threshold | PSNR=24.260, sym32 | d- | Hard Th, with removing D1 | PSNR=24.286,sym6 |
| e- | Hard Th, with removing V1 | PSNR=24.576, bior3.7 | f- | Hard Th, with removing H1 | PSNR=22.278, bior3.7 |
| g- | Hard Th, with removing D1 &V1 | PSNR=24.381, bior3.7 | h- | Hard Th, with removing D1&H1 | PSNR=24.687, bior3.5 |
| i- | Hard Th, with removing V1&H1 | PSNR=24.746, bior3.5 | j- | Hard Th, with removing D1,V1,&H1 | PSNR=24.822, bior3.5 |

4.3. Experimental Results of the Camera Image

The original camera image without noise showed in Figure 3.2, as an image with size 256x256 pixels gray level with a standard deviation equal to (63.3729). The two ratios of the noise ($\sigma=15$ and $\sigma=25$) with the type Additive Gaussian Noise are added to the original image to generate the two noisy images, and the standard deviation become (64.3469) and (65.9484) respectively. After applying 2D-DWT for 3-analysis levels, the image will be transformed into the wavelet domain as ten bands, the approximation band (A3) which contains a shrinking copy to the original image, and nine details bands (H1,V1,D1, H2,V2,D2, H3,V3,and D3) which they are the high frequencies bands.

The denoising algorithm needs the value of the noise ratio in each noisy image; the Robust Median Estimator by equation 5, has been used to estimate the noise ratio. The results for the estimation noise ratio for the noisy camera image shown in Table 3.1, and for the two ratios $\sigma=15$ and $\sigma=25$ they were equal to 14.6082, and 26.8597 respectively.

4.3.1. Results of Camera Image denoising by the hard threshold methods

In this part, the results for implementing all the cases belong to the denoising the Camera image by the hard threshold methods and for the two ratios $\sigma=15$ and $\sigma=25$ are shown in the Figures 4.17, 4.18, 4.19, and 4.20 below.

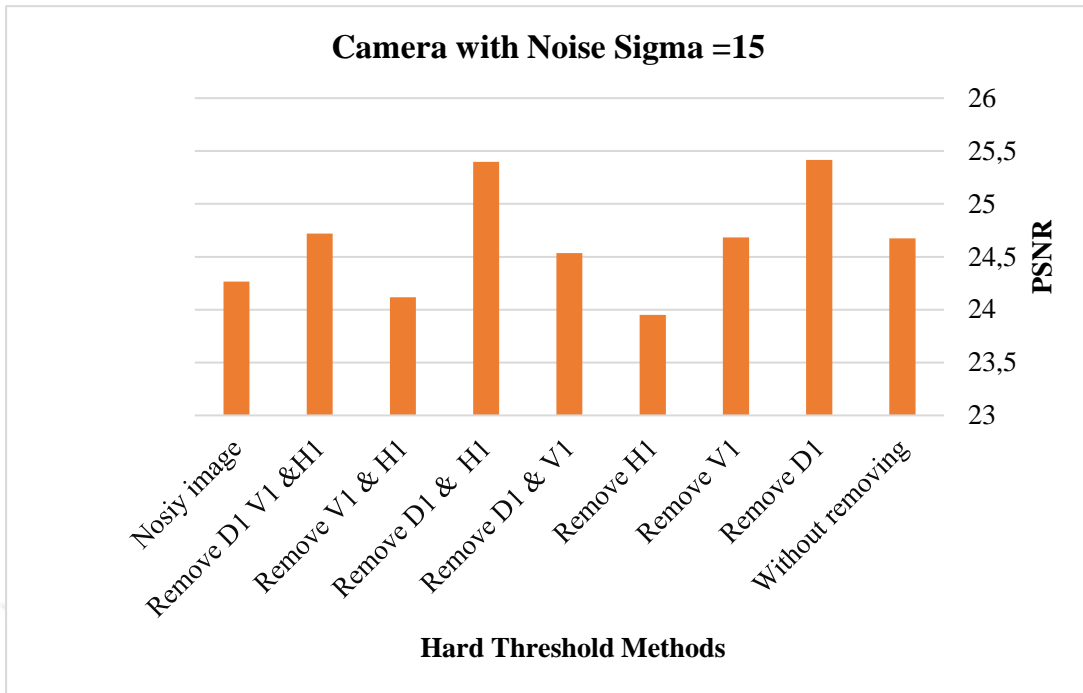


Figure 4.17. The Results of the Camera Image with Noise Sigma = 25, by Using the Hard Threshold Methods.

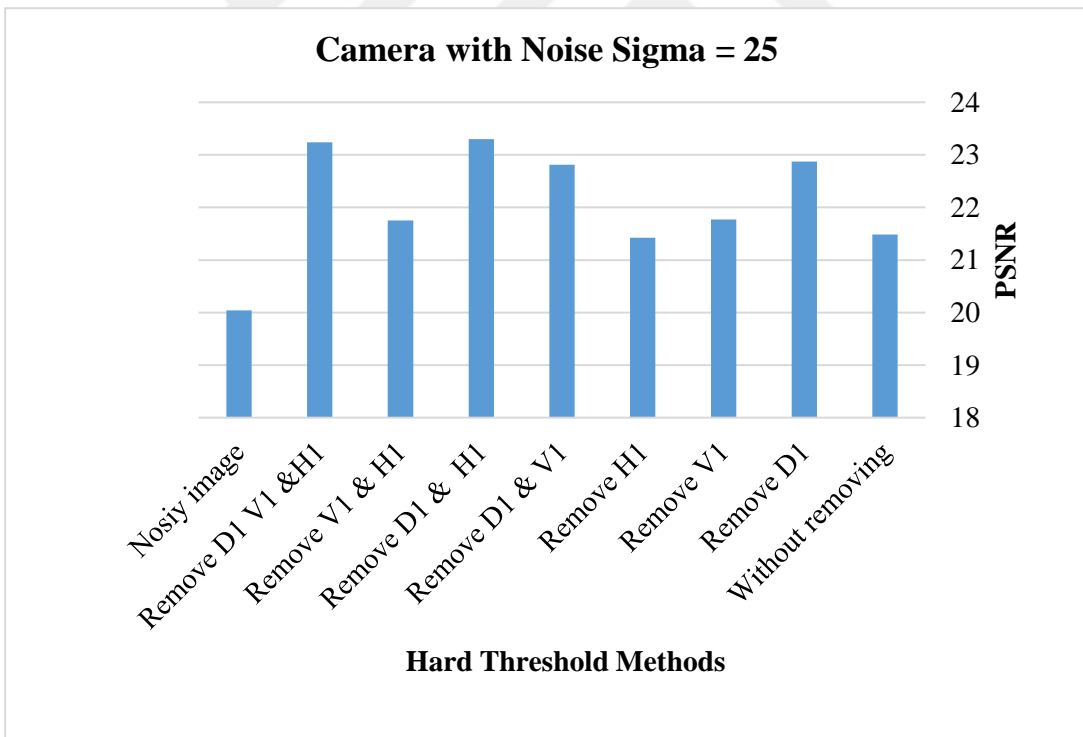


Figure 4.18. The Results of the Camera Image with Noise Sigma = 25, by Using the Hard Threshold Methods

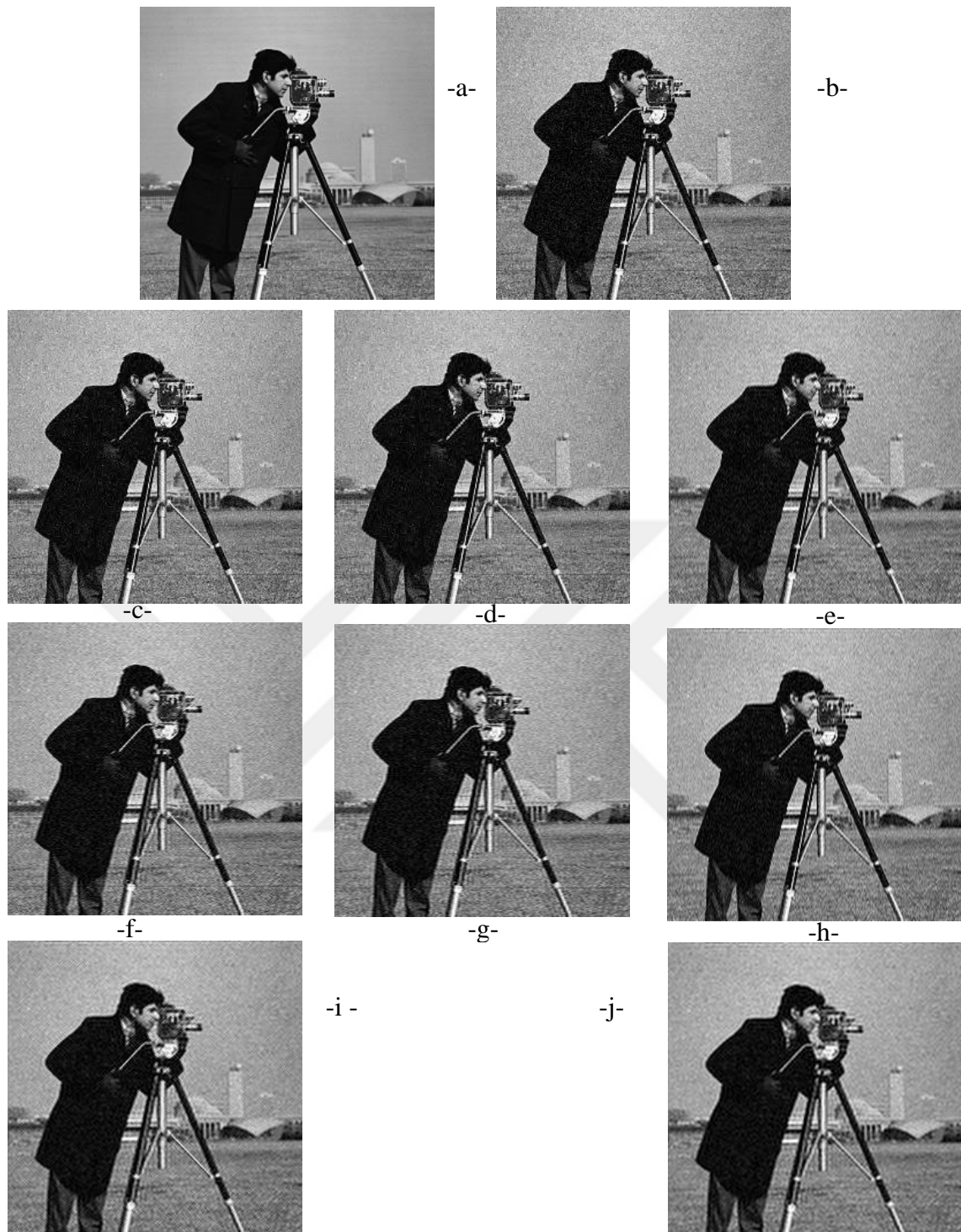


Figure 4.19. The Camera Image Results with Noise Sigma =15, by Using the Hard Threshold Methods.

| | | | | | |
|----|------------------------------|----------------------|----|----------------------------------|----------------------|
| a- | Original image | | b- | Nosiy image | PSNR= 24.264 |
| c- | Hard Threshold | PSNR=24.674, rbio2.4 | d- | Hard Th, with removing D1 | PSNR=25.414, rbio2.4 |
| e- | Hard Th, with removing V1 | PSNR=24.682, db44 | f- | Hard Th, with removing H1 | PSNR=23.949, db44 |
| g- | Hard Th, with removing D1 | PSNR=24.535, db44 | h- | Hard Th, with removing D1&H1 | PSNR=25.396, db17 |
| i- | Hard Th, with removing V1&H1 | PSNR=24.115, db44 | j- | Hard Th, with removing D1,V1,&H1 | PSNR=24.719, db44 |

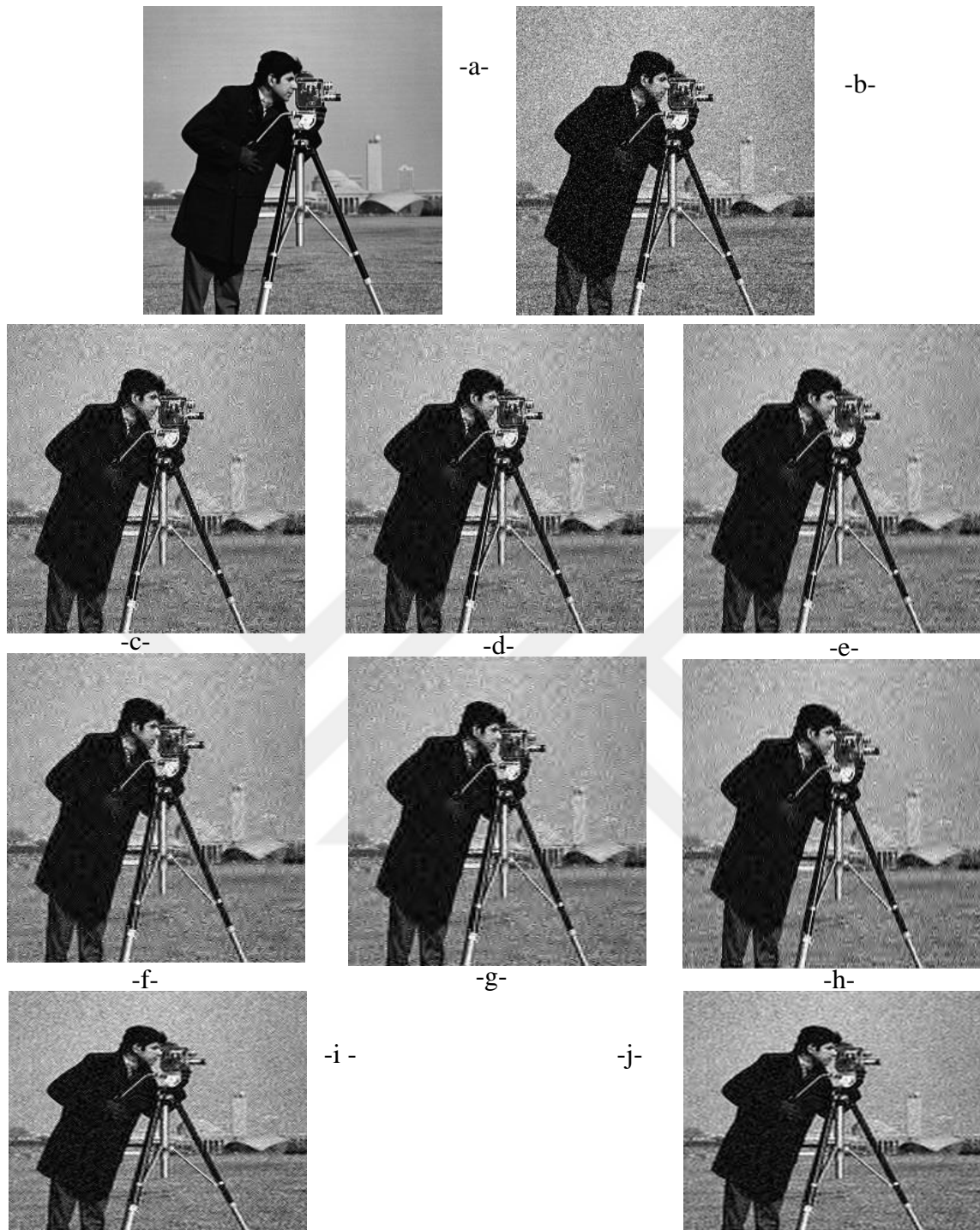


Figure 4.20. The Camera Image Results with Noise Sigma =25, by Using the Hard Threshold Methods.

| | | | | | |
|----|------------------------------|----------------------|----|----------------------------------|----------------------|
| a- | Original image | | b- | Nosiy image | PSNR= 20.041 |
| c- | Hard Threshold | PSNR=21.483, rbio2.8 | d- | Hard Th, with removing D1 | PSNR=22.874, rbio2.8 |
| e- | Hard Th, with removing V1 | PSNR=21.770, rbio2.8 | f- | Hard Th, with removing H1 | PSNR=21.422, rbio2.8 |
| g- | Hard Th, with removing D1&V1 | PSNR=22.812, rbio2.8 | h- | Hard Th, with removing D1&H1 | PSNR=23.296, rbio2.8 |
| i- | Hard Th, with removing V1&H1 | PSNR=21.754, sym29 | j- | Hard Th, with removing D1,V1,&H1 | PSNR=23.239, sym29 |

4.3.2. Results of Camera Image denoising by the soft Penalized threshold methods

In this part, the results for implementing all the cases belong to the denoising the Camera image by the soft threshold methods and for the two ratios $\sigma=15$ and $\sigma=25$ are shown in Figures 4.21, 4.22, 4.23 and 4.24 below.

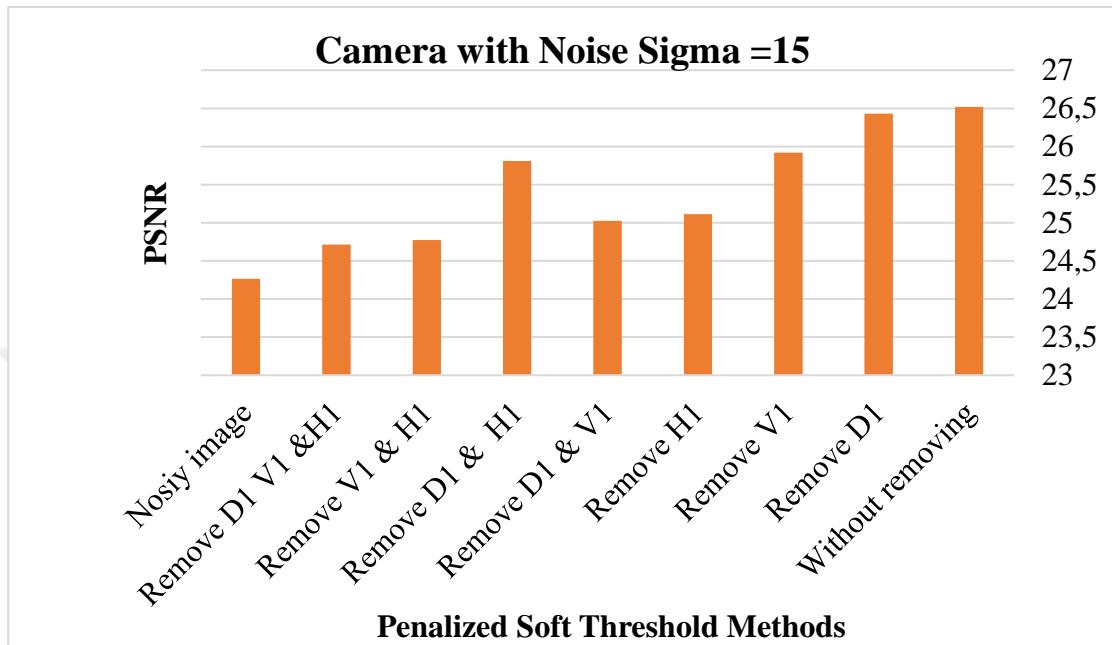


Figure 4.21. The results of the Camera Image with Noise Sigma = 15, by Using the Soft Penalized Threshold Methods.

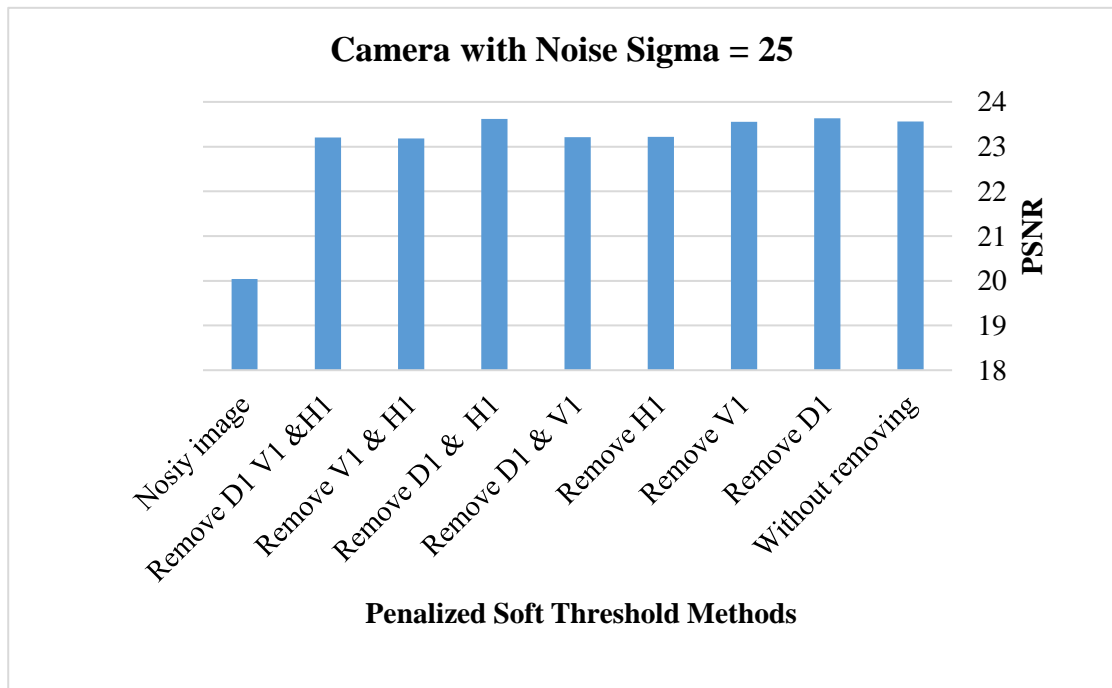


Figure 4.22. The Results of the Camera Image With Noise Sigma = 25, by Using the Soft Penalized Threshold Methods.

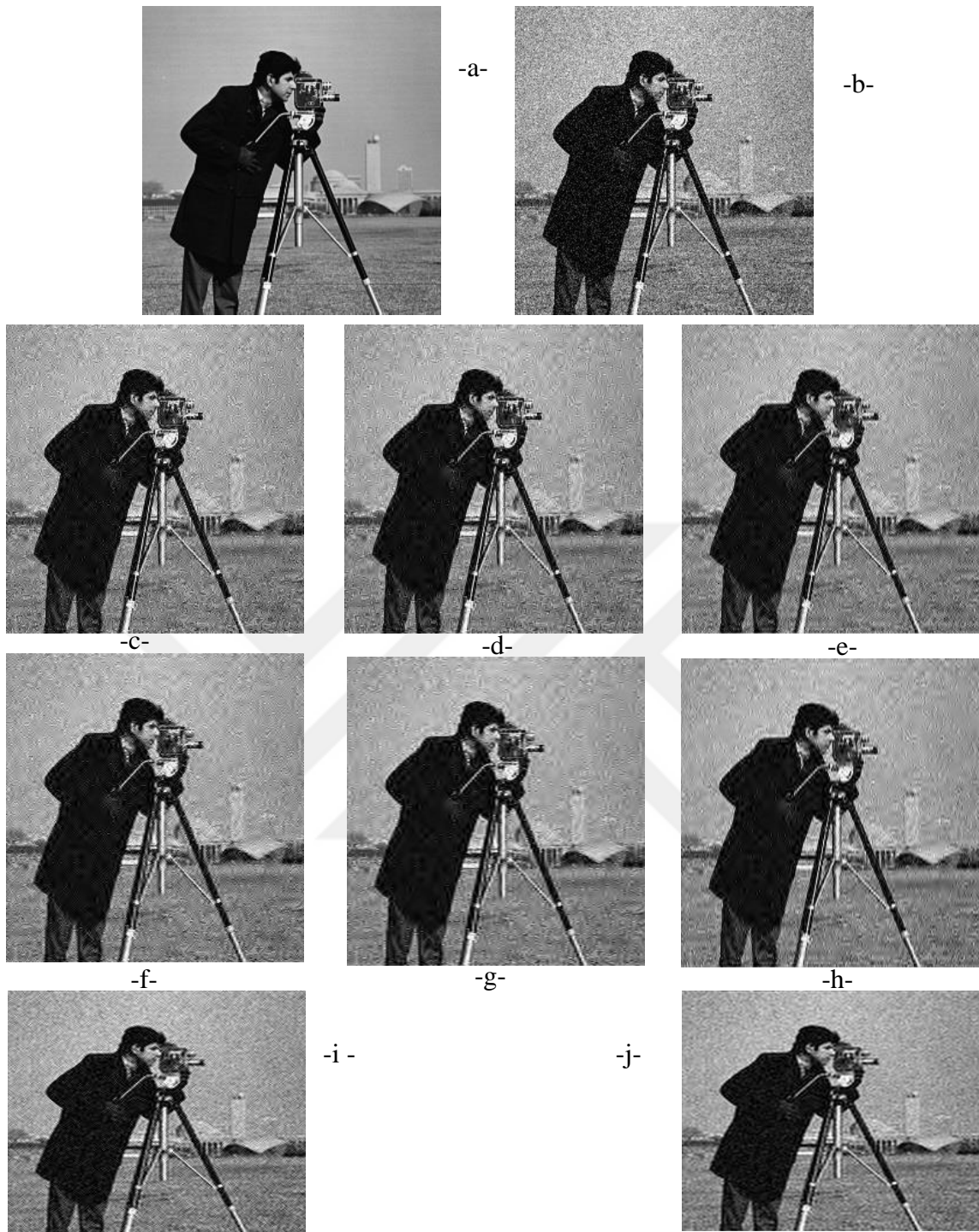


Figure 4.23. The Results of the Camera Image With Noise Sigma =15, by Using Soft Penalized Threshold Methods

| | | | | | |
|----|----------------------------------|-------------------------|----|-------------------------------------|----------------------|
| a- | Original image | | b- | Nosiy image | PSNR= 24.264 |
| c- | Hard Threshold | PSNR=26.520, bior3.9 | d- | Hard Th, with removing D1 | PSNR=26.429, bior3.9 |
| e- | Hard Th, with removing V1 | PSNR=25.917, sym19 | f- | Hard Th, with removing H1 | PSNR=25.113, sym23 |
| g- | Hard Th, with removing D1 &V1 | PSNR=25.025, sym23 | h- | Hard Th, with removing D1&H1 | PSNR=25.809, sym19 |
| i- | Hard Th, with removing V1&H1 | PSNR=24.771, sym23 | j- | Hard Th, with removing D1,V1,&H1 | PSNR=24.713, db41 |

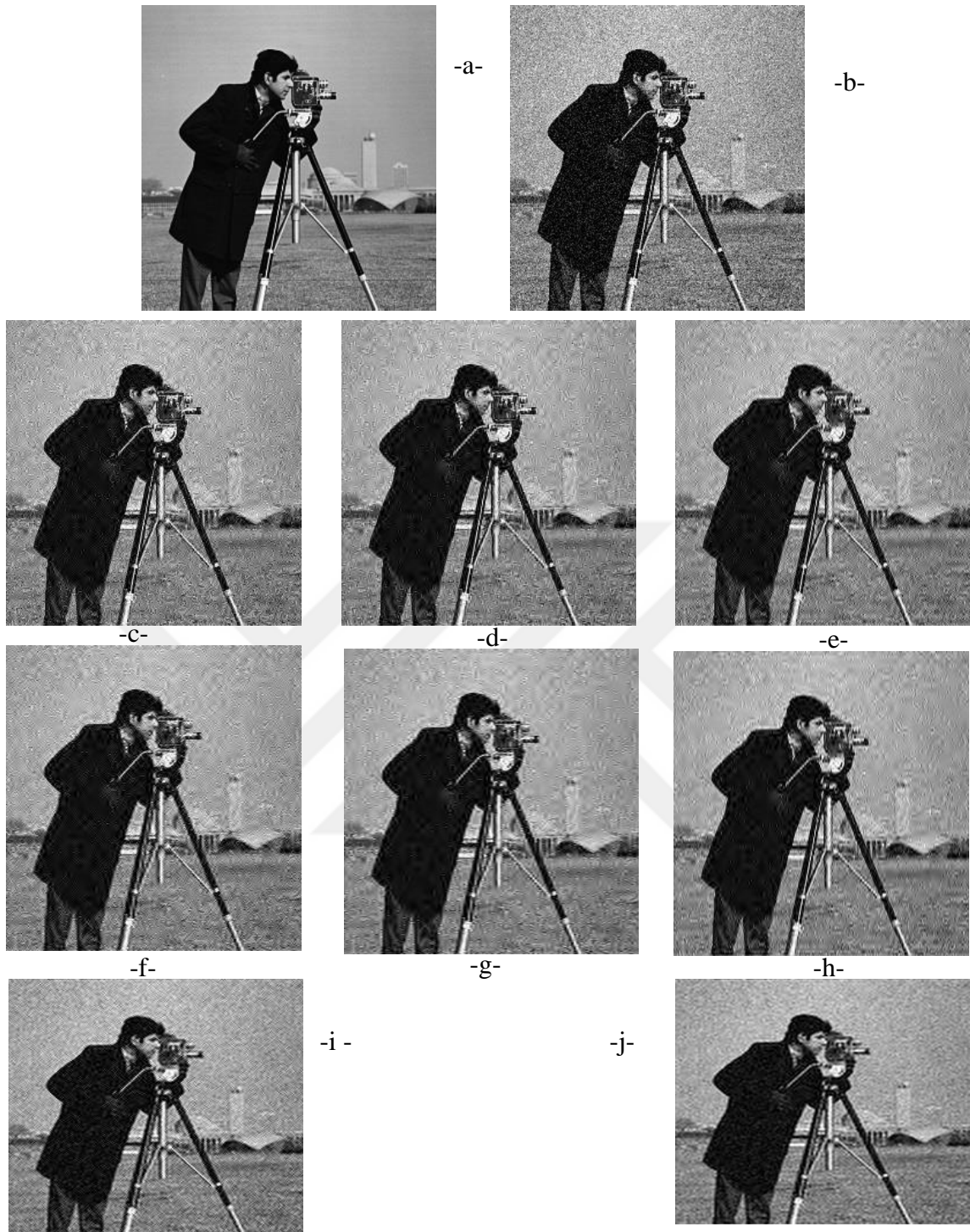


Figure 4.24. The Results of the Camera Image with Noise Sigma =25, by Using Soft Penalized Threshold Methods

| | | | | | |
|----|-------------------------------|----------------------|----|----------------------------------|----------------------|
| a- | Original image | | b- | Nosiy image | PSNR= 20.041 |
| c- | Hard Threshold | PSNR=23.563, bior3.9 | d- | Hard Th, with removing D1 | PSNR=23.632, rbio3.9 |
| e- | Hard Th, with removing V1 | PSNR=23.555, bior3.7 | f- | Hard Th, with removing H1 | PSNR=23.218, sym23 |
| g- | Hard Th, with removing D1 &V1 | PSNR=23.214, bior3.9 | h- | Hard Th, with removing D1&H1 | PSNR=23.618, rbio3.9 |
| i- | Hard Th, with removing V1&H1 | PSNR=23.184, sym36 | j- | Hard Th, with removing D1,V1,&H1 | PSNR=23.201, bior3.9 |

4.4. Experimental Results of the peppers Image

The original peppers image without noise revealed in Figure 3.2, as an image with size 256x256 pixels gray level with a standard deviation equal to (53.8455). The two ratios of the noise ($\sigma=15$ and $\sigma=25$) with the type Additive Gaussian Noise are added to the original image to generate the two noisy images, and the standard deviation become (56.0944) and (59.2166) respectively. After applying 2D-DWT for 3-analysis levels, the image will be transformed into the wavelet domain as ten bands, the approximation band (A3) which contains a shrinking copy to the original image, and nine details bands (H1,V1,D1, H2,V2,D2, H3,V3,and D3) which they are the high frequencies bands.

The denoising algorithm needs the value of the noise ratio in each noisy image; the Robust Median Estimator by equation 5, has been used to estimate the noise ratio. The results for the estimation noise ratio for the noisy peppers image shown in Table 3.1, and for the two ratios $\sigma=15$ and $\sigma=25$ they were equal to 15.6405, and 27.6837 respectively.

4.4.1. Results of Peppers Image Denoising by the Hard Threshold Methods

In this part, the results for implementing all the cases belong to the denoising the peppers image by the hard threshold methods and for the two ratios $\sigma=15$ and $\sigma=25$ are shown in the Figures 4.25, 4.26, 4.27 and 4.28 below.

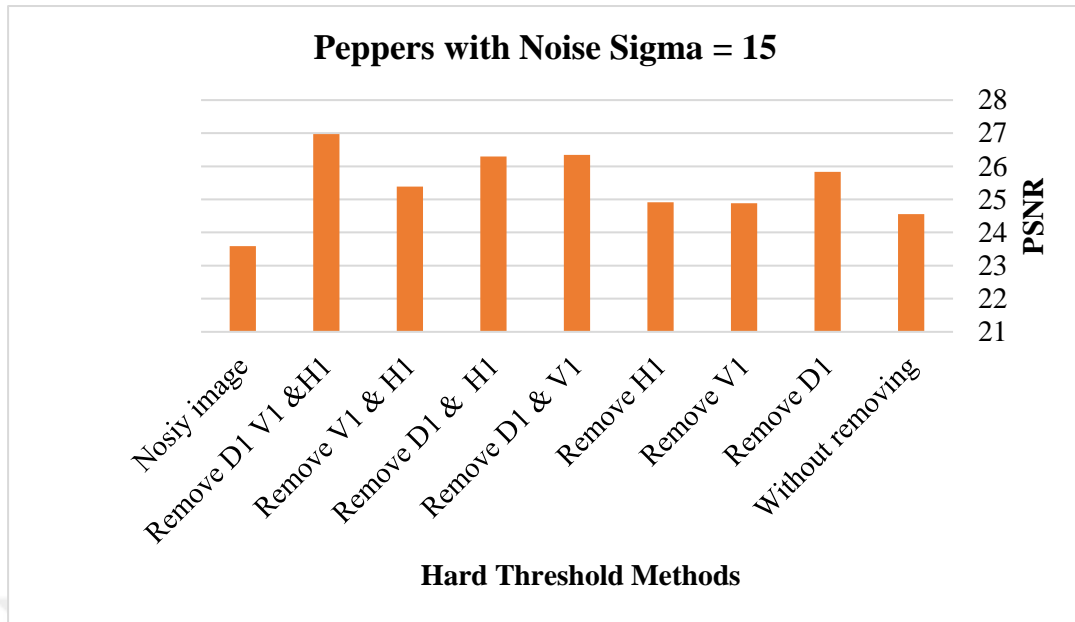


Figure 4.25. The Results of the Peppers Image with Noise Sigma = 15, by Using the Hard Threshold Methods.

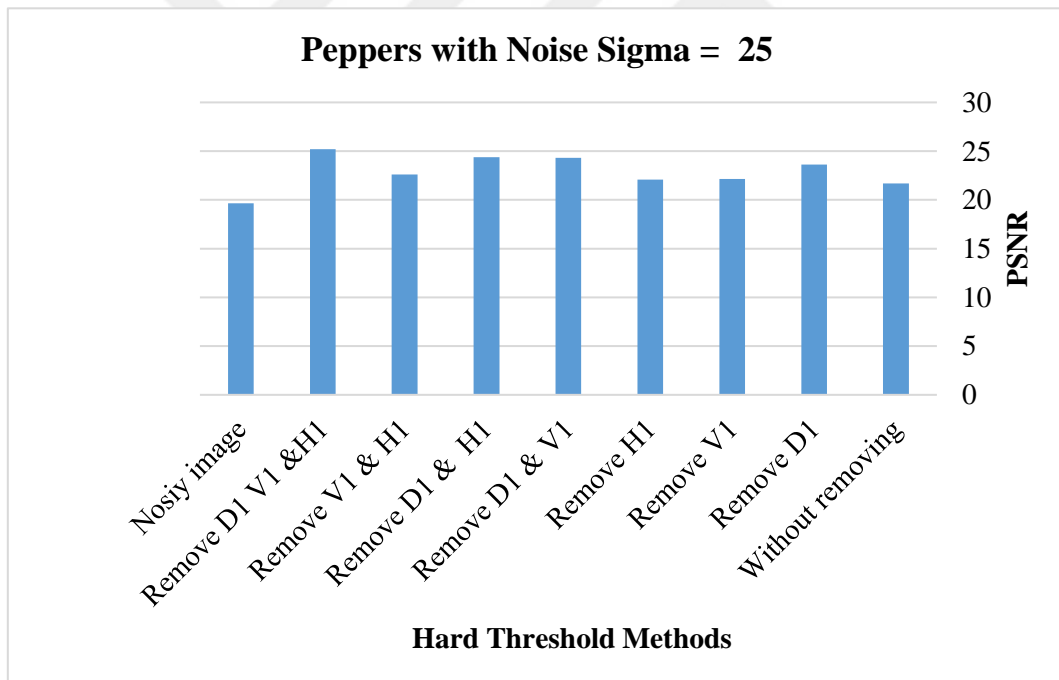


Figure 4.26. The Results of the Peppers Image with Noise Sigma = 25, by Using the Hard Threshold Methods.

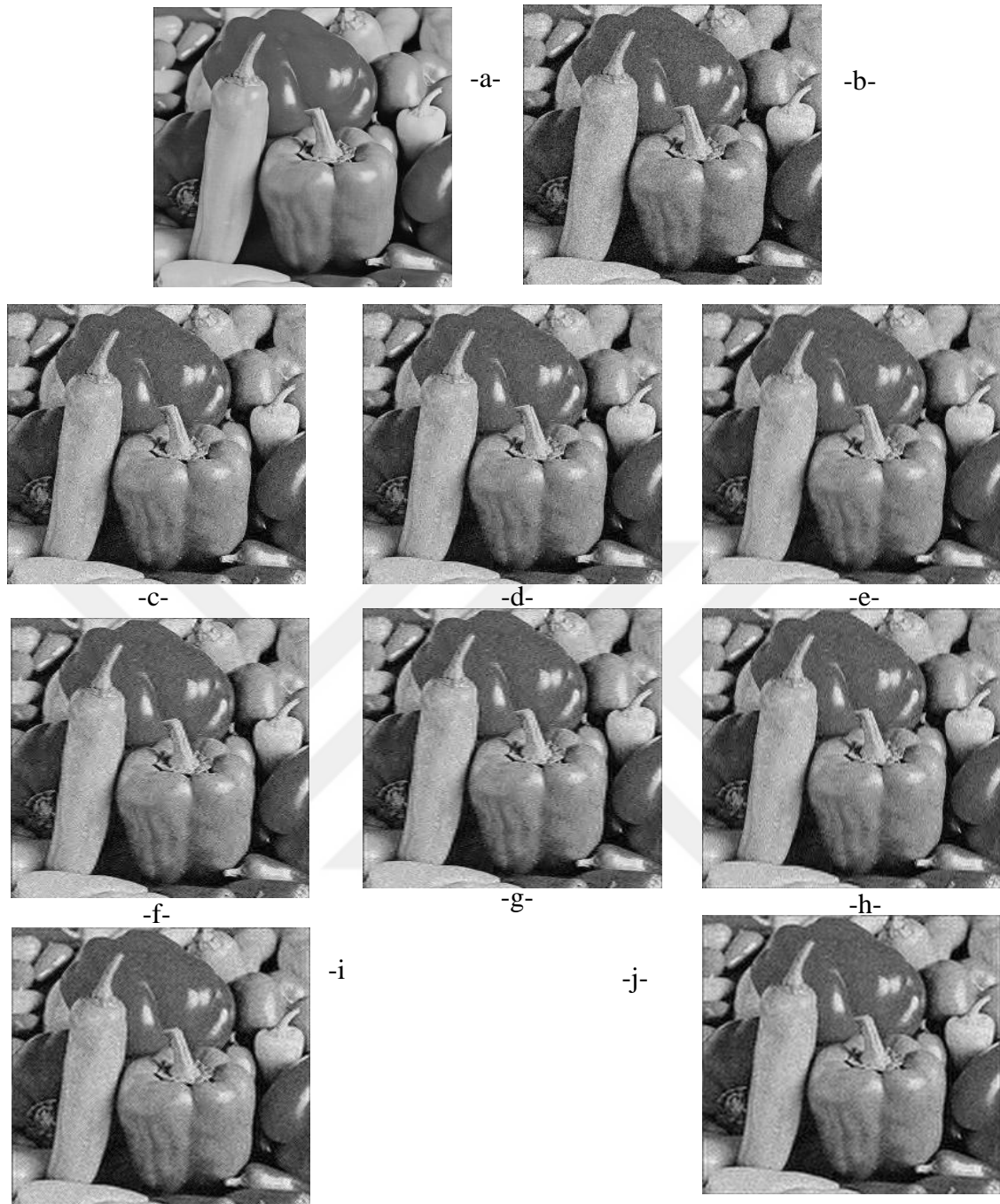


Figure 4.27. The Peppers Image Results with Noise Sigma =15, by Using the Hard Threshold Methods.

| | | | | | |
|----|--------------------------------|----------------------|----|----------------------------------|----------------------|
| a- | Original image | | b- | Noisy image | PSNR= 23.589 |
| c- | Hard Threshold | PSNR=24.559, rbio2.4 | d- | Hard Th, with removing D1 | PSNR=25.831, rbio2.4 |
| e- | Hard Th, with removing V1 | PSNR=24.885, rbio2.6 | f- | Hard Th, with removing H1 | PSNR=24.918, rbio2.6 |
| g- | Hard Th, with removing D1 & V1 | PSNR=26.343, rbio2.6 | h- | Hard Th, with removing D1&H1 | PSNR=26.295, rbio2.6 |
| i- | Hard Th, with removing V1&H1 | PSNR=25.384, db19 | j- | Hard Th, with removing D1,V1,&H1 | PSNR=26.976, sym30 |



Figure 4.28. The Peppers Image Results with Noise Sigma =25, by Using the Hard Threshold Methods.

| | | | | | |
|----|--------------------------------|----------------------|----|----------------------------------|----------------------|
| a- | Original image | | b- | Nosiy image | PSNR= 19.645 |
| c- | Hard Threshold | PSNR=21.693, rbio2.4 | d- | Hard Th, with removing D1 | PSNR=23.624, rbio2.8 |
| e- | Hard Th, with removing V1 | PSNR=22.144, rbio2.4 | f- | Hard Th, with removing H1 | PSNR=22.084, rbio2.4 |
| g- | Hard Th, with removing D1 & V1 | PSNR=24.306, rbio2.8 | h- | Hard Th, with removing D1&H1 | PSNR=24.376, rbio2.8 |
| j- | Hard Th, with removing V1&H1 | PSNR=22.590, rbio2.6 | j- | Hard Th, with removing D1,V1,&H1 | PSNR=25.202, rbio2.8 |

4.4.2. Results of Peppers Image denoising by the soft Penalized threshold methods

In this part, the results for implementing all the cases belong to the denoising the peppers image by the soft threshold methods and for the two ratios $\sigma=15$ and $\sigma=25$ are shown in the Figures 4.29, 4.30, 4.31, and 4.32 below.

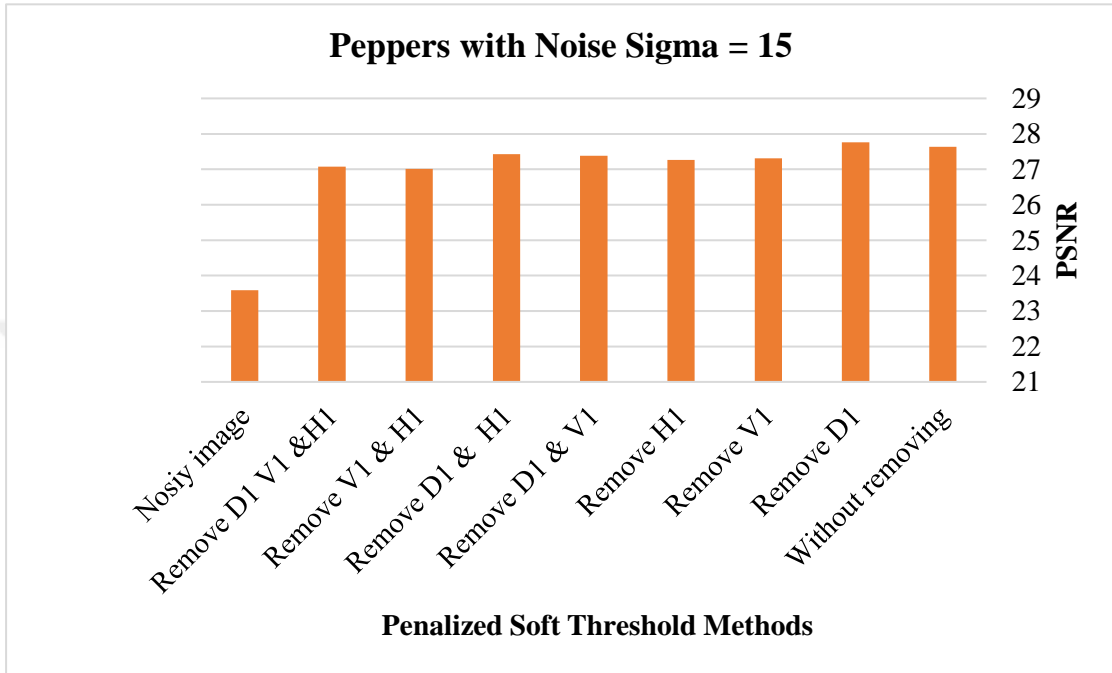


Figure 4.29. The Results of the Peppers Image with Noise Sigma = 15, by Using the Soft Penalized Threshold Methods.

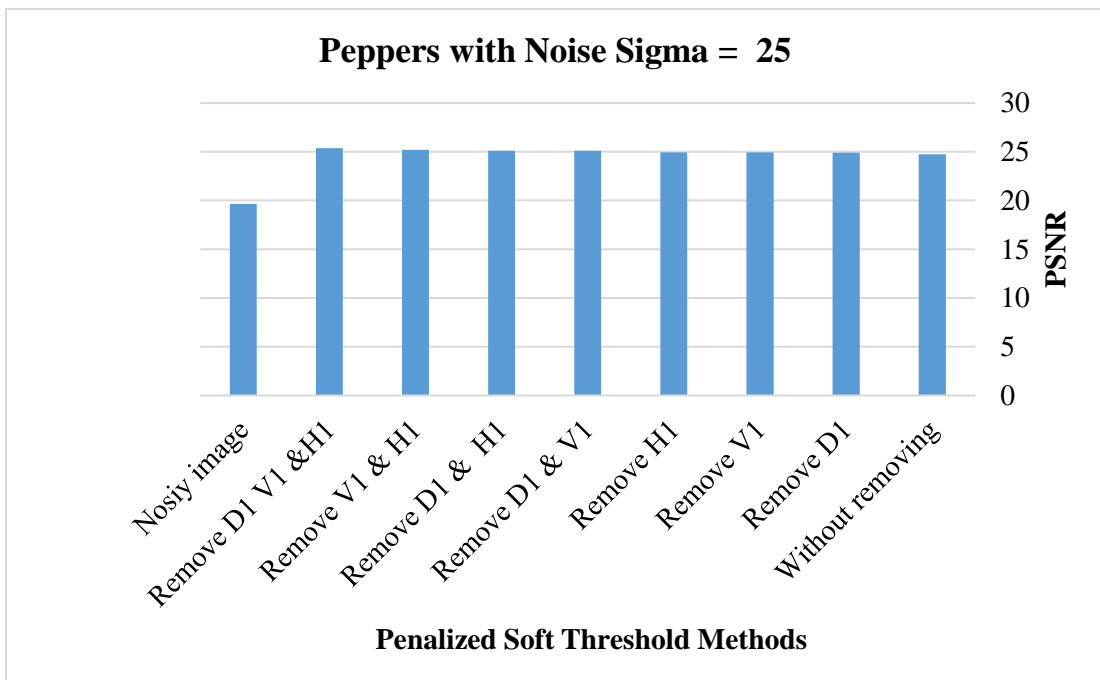


Figure 4.30. The Results of the Peppers Image with Noise Sigma = 25, by Using the Soft Penalized Threshold Methods.

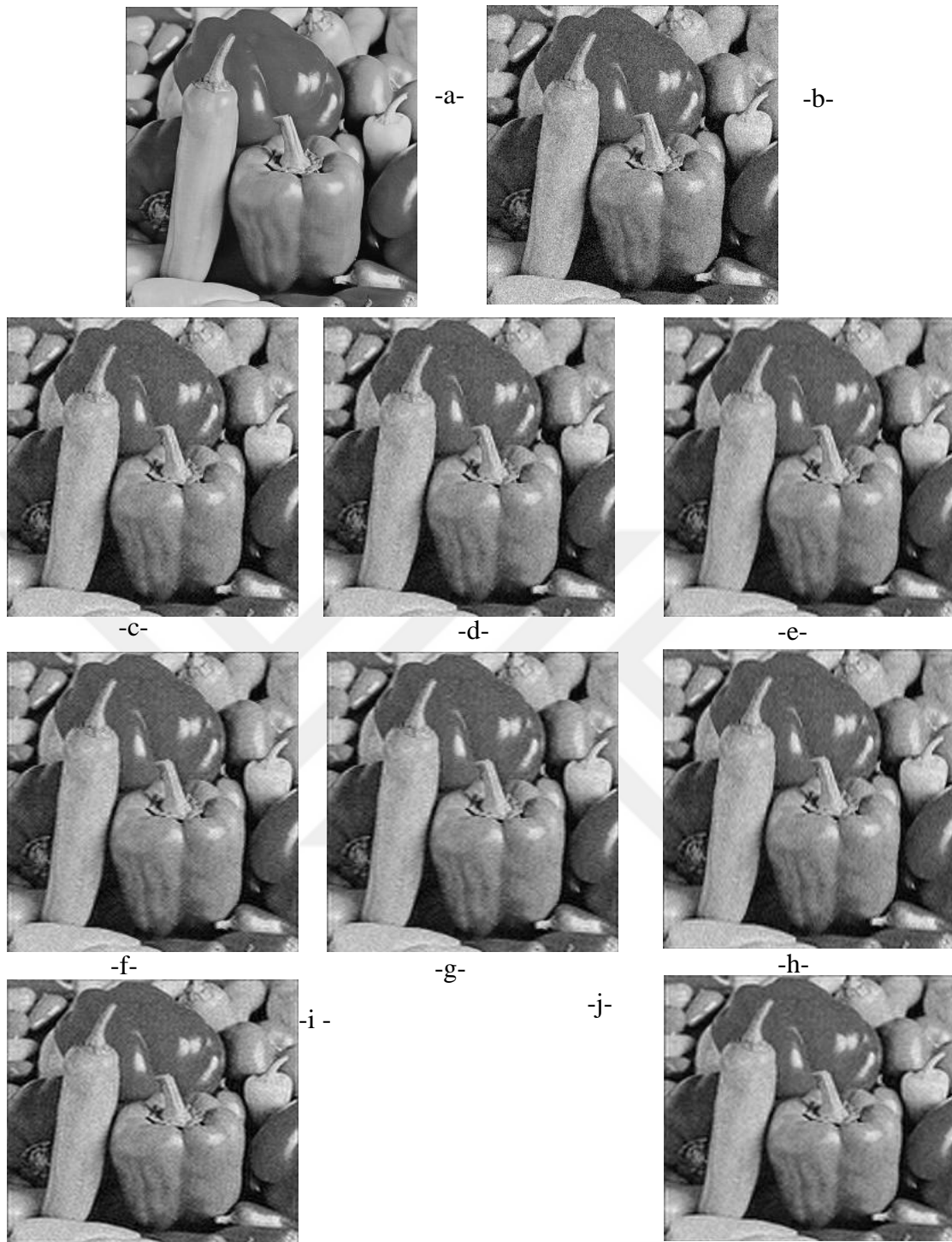


Figure 4.31. The Results Of The Peppers Image with Noise Sigma =15, by Using Soft Penalized Threshold Methods

| | | | | | |
|----|--------------------------------|----------------------|----|----------------------------------|----------------------|
| a- | Original image | | b- | Nosiy image | PSNR= 23.589 |
| c- | Hard Threshold | PSNR=27.637, bior3.9 | d- | Hard Th, with removing D1 | PSNR=27.758, bior3.7 |
| e- | Hard Th, with removing V1 | PSNR=27.309, bior3.7 | f- | Hard Th, with removing H1 | PSNR=27.266, bior3.9 |
| g- | Hard Th, with removing D1 & V1 | PSNR=27.381, bior3.7 | h- | Hard Th, with removing D1&H1 | PSNR=27.423, bior3.7 |
| i- | Hard Th, with removing V1&H1 | PSNR=27.014, sym28 | j- | Hard Th, with removing D1,V1,&H1 | PSNR=27.073, bior3.7 |

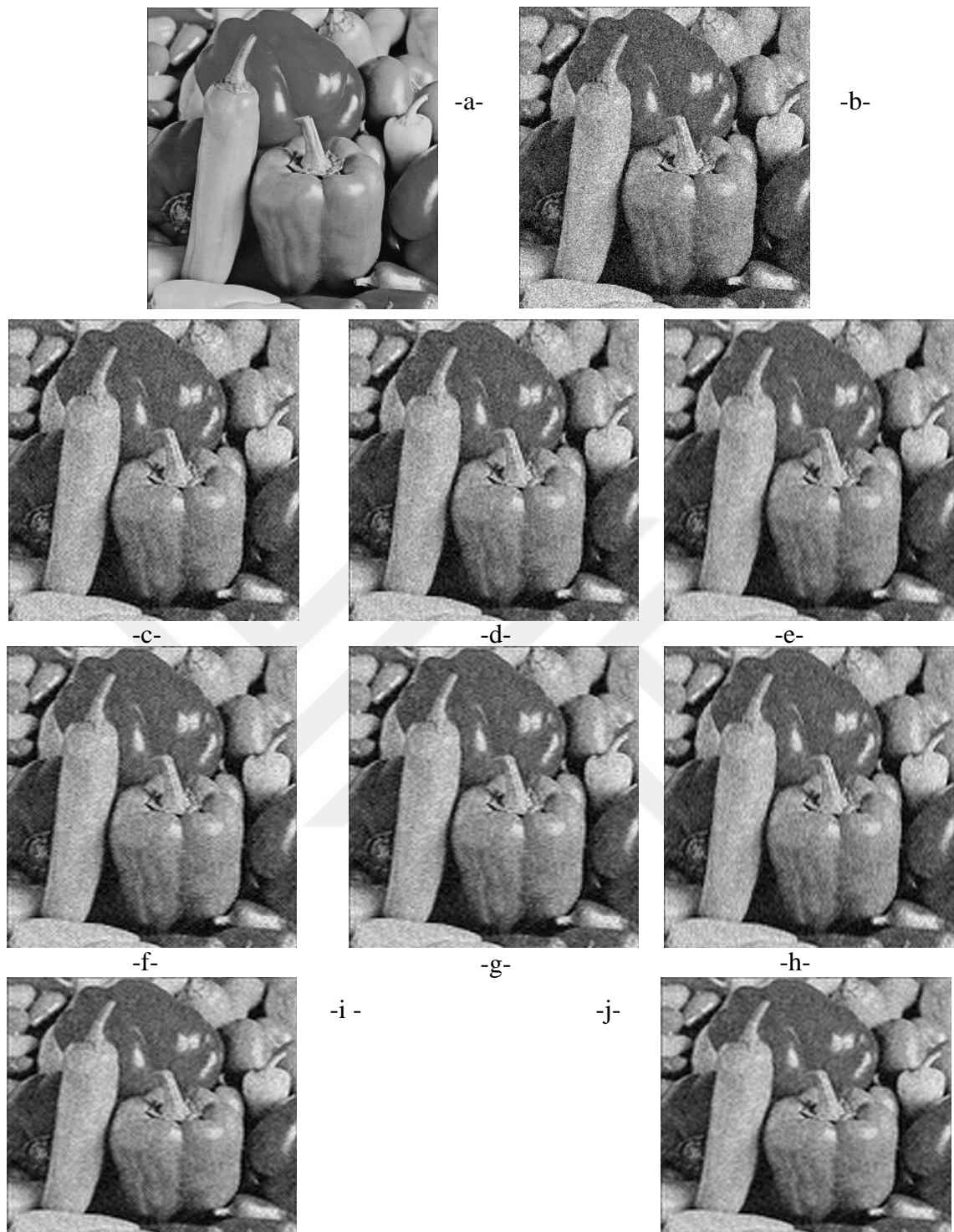


Figure 4.32. The Results of the Peppers Image with Noise Sigma =25, by Using Soft Penalized Threshold Methods

| | | | | | |
|----|--------------------------------|----------------------|----|----------------------------------|----------------------|
| a- | Original image | | b- | Nosiy image | PSNR= 19.645 |
| c- | Hard Threshold | PSNR=24.753, sym23 | d- | Hard Th, with removing D1 | PSNR=24.902,bior3.7 |
| e- | Hard Th, with removing V1 | PSNR=24.949, bior3.7 | f- | Hard Th, with removing H1 | PSNR=24.926,bior3.7 |
| g- | Hard Th, with removing D1 & V1 | PSNR=25.097, bior3.7 | h- | Hard Th, with removing D1&H1 | PSNR=25.122, bior3.7 |
| i- | Hard Th, with removing V1&H1 | PSNR=25.195, bior3.5 | j- | Hard Th, with removing D1,V1,&H1 | PSNR=25.357, bior3.5 |

4.5. Comparisons of the Threshold Techniques

In this study, two of the threshold techniques used, each of them is applied for eight cases with the removing details bands in the wavelet domain and for 3 levels of the DWT analysis operation. The steps for each case implemented to a specific image of the four test images which used for two noise ratios ($\sigma=15$ and $\sigma=25$). Table 4.1, and Table 4.2, below shows the best results for each case by recording that results from all values measured by applying the 110 filters of the wavelet filter families. The cells with a dark background represent the best result for each image.

Table 4.1. The Comparison Between the Hard Threshold, and Soft Penalized Threshold Cases for the Four Test Images with the Noise Sigma =15.

| Threshold Type (Th) | Denoising Case | Images, with Noise Sigma = 15 | | | | | | | |
|---|-------------------------|-------------------------------|---------|--------------------------|---------|----------------------------|---------|-----------------------------|---------|
| | | Butterfly PSNR = 23.781753 | | Lena PSNR = 23.810283 | | camera PSNR = 24.264110 | | peppers PSNR = 23.589858 | |
| | | PSNR | Filter | PSNR | Filter | PSNR | Filter | PSNR | Filter |
| Hard Threshold with 3_Levels 2D-DWT | Th. Only | 24.325 | rbio2.8 | 24.836 | rbio2.6 | 24.674 | rbio2.4 | 24.559 | rbio2.4 |
| | Th. with removing D1 | 24.966 | rbio2.8 | 25.866 | rbio2.6 | 25.414 | rbio2.4 | 25.831 | rbio2.4 |
| | Th. with removing V1 | 23.391 | db41 | 25.170 | rbio2.6 | 24.682 | db44 | 24.885 | rbio2.6 |
| | Th. with remove H1 | 23.738 | rbio2.8 | 24.788 | rbio2.6 | 23.949 | db44 | 24.918 | rbio2.6 |
| | Th. with remove D1 & V1 | 24.285 | rbio2.8 | 25.803 | rbio2.6 | 24.535 | db44 | 26.343 | rbio2.6 |
| | Th. with remove D1 & H1 | 23.892 | sym36 | 26.303 | rbio2.6 | 25.396 | db17 | 26.295 | rbio2.6 |
| | Th. with remove V1 & H1 | 23.056 | sym25 | 25.262 | sym25 | 24.115 | db44 | 25.384 | db19 |
| Th. with remove D1 V1 & H1 | 23.528 | sym25 | 26.345 | sym25 | 24.719 | db44 | 26.976 | sym30 | |
| Soft Threshold Penalized with 3_Levels 2D-DWT | Th. Only | 25.696 | bior3.9 | 26.988 | bior3.9 | 26.52 | bior3.9 | 27.637 | bior3.9 |
| | Th. with removing D1 | 25.506 | bior3.9 | 26.945 | bior3.9 | 26.429 | bior3.9 | 27.758 | bior3.7 |
| | Th. with removing V1 | 24.334 | sym35 | 27.065 | bior3.7 | 25.917 | sym19 | 27.309 | bior3.7 |
| | Th. with remove H1 | 24.604 | bior3.9 | 26.425 | sym35 | 25.113 | sym23 | 27.266 | bior3.9 |
| | Th. with remove D1 & V1 | 24.452 | bior3.9 | 26.388 | sym35 | 25.025 | sym23 | 27.381 | bior3.7 |
| | Th. with remove D1 & H1 | 24.255 | sym35 | 27.012 | bior3.9 | 25.809 | sym19 | 27.423 | bior3.7 |
| | Th. with remove V1 & H1 | 23.584 | sym25 | 26.449 | bior3.5 | 24.771 | sym23 | 27.014 | sym28 |
| Th. with remove D1 V1 & H1 | 23.516 | sym25 | 26.372 | bior3.9 | 24.713 | db41 | 27.073 | bior3.7 | |

Table 4.2. The Comparison Between The Hard Threshold, And Soft Penalized Threshold Cases for the Four Test Images with the Noise Sigma =25.

| Threshold Type (Th) | Denoising case | Images, with Noise Sigma = 25 | | | | | | | |
|---|----------------------------|-------------------------------|---------|---------------|---------|-----------------|---------|----------------|---------|
| | | Butterfly | | Lena | | camera | | peppers | |
| | | PSNR = 19.69711 | | PSNR = 19.665 | | PSNR = 20.04154 | | PSNR = 19.6454 | |
| | | PSNR | Filter | PSNR | Filter | PSNR | Filter | PSNR | Filter |
| Hard Threshold with 3_Levels 2D-DWT | Th. Only | 21.189 | rbio2.8 | 21.693 | rbio2.8 | 21.483 | rbio2.8 | 21.693 | rbio2.4 |
| | Th. with removing D1 | 22.503 | rbio2.8 | 23.435 | rbio2.8 | 22.874 | rbio2.8 | 23.624 | rbio2.8 |
| | Th. with removing V1 | 21.033 | rbio2.8 | 22.051 | rbio2.8 | 21.770 | rbio2.8 | 22.144 | rbio2.4 |
| | Th. with remove H1 | 21.173 | rbio2.8 | 22.014 | rbio2.8 | 21.422 | rbio2.8 | 22.084 | rbio2.4 |
| | Th. with remove D1 & V1 | 22.483 | rbio2.8 | 23.954 | rbio2.8 | 22.812 | rbio2.8 | 24.306 | rbio2.8 |
| | Th. with remove D1 & H1 | 22.314 | rbio2.8 | 23.998 | rbio2.8 | 23.296 | rbio2.8 | 24.376 | rbio2.8 |
| | Th. with remove V1 & H1 | 21.060 | sym17 | 22.413 | rbio2.6 | 21.754 | sym29 | 22.59 | rbio2.6 |
| | Th. with remove D1 V1 & H1 | 22.335 | sym29 | 24.596 | rbio2.8 | 23.239 | sym29 | 25.202 | rbio2.8 |
| Soft Threshold Penalized with 3_Levels 2D-DWT | Th. Only | 22.982 | bior3.9 | 24.260 | sym32 | 23.563 | bior3.9 | 24.753 | sym23 |
| | Th. with removing D1 | 23.012 | bior3.9 | 24.286 | sym6 | 23.632 | rbio3.9 | 24.271 | bior3.7 |
| | Th. with removing V1 | 22.576 | sym36 | 24.576 | bior3.7 | 23.555 | bior3.7 | 24.949 | bior3.7 |
| | Th. with remove H1 | 22.716 | bior3.7 | 24.278 | bior3.7 | 23.218 | sym23 | 24.926 | bior3.7 |
| | Th. with remove D1 & V1 | 22.738 | bior3.9 | 24.381 | bior3.7 | 23.214 | bior3.9 | 25.097 | bior3.7 |
| | Th. with remove D1 & H1 | 22.574 | sym36 | 24.687 | bior3.5 | 23.618 | rbio3.9 | 25.122 | bior3.7 |
| | Th. with remove V1 & H1 | 22.279 | sym29 | 24.746 | bior3.5 | 23.184 | sym36 | 25.195 | bior3.5 |
| | Th. with remove D1 V1 & H1 | 22.275 | sym29 | 24.822 | bior3.5 | 23.201 | bior3.9 | 25.357 | bior3.5 |

5. CONCLUSIONS AND RECOMMENDATIONS

In this part, a discussion made for the results that obtained by applying all cases of the denoising which they belong to the two threshold techniques that used to the four test images with the two noise ratios ($\sigma=15$ and $\sigma=25$). Also, present the conclusions extracted from the total results of all of the case in this study.

5.1 Results Recommendation

Depends on the results shown in Table 4.1, and Table 4.2, the results will be discussed into two parts, each with one of the threshold techniques.

5.1.1 Results Recommendation for the Hard Threshold Cases

1. Apply the threshold technique only:

Through applying only the threshold technique without removing any bands of the details bands, and for both levels of the noise 15, and 25, the wavelet filter family (reverse biorthogonal) is the superior filters which give the best results obtained by using the filter (rbio2.8).

1. Apply the threshold technique with removing the band D1:

By applying the threshold technique with removing the details band D1, the wavelet filter family (reverse biorthogonal) is the superior filters which give the best results that have been obtained by using the filters (rbio2.4 and rbio2.8) with the noise level 15, while when the noise is 25, the filter (rbio2.8) gives the superior result.

2. Apply the threshold technique with removing the band V1:

By applying the threshold technique with removing the details band V1, the wavelet filter families (reverse biorthogonal) and (Daubechies) are the superior filters which give the best results that have been obtained by using the filters (rbio2.6) from (reverse Biorthogonal) filter family, and the filters (db41, and db44) from the Daubechies filters family with the noise level 15. With the noise equal to 25, the filter (rbio 2.8) from (reverse biorthogonal) filter family, gives the superior result.

3. Apply the threshold technique with removing the band H1:

By applying the threshold technique with removing the details band H1, the wavelet filter family (reverse biorthogonal) also is the superior filters which give the best results that have been obtained with the noise equal to 25 by using the filters

(rbio2.4 and rbio2.8). While with the noise equal to 15, the wavelet filter families (reverse biorthogonal) and (Daubechies) are shared the superior results that obtained by using the filters (rbio 2.6), and (db44) respectively.

4. Apply the threshold technique with removing two details bands:

By applying the threshold technique with removing the two details bands (D1 with V1, or D1 with H1, or V1 with H1), and at the noise level 15, the results showed that the three wavelet filter families (reverse biorthogonal), (Daubechies), and (Symmetry) shared the superior by giving the best results that have been obtained by using the filters (rbio2.6, and rbio2.8) from the reverse Biorthogonal family, and the filters (db19, db17, and db44) from the Daubechies filter family, and the filters (sym25, and sym36) from the Symmetry filter family. While when the noise level is 25, the wavelet filter families (reverse Biorthogonal) and (Symmetry) are the superior filters which give the best results that have been obtained by using the filters (rbio2.6, and rbio2.8) from (reverse biorthogonal) filter family, and the filters (sym17, and sym29) from the Symmetry filters family.

5. Apply the threshold technique by removing all of the details bands:

By applying the threshold technique with removing all of the details bands (D1, V1, and H1), and at the noise level 15, the results showed that the two wavelet filter families (Daubechies), and (Symmetry) shared the superior by giving the best results that have been obtained by using the filters (sym25, and sym30) from the Symmetry filter family, and the filter (db44) from the Daubechies filter family. While when the noise level is 25, the wavelet filter families (reverse biorthogonal) and (Symmetry) are the superior filters which give the best results that have been obtained by using the filter (rbio2.8) from (reverse Biorthogonal) filter family, and the filter (sym29) from the Symmetry filters family.

5.1.2 Results Recommendation for the Soft Penalized Threshold Cases

1. Apply the threshold technique only:

Through applying just the threshold technique without removing any bands of the details bands, the wavelet filter family (Biorthogonal) is the superior filters which give the best results that obtained with the noise equal to 15 by using the filter (bior3.9). While with the noise equal to 25, the wavelet filter families (Biorthogonal) and (Symmetry) shared the superior results that obtained by using the filter (bior3.9) from the family (Biorthogonal), and the filters (sym32, and sym32) from (Symmetry) family.

2. Apply the threshold technique with removing the band D1:

By applying the threshold technique with removing the details band D1, the wavelet filter family (Biorthogonal) is the superior filters which give the best results that obtained by using the filters (bior3.9 and bior3.7) with the noise level 15. While when the noise level is 25, and in addition to the filters (bior3.9, and bior3.7) from (Biorthogonal) family, the filter (rbio3.9), and the filter (sym6) from families (reverse biorthogonal) and (Symmetry) respectively are gives the superior result.

3. Apply the threshold technique with removing the band V1:

By applying the threshold technique with removing the details band V1, with the noise level 15, the wavelet filter families (Biorthogonal) and (Symmetry) shared the superior results that obtained by using the filter (bior3.7) from the family (Biorthogonal), and the filters (sym 19, and sym 35) from (Symmetry) family. While with the noise equal to 25, the filter (bior3.7) from the family (Biorthogonal), and the filter (sym36) from (Symmetry) family are given the superior result.

4. Apply the threshold technique with removing the band H1:

By applying the threshold technique with removing the details band H1, with the noise level 15, the wavelet filter families (Biorthogonal) and (Symmetry) shared the superior results that obtained by using the filter (bior3.9) from the family (Biorthogonal), and the filters (sym23, and sym35) from (Symmetry) family. While with the noise equal to 25, the filter (bior3.7) from the family (Biorthogonal), and the filter (sym23) from (Symmetry) family are given the superior result.

5. Apply the threshold technique with removing two details bands:

By applying the threshold technique with removing the two details bands (D1 with V1, or D1 with H1, or V1 with H1), and at the noise level 15, the results showed that the two wavelet filter families (Biorthogonal) and (Symmetry) shared the superior by giving the best results that have been obtained by using the filters (bior3.9, bior3.7 and bior3.5) from the Biorthogonal family, and the filters (sym19, sym23, sym25, sym28, and sym35) from the Symmetry filter family. While when the noise level is 25, the wavelet filter families (reverse biorthogonal), (Symmetry), and (Biorthogonal) are the superior filters which give the best results that have been obtained by using the filter (rbio3.9) from (reverse biorthogonal) filter family, and the filters (sym29, and sym36) from the Symmetry filters family, and the filters (bior3.9, bior3.7 and bior3.5) from the Biorthogonal family.

6. Apply the threshold technique by removing all of the details bands:

By applying the threshold technique with removing all of the details bands (D1, V1, and H1), and at the noise level 15, the results showed that the three wavelet filter families (Daubechies), (Biorthogonal), and (Symmetry) shared the superior by giving the best results that have been obtained by using the filter (sym25) from the Symmetry filter family, and the filter (db41) from the Daubechies filter family, and filters (bior3.9, and bior3.5) from the Biorthogonal family. While when the noise level is 25, the wavelet filters (bior3.9, and bior3.5) from the Biorthogonal family and the filter (sym29) from the Symmetry filters family is the superior filters which give the best results.

5.2 THE CONCLUSION

From all of the results and the discussion cases, the following points can be concluded:

1. The amount of noise that concentrates and distributes into the details bands for the first analysis level for the 2D-DWT have the significant effect to the results of the image denoising, and this reason will make a deal with that bands plays a very critical role on the results and the performance of the denoising system.
2. Through increasing the level of the analysis phase in 2D-DWT, the increasing of the image enhancement was been noticed. This enhancement will be limit through the limit number of analysis levels because there will be no improvement due to the saturation of the denoising operation. The saturation of the denoising operation means that the number of points in the data is very small and will not affect the result at all.
3. From all of the results in this study, the best results that were the results that obtained by using the filters (bior 3.9, bior 3.7 and bior 3.5) which they are belongs to the wavelet filters family called the Biorthogonal filters family.
4. The filter (bior 3.9) from the Biorthogonal filters family, gave the best results of the images denoising operation in this study and gave compatibility properties with the distribution of the noise itself into the high frequencies in the details bands for the wavelet transformation.
5. Through the results obtained, a variation was observed in the effect of using the same filter with the change of the band from the details bands that removed in the wavelet domain. This variation indicates that each wavelet filter has specific properties that may be compatible with a particular band and not consistent with the others.
6. In the case when all the details bands for the first analysis level in 2D-DWT removed, and for both of the threshold technique, the results showed that for a large set of the filters in wavelet filters families the effect was small. The reason is that a large amount of the noise has been removed directly with removing the details bands for the first analysis level in 2D-DWT.

6. REFERENCES

- Abdullah, H.N., Aziz, J.S., Mohammed, A.N., 2011. Complex Discrete Wavelet Transform-Based Image Denoising, *Engineering and Technology*, 29(5), 833-850.
- Abinaya, M. and Amudha. J., 2015. Image Denoising and Quality Measurements Using Wavelet Thresholding, *International Journal of Science and Innovative Engineering and Technology*, 2, 1-6.
- Agrawal, S. and Sahu, R., 2012. Wavelet Based MRI Image Denoising Using Thresholding Technique. *International Journal of Science, Engineering and Technology Research*, 1(3), 32-35.
- Al Jumah, A., 2013. Denoising of an Image Using Discrete Stationary Wavelet Transform and Various Thresholding Techniques, *Journal of Signal and Information Processing*, 4(01), 33-41.
- Alessio, S.M., 2016. Digital Signal Processing and Spectral Analysis for Scientists Concepts and Application, Springer.
- Anutam, R., 2014. Performance Analysis of Image Denoising With Wavelet Thresholding Methods For Different Levels of Decomposition, *International Journal of Multimedia and Its Applications*, 6(3), 35-46.
- Argenti, F., Benelli, G., Kutufa, C., 1993. Transmission of Wavelet Transform Coded TV Images on a Noisy Channel, In *Proceedings of ICC'93-IEEE International Conference on Communications*, 1, 386-390.
- Moghtased-Azar, K. and Gholamnia, M., 2014. Effect of Using Different Types of Threshold Schemes in Wavelet Space on Noise Reduction over GPS Times Serie, *Journal of Geomatics Science and Technology*, 4(1), 51-66.
- Mohideen, S.K., Perumal, S.A., Sathik, M.M., 2008. Image de-noising using discrete wavelet transform. *International Journal of Computer Science and Network Security*, 8(1), 213-216.
- Birgé, L. and Massart, P., 2007. Minimal penalties for Gaussian model selection, *Probability theory and related fields*, 138(1-2), 33-73.
- Boyat, A.K. and Joshi, B.K., 2015. A Review Paper: Noise Models in Digital Image Processing, *Signal and Image Processing: An International Journal*, 6, 2.
- Bregovic, R. and Gotchev, A., 2014. On the Performance of Multirate Filterbanks: Quantification of Shift Variance and Cyclostationarity in the works of Till Aach, *Image Processing: Algorithms and Systems XII*, 9019,9019.
- Burrus, C.S., 2012. Fast fourier transforms, *OpenStax CNX*,
- Dixit A. and Sharma, P., 2014. A Comparative Study of Wavelet Thresholding for Image Denoising: I.J. Image, Graphics, and Signal Processing, 12, 39-46.
- Ergen, B., 2012. Signal and Image Denoising Using Wavelet Transform, *Advances in Wavelet Theory and Their Applications in Engineering, Physics and Technology*.
- Gomes, J. and Velho, L., 2015. From Fourier Analysis to Wavelets, 3, New York: Springer.

- Graps, A., 1995. An introduction to wavelets. *IEEE computational science and engineering*, 2(2), pp.50-61.
- Levicky, D., Drutarovsky, M., Galajda, P., Kocur, D., Marchevsky, S., 1996. Adaptive Goertzel's Algorithm for DFT Computation with Higher Accuracy, *Radloengineering*, 5, 1.
- Liu, Y., 2015. Image Denoising Method based on Threshold, Wavelet Transform, and Genetic Algorithm, *International Journal of Signal Processing, Image Processing and Pattern Recognition*, (8)2, 29-40.
- Liu, Z., Mi, Y., Mao, Y., 2014. An Improved Real time Denoising Method Based on Lifting Wavelet Transform, *Measurement Science Review*, (14)3, 152-159.
- Chun Lin, L., 2010. A Tutorial of the Wavelet Transform, *NTUEE, Taiwan*.
- Mallat, S.G., 1989. A Theory for Multiresolution Signal Decomposition: The Wavelet Representation, *Transactions on Pattern Analysis And Machine Intelligence*, 7, 674-693.
- Misiti, M., Misiti, Y., Oppenheim, G., Poggi, J.M., 1997. Wavelet Toolbox Getting Started Guide, *The Mathworks*.
- Newland, D.E., 1993. Harmonic Wavelet Analysis, *Proceedings of the Royal Society of London. Series A: Mathematical and Physical Sciences*, 443(1917), 203-225.
- Pang, J., 2017. Improved Image Denoising Based on Haar Wavelet Transform, *SmartWorld, Ubiquitous Intelligence and Computing, Advanced and Trusted Computed, Scalable Computing and Communications, Cloud and Big Data Computing, Internet of People and Smart City Innovation*, 1-6.
- Niblack, W., 1986. An introduction to digital image processing, (34). Englewood Cliffs: Prentice-Hall.
- Preibisch, S., Saalfeld, S., Tomancak, P., 2009. Globally optimal stitching of tiled 3D microscopic image acquisitions. *Bioinformatics*, 25(11), 1463-1465.
- Ramadhan, A., Mahmood, F., Elci, A., 2017. Image Denoising by Median Filter in Wavelet Domain, *the International Journal of Multimedia and Its Applications* (9), 1.
- Ismael, S.H. and Mustafa, F.M., 2016. A new approach of image denoising based on discrete wavelet transform. 2016 World Symposium on Computer Applications & Research (WSCAR), 36-40
- Saxena, C. and Kourav, D., 2014. Noises and Image Denoising Techniques: A Brief Survey, *International Journal of Emerging Technology and Advanced Engineering*, 4(3), 878-885.
- Selami, A.M.A.A. and Fadhil, A.F., 2016. A Study of the Effects of Gaussian Noise on Image Feature, *Kirkuk University Journal /Scientific Studies (KUJSS)*, 11, 3, 152-169.
- Sontakke, M.D. and Kulkarni, M.S., 2015. Different Types of Noises in Images and Noise Removing Technique, *International Journal of Advanced Technology in Engineering and Science*, 03(1).

Toufik, B. and Mokhtar, N., 2012. The Wavelet Transform for Image Processing Applications, *Advances in Wavelet Theory and Their Applications in Engineering, Physics and Technology*.



CURRICULUM VITAE

PERSONAL INFORMATION

Name : Sleman Saeed Hassan
Nationality : IRAQ
Date of birth : 10 December 1992
Telephone:
Email : salmansaeed09876@gmail.com

EDUCATION

In 07.10.2016, i started master study in the department of electrical and electronic engineering at Siirt University.

| <u>DEGREE</u> | <u>INSTITUTE</u> | <u>YEAR OF GRADUATION</u> |
|----------------------|---------------------------------------|----------------------------------|
| High School | Kawa High School | 2011 |
| B. Eng. | Computer Scince College of Sulaimanya | 2015 |
| M.Sc. | Siirt University | 2019 |

RESEARCH INTERESTS

- Signal and Image Processin
- Image Denoising

FOREIGN LANGUAGE

Kurdish, English, Arabic.